Astbury Centre for Structural Molecular Biology

UNIVERSITY OF LEEDS

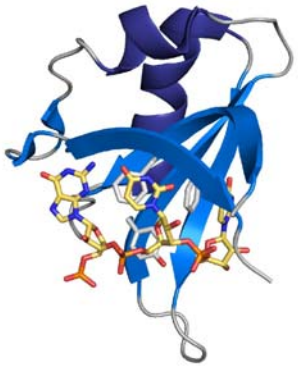

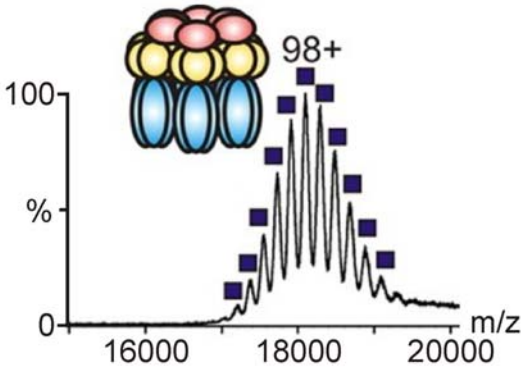

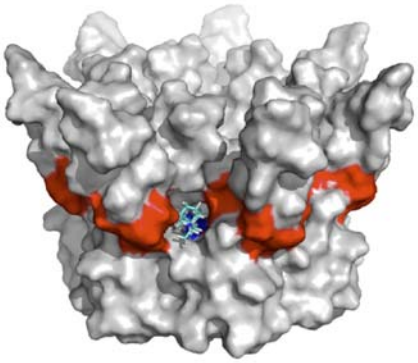

ASTBURY CENTRE

Annual Report 2011

Front cover illustration: some research highlights from 2011 by Astbury members. **Left:** crystal structure of DAZL RRM in complex with a sequence from the 3′-UTRs of mRNA. This work was published in *Proc. Natl. Acad. Sci USA* and further details can be found in the Edwards group entry (p. 16). **Middle:** ESI-MS spectrum of the intact TP901-1 lactococcal phage baseplate – a large (~ 1.8 MDa) non-covalent protein complex. This work was published in *Mol. Cell. Prot.* and further details can be found in the Ashcroft group entry (p. 1). **Right:** model of the Hepatitis C virus-coded p7 ion channel or "viroporin". Rimantadine is shown docked into the peripheral binding site. This work, led by Stephen Griffin, together with Fishwick and Foster (Chemistry) and Harris (Institute of Molecular and Cellular Biology) was published in *Hepatology*. Further details can be found in the Griffin group entry (p. 22)

Acknowledgement

The Astbury Centre for Structural Molecular Biology thanks its many sponsors for support of the work and its members for writing these reports. The report is edited by David Brockwell.

This report is also available electronically via http://www.astbury.leeds.ac.uk

Mission Statement

The Astbury Centre for Structural Molecular Biology will promote interdisciplinary research of the highest standard on the structure and function of biological molecules, biomolecular assemblies and complexes using physico-chemical, molecular biological and computational approaches.

Introduction

It is with great pleasure that I write this introduction, my first as the new Director of the Astbury Centre. The Centre continues to be buoyant, diverse and successful, engaging in all aspects of research as you will see from some of the highlights detailed below. It is with much excitement that we look to the future and to meeting the challenges of our interdisciplinary research in the year ahead. The successes of the Centre over the last three years have come about in a large part thanks to the enormous efforts of our previous Director, Adam Nelson. Adam worked tirelessly for the Centre over the last three years and will continue to play a leading role in the Centre (as Director of the Industry Hub, see below, and by continuing as a member of the Executive). On behalf of all the Astbury members I would like to take this opportunity to thank Adam for all of his hard work and many contributions.

This annual report provides a snapshot of the Astbury Centre's activities in 2011. In its pages you will find reports that describe new and exciting research stories, which span fundamental research into Structural Molecular Biology in its widest context, as well as the various applications of our research in bio(nano)technology, bioengineering, medicine and synthetic biology. The pages and co-authors of each report demonstrate the successes made possible by the interdisciplinary research within the Centre. They also highlight the breadth of activity in the Centre that spans studies of molecular interactions within cells, to the development of new physical and chemical methods for studying biological systems.

2011 saw continuing success of the members of the Astbury Centre in terms of peer recognition. Our student and post-doc members again received several awards at a variety of international meetings, including best oral presentation (Scott Jackson (Peter Henderson's laboratory)); best poster (James Ross (Bruce Turnbull's laboratory)) and best paper (Tom Knapman (Alison Ashcroft's group) for his manuscript on ion mobility spectrometry-mass spectrometry published in the International Journal of Mass Spectrometry in 2011). Well done everyone! Members of the Centre were also proud to take part in a ceremony in which Professor David Stuart, FRS (University of Oxford) was awarded an Honorary Degree, which was performed by our Chancellor, Lord Bragg, FRS, FBA, FRSA, FRSL, FRTS. The Degree was awarded in recognition of Professor Stuart's phenomenal contributions to Structural Molecular Biology, specifically in the context of X-ray crystallography of viruses.

The Centre welcomed 6 new academic staff members in 2011 (Michelle Peckham, Paul Beales, Steve Evans, Narcis Fernandez-Fuentes, Steve Johnson, Darren Tomlinson) and we were also delighted to welcome many new PhD students and postdoctoral members to the Centre this year. This takes our current numbers to 60 academic staff, 183 students and 58 postdoctoral fellows. We were sorry to see Steve Homans leave the University in 2011. We wish him all the best in his new role. He will maintain his links with Astbury as a Visiting Member and we look forward to seeing him at Astbury events during 2012.

Astbury Centre members continued to be very successful in publishing their research in 2011. In total, we published >130 manuscripts in 2011, including 18 papers in high impact journals. These reflect the remit of the Astbury Centre and include *Nature* and *Cell* series, *Proc. Natl. Acad. Sci.USA*; molecular and cellular focussed journals, *J. Am. Chem. Soc.*, *Angew. Chem. Intl. Ed*. and health/disease oriented journals such as *PloS Pathog.*, *Blood* and *Hepatol*. Highlights included (i) measurement of the intramolecular and intermolecular electron transfer rates of nitrite reductase (Evans, Jeuken); (ii) the use of mass spectrometry to delineate the effects of an amyloid inhibitor on the aggregation of β_2m (Ashcroft, Radford) and (iii) identification of a novel interaction between ORF57 protein from Karposi's sarcoma-associated herpesvirus and the cellular proteiin UIF (Whitehouse). In terms of grant income, Astbury members also enjoyed success in 2011. Highlights included a large (£0.7M) Equipment Grant funded by the Wellcome Trust (led by Peter Stockley and Arwen Pearson and involving 10 Astbury PIs) that funded the purchase of new X-ray facilities and instruments for EM, CD and ITC, as well as an upgrade to our NMR facilities. Our success in applications to the ERC for Starting grants also continued this year, with Lars Jeuken joining Andy Wilson and Lorna Dougan as holders of these prestigious awards. Congratulations also to Mark Harris who was awarded a Wellcome Trust Senior Investigator Award: the first in Leeds and the first in our Centre. Finally, working together with the White Rose and the Universities of York and Sheffield (in partnership with the Food and Environment Research Agency (FERA) and the Research Complex at Harwell) we were delighted to learn that an application for a BBSRC Doctoral Training Partnership entitled "Mechanistic Biology and its Strategic Application" in which many Astbury members were involved was funded to a very high level, with 20 PhD studentships p.a. funded across the three Institutions by BBSRC, supplemented by 9 studentships from the three participating Universities and 9 from the White Rose. At the end of 2011, Astbury Centre members held a £22M share of grants totalling £37M from funding agencies spanning MRC, EPSRC, BBSRC, Wellcome Trust, British Heart Foundation, to name but a few.

Developing strong and sustained links with relevant industries has been a major objective within the Centre over the last three years and this will continue to be a major focus of our activities in, and beyond, 2012. We thank Alison Ashcroft for driving the development of these links over the last three years. We were delighted to host over 30 delegates from about 20 companies to our third event for industrial partners, which focused on the themes "Protein Aggregation and Bioprocessing" (led by David Brockwell) and "Targeted Molecular Delivery" (led by Peter Stockley). The Industry Advisory board was also expanded to align with our growing links with industry. These newly formed links are now bearing fruit, and our partnerships with AstraZeneca and Medimmune alone resulted in 6 new collaborative PhD studentships in 2011. In recognition of the success of this initiative, and its importance for the Astbury Centre, Adam Nelson has now taken on the role of Director of the University's Pharmaceutical & Biopharmaceutical Sector hub, an £550k initiative which seeks to align relevant research within the University with the specific needs of these sectors.

The Astbury Society, led by the co-presidents Adam Daniels and Lucy Woods, played a magnificent role in Astbury activities in 2011, hosting social events (including the now famous pub quiz and pizza night) and providing much-needed cakes, coffee and tea at various events. Thank you! They also organised a fantastic brain-teasing and muscle-stretching team building event at the Annual Retreat, this year held over 2 days in Shrigley Hall Hotel (Derbyshire) which was attended by 155 members. The society also hosted the barbeque and Sports Day at the fifth Annual Astbury Lecture which this year was given by Professor Sir Alec Jeffreys, FRS. Finally, three Astbury Society members (Adam Daniels, Lucy Woods and Bethny Morrissey), led by a previous society president (Nicole Timms (2010)) organised a very successful Young Life Scientist Conference in August, as part of the centenary celebrations of the Biochemical Society. The meeting, entitled "Protein Evolution and Engineering: From Research to the Real World', attracted 90 participants from 7 countries, with Professors Don Hilvert (ETH Zurich) and Dan Tawfik (Weizmann Institute, Israel), giving keynote lectures. A new Astbury Society Committee (chaired by James Towey and Heather Cox) has taken the helm for 2012. Watch out for news and events!

I hope that you enjoy reading this Annual Report, whether you are a member of the Centre, a visitor, a member of our Industrial Advisory Board, a funding agency that supports our activities, or a passing reader with an interest in Structural Molecular Biology and the activities of our Centre. Finally, thanks to David Brockwell for preparing this report, everyone who contributed to it, and everyone who participated in Astbury's activities in 2011 and made them such a success.

Sheena E Radford

Director, Astbury Centre for Structural Molecular Biology,

Leeds, April 2012

Contents

Contributions indexed by Astbury Centre Principal Investigator

Biomolecular mass spectrometry

James Ault, Helen Beeston, Henry Fisher, Aneika Leney, Bethny Morrissey, George Preston, Caroline Pritchard, Charlotte Scarff, Dale Shepherd, Lucy Woods, Lydia Young and Alison Ashcroft

Introduction

The main focus of our research is the development and application of mass spectrometric techniques to investigate the tertiary and quaternary structures of biomolecules. We use non-covalent electrospray ionisation mass spectrometry (ESI-MS) and tandem mass spectrometry (MS/MS) to determine the mass, conformational properties, stoichiometry, stability, and binding characteristics of proteins and protein complexes. We are also pioneers of ion mobility spectrometry-mass spectrometry (IMS-MS), which offers a unique opportunity to separate co-populated biomolecular entities on the basis of their physical shape and to measure their mass and cross-sectional area (Ω) in a single, rapid (≤ 2 mins) experiment.

Results

In collaboration with Prof. Christian Cambillau (Université de Marseilles, France), we have used ESI-(IMS)-MS to study the mass and stoichiometry of the intact, non-covalently bound baseplate complexes of two siphophages, p2 and TP901-1, as well as several significant structural sub-complexes generated by a "block cloning" strategy. Both p2 and TP901-1 infect different strains of the gram+ lactic acid bacterium *Lactococcus lactis*. They possess a large multi-protein organelle (1-2 MDa) at their distal tail end, termed the baseplate, which is responsible for specific host recognition, attachment and initiation of infection. However, despite X-ray crystallography and/or electron microscopy of the final baseplate, the pathways leading to these large complexes remain ill-defined.

The masses of the intact phage baseplates, and a range of associated sub-complexes, were etermined within an error of ≤0.2 %. Thus, the stoichiometries of the intact baseplates were confirmed and the identities of the multi-protein sub-complexes assigned unambiguously. For example, the stoichiometry of the intact TP901-1 baseplate (mass 1.769 MDa) was confirmed as [(6 x Dit) + (18 x BppU) + (54 x BppL] subunits (Figure 1).

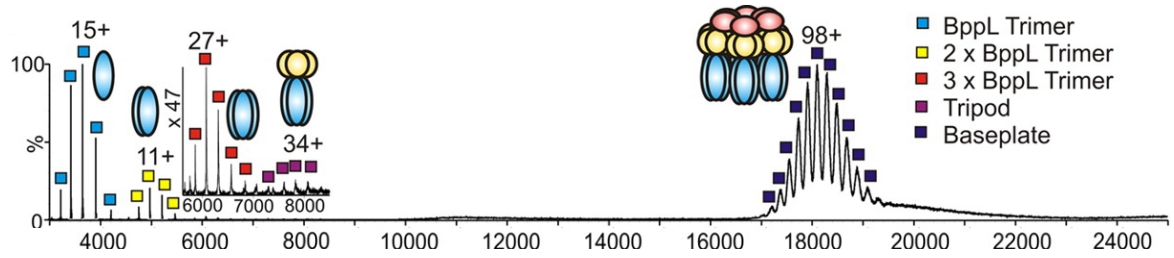

Figure 1: ESI-MS spectrum of the intact TP901-1 lactococcal phage baseplate (mass 1.769 MDa; m/z ca 18,000) and associated sub-complexes. Key: pink = distal tail protein (Dit); yellow = baseplate protein upper (BppU); blue = baseplate protein lower (BppL).

The characterisation of these sub-complexes has provided valuable insights into the assembly of the organelles and we have been able to propose plausible baseplate assembly pathways for the p2 and TP901-1 lactococcal phages (Figure 2). The collision cross-sectional areas measured by ESI-IMS-MS were compared with solution-phase dynamic light scattering data to support the notion that the structure of a protein complex can be maintained in the gas phase. Together the data illustrate the value of ESI-(IMS)-MS for studying heterogeneous, megaDalton, macromolecular baseplate complexes.

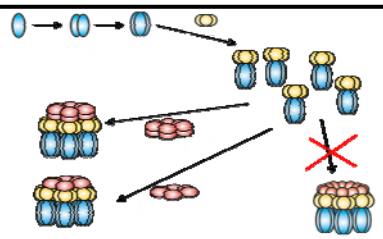

Figure 2: proposed TP901-1 baseplate assembly pathway from baseplate complex and sub-complexes characterised by ESI-MS and ESI-IMS-MS. Key: pink = distal tail protein (Dit); yellow = baseplate protein upper (BppU); blue = baseplate protein lower (BppL).

Publications

Filby, M., Muldoon, J., Dabb, S., Fletcher, N., Ashcroft, A. & Wilson, A. (2011) Protein surface recognition using geometrically pure Ru(II) tris(bipyridine) derivatives. *Chem. Commun*. **47:**559-561.

Goulet, A., Kee Him, J., Veesler, D., Auzat, I., Robin, G., Shepherd, D., Ashcroft, A., Richard, E., Lichière, J., Tavares, P., Cambillau, C. & Bron, P. (2011) The opening of SPP1 bacteriophage tail, a prevalent mechanism in gram+ infecting siphophages. *J. Biol. Chem*. **286:**25397-25405.

Kaur-Atwal, G., Reynolds, J., Mussell, C., Champarnaud, E., Knapman, T., Ashcroft, A., O'Connor, G., Christie, S. & Creaser, C. (2011) Determination of testosterone and epi-testosterone glucuronides in urine by ultra performance liquid chromatography combined ion mobility-mass spectrometry. *Analyst* **136:**3911-3916.

Leney, A., Phan, G., Allen, W., Verger, D., Waksman, G., Radford, S. & Ashcroft, A. (2011) Second order rate constants of donor strand exchange reveal individual amino acid residues important in determining the subunit specificity of pilus biogenesis. *J. Amer. Soc. Mass Spectrom.* **22:**1214-1223.

Pritchard, C., Quaglia, M., Ashcroft, A. & O'Connor, G. (2011) Considering the advantages and pitfalls of the use of isotopically labelled protein standards for accurate protein identification. *Bioanalysis* **3:**2797-2802.

Shepherd, D., Veesler, D., Lichière, J., Ashcroft, A. & Cambillau, C. (2011) Unravelling lactococcal phages baseplates assembly through mass spectrometry. *Mol. Cell. Prot*. DOI: 10.1074/mcp.M111.009787

Smith, D., Woods, L., Radford, S. & Ashcroft, A. (2011) Structure and dynamics of oligomeric intermediates in beta2-microglobulin self-assembly. *Biophys. J*. **101:**1238-1247.

Woods, L., Platt, G., Hellewell, A., Hewitt, E., Homans, S., Ashcroft, A. & Radford, S. (2011) Ligand binding to distinct precursor states diverts the aggregation pathway of an amyloid-forming protein. *Nat. Chem. Biol.* **7:**730–739.

Funding

This work was funded by the BBSRC, the EPSRC, the Wellcome Trust, Waters UK Ltd., LGC, AZ, and GSK. We thank the BMSS for student travel grants.

Collaborators

External: R. Griffin (M.I.T.), S. Macedo-Ribeiro (Universidade do Porto), H. Saibil, (Birkbeck College), D. Middleton (University of Liverpool), M. Vendruscolo (University of Cambridge) and A. Rodger (University of Warwick).
Leeds: S. Harris, E. Hewitt, S. Homans, I. Manfield, P. Stockley and S. Warriner.

Applying classical nucleation theory to describe amyloid fibril formation

Raffaela Cabriolu and Stefan Auer

Introduction

One goal of our research is to reveal the physical aspects of the self-assembly and nucleation of polypeptide chains into amyloid-like structures. In order to achieve our goals we use computational/theoretical methods developed to investigate phase transitions in atomic and colloidal systems and apply them to investigate the transitions in the more complex biomolecular systems. In the last year we have been able to provide insight into the fibrillation kinetics of amyloid fibrils from atomistic nucleation theory, and to determine the size distribution of amyloid nanofibrils.

Amyloid fibrillation kinetics: Insight from atomistic nucleation theory

In this work we consider the nucleation of nanosized amyloid fibrils composed of successively layered β-sheets at the molecular level when this process takes place by direct polymerization of protein segments (β-strands) into β-sheets. Application of atomistic nucleation theory (ANT) to amyloid nucleation of β_2-microglobulin and amyloid β_{40} allows us to predict the fibril nucleus size and the fibril nucleation rate as functions of the supersaturation of the protein solution. The ANT predictions are compared to recent time-resolved optical experiments where they measure the effect of the protein concentration and mutations on the initial lag time before amyloid fibrils form in the protein solution. The presented analysis reveals the general principles underlying the nucleation kinetics of nanosized amyloid fibrils and indicates that it can be treated in the framework of existing general theories of the nucleation of new phases.

Size distribution of amyloid nanofibrils

In this work we consider the size distribution of amyloid nanofibrils (protofilaments) in nucleating protein solutions when the nucleation process occurs by the mechanism of direct polymerization of β-strands (extended peptides or protein segments) into β-sheets. Employing the atomistic nucleation theory, we derive a general expression for the stationary size distribution of amyloid nanofibrils constituted of successively layered β-sheets. The application of this expression to amyloid $\beta_{1\text{-}40}$ ($A\beta_{40}$) fibrils allows us to determine the nanofibril size distribution as a function of the protein concentration and temperature. The distribution is most remarkable with its exhibiting a series of peaks which are positioned at "magic" nanofibril sizes (or lengths) and which are due to deep local minima in the work for fibril formation. This finding of "magic" sizes or lengths is consistent with experimental results for the size distribution of aggregates in solutions of $A\beta_{40}$ proteins. Also, our approach makes it possible to gain insight into the effect of point mutations on the nanofibril size distribution, an effect that may play a role in experimentally observed substantial differences in the fibrillation lag-time of wild-type and point-mutated amyloid-beta proteins.

Publications

Cabriolu, R. & Auer, S. (2011) Amyloid fibrillation kinetics: insight from atomistic nucleation theory *J. Mol. Biol.* **411:**275-285.

Cabriolu, R., Kashchiev, D. & Auer, S. (2011) Size distribution of amyloid nanofibrils *Biophys. J.* **101**, 2232-2241.

Funding

This work was supported by the EPSRC.

Collaborators
Professor Dimo Kashchiev, Institute of Physical Chemistry, Bulgarian Academy of Sciences, Sofia, Bulgaria.

DNA-directed assembly of giant Janus vesicles

Paul Beales

Overview

The interactions between patchy particles do not only depend upon their relative separations but also their relative orientations. This added complexity introduced by heterogeneous surface chemistry affords the assembly of a greater array of supra-particulate materials.

We use liquid-liquid phase separation in lipid mixtures to form Janus-textured giant vesicles. We investigate the partitioning of lipid-DNA and cholesterol-DNA conjugates between the coexisting domains. Inclusion of highly unsaturated lipids in the membrane mixtures enhances partitioning of these functionalities into liquid-ordered (L_o) domains with cardiolipin driving the strongest enhancement into the L_o phase (greater than an order of magnitude enhancement). DNA-directly assembly of populations of Janus vesicles expressing complementary DNA sequences results in the formation of size-limited vesicle clusters: L_o domains saturate in adhesion plaques leaving DNA-depleted membrane exposed on the exterior of the clusters that do not favour further binding.

This ability to control the size of multicompartment structures may have application in designing nanomedicines for combination therapies or synthetic biology approaches to mimic the compartmentalization of chemistry within cells and tissues.

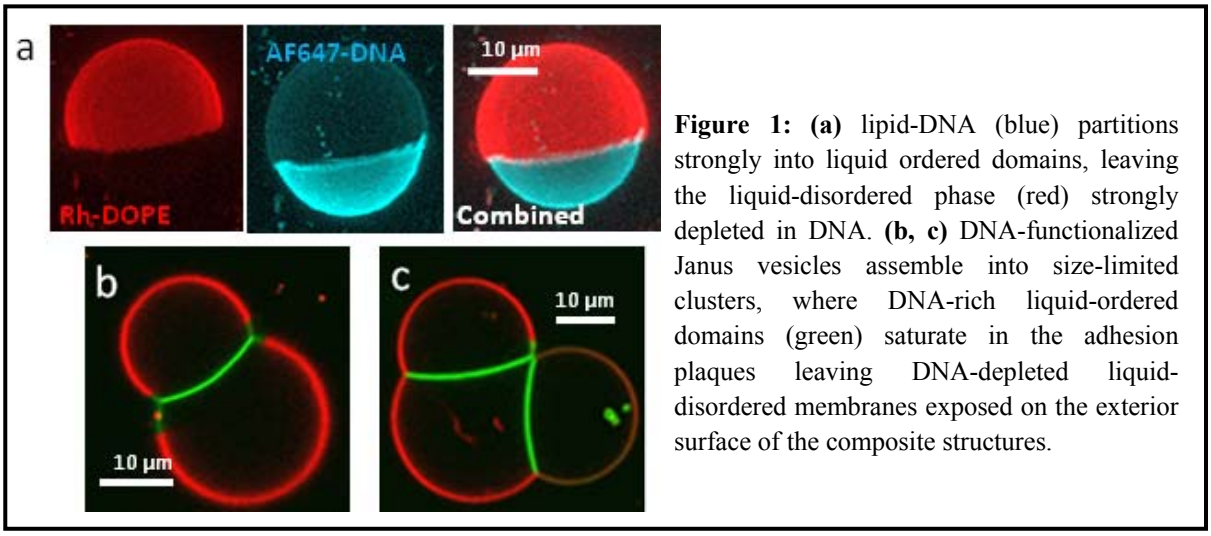

Figure 1: (a) lipid-DNA (blue) partitions strongly into liquid ordered domains, leaving the liquid-disordered phase (red) strongly depleted in DNA. **(b, c)** DNA-functionalized Janus vesicles assemble into size-limited clusters, where DNA-rich liquid-ordered domains (green) saturate in the adhesion plaques leaving DNA-depleted liquid-disordered membranes exposed on the exterior surface of the composite structures.

Publications

Beales, P., Nam, J. & Vanderlick, T. (2011) Specific adhesion between DNA-functionalized "Janus" vesicles: size-limited clusters. *Soft Matter* **7:**1747-1755.

Funding

This work was funded by Yale University.

Collaborators

This work was conducted in conjunction with Prof. Kyle Vanderlick and Dr. Jin Nam (Yale University).

QM/MM modelling of the reaction mechanism and chemical incorporation of non-natural amino acids into the active site of *N*-acetylneuraminic acid lyase

Nicole Timms, Adam Daniels, Sasha Derrington, Claire Windle, Jennifer Stockwell, Alun Myden, Adam Nelson, Arwen Pearson, Chi Trinh and Alan Berry

Introduction

N-Acetylneuraminic acid lyase (NAL) is a Class I aldolase that catalyses the reversible aldol condensation between *N*-acetyl-d-mannosamine, **1**, and pyruvate, **2**, to yield *N*-acetylneuraminic acid, **3** (Figure 1). We have previously demonstrated that directed evolution is a powerful tool in the discovery of synthetically valuable aldolase variants. For example, we discovered the NAL variant E192N whose substrate specificity was switched towards the alternative aldehyde substrate **4**; condensation of the aldehyde, **4**, with pyruvate, **2**, yields the product **5**, which is a potential precursor of some influenza A sialidase inhibitors. In addition, we have used directed evolution to create a pair of stereoselective aldolase enzymes that may be used to prepare stereoselectively the 4*S* and 4*R* diastereomers of **5**.

Previously, there has only been speculation as to how the aldehyde oxygen is protonated

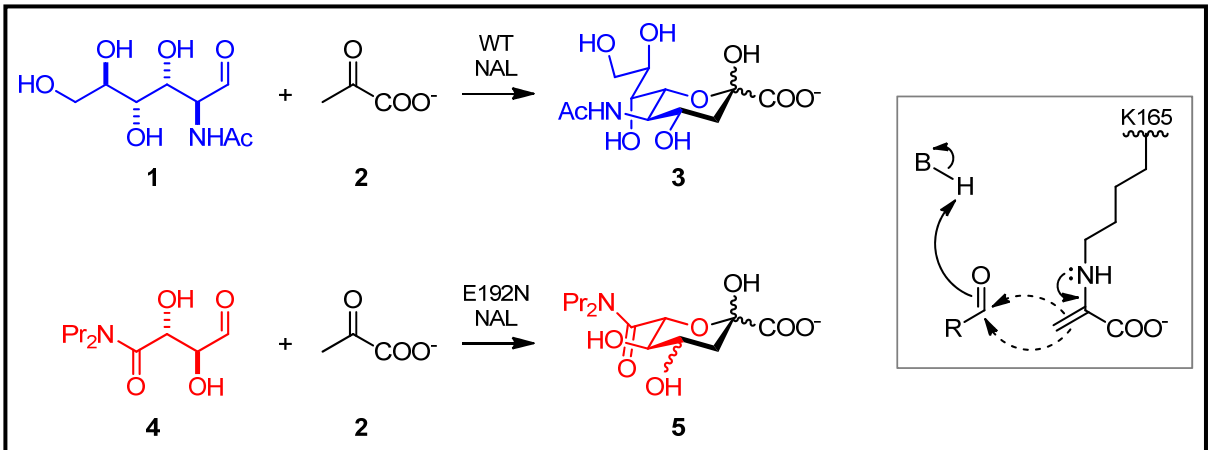

Figure 1: left - the reactions catalysed by wild-type NAL and NAL variant E192N. **Right -** the carbon-carbon bond formation and subsequent protonation of the aldehyde oxygen in the NAL-catalysed reaction.

during the NAL-catalysed reaction, whether it is by an active site residue, a water molecule or *via* substrate-assisted catalysis. There has been similar speculation as to why the reaction catalysed by NAL variant E192N between aldehyde **4** and pyruvate, **2**, shows a lack of stereoselectivity, unlike in the wild-type reaction. These questions we have tried to address through the computational modelling of each of these reaction mechanisms.

Traditionally we have only been able to utilise the 20 standard proteogenic amino acids in directed evolution experiments. Although highly diverse, this range of amino acids does not cover the full spectrum of structures and functional groups. The incorporation of non-natural amino acids into a protein allows new functionality to be introduced. The chemical incorporation of non-natural amino acids has many advantages over genetic incorporation as it is post-translational, allowing high yields of the protein to be purified initially, and also larger libraries of amino acids can be created without the costly need for finding new translational machinery.

QM/MM modelling of the NAL reaction mechanism

Previously, we have solved the 3D structures of a number of NAL variants, including substrate- and inhibitor-bound structures which we have used as starting points for modelling of the NAL reaction mechanism. Using quantum mechanical and molecular mechanical

(QM/MM) methods we have performed restrained molecular dynamics and energy minimisations to simulate the formation of the carbon-carbon bond between pyruvate, **2**, and the corresponding aldehydes **1** and **4** in the wild-type and E192N NAL-catalysed reactions, respectively. These simulations have elucidated key residues involved in the stabilisation of a high energy reaction intermediate, and allowed us to hypothesise on the movement on protons during the reaction (Figure 2). Furthermore, this work has offered new evidence towards the explanation of the stereoselectivity of wild-type NAL and the lack of stereoselectivity of the E192N variant. These methods can be used to estimate the structure-function relationship of both the enzyme and substrate(s) during the NAL-catalysed reaction. This will allow us to make much more informed decisions in the future rational design of this enzyme to produce variants with greater catalytic activity or altered substrate specificity.

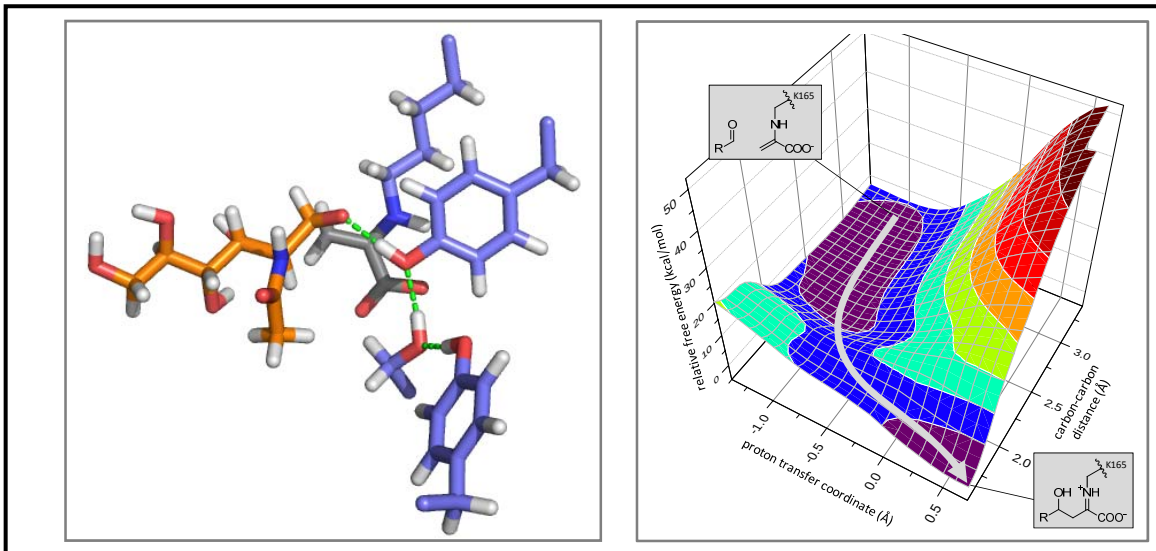

Figure 2: left - A modelled 'transition state' for the NAL-catalysed reaction. **Right** - A potential energy landscape of the NAL-catalysed reaction showing the minimum energy pathway between the substrates, **1** and **2**, and the product, **3**.

Chemical incorporation of non-natural amino acids into the NAL active site

We have developed the methodology for the chemical incorporation of non-natural amino acids in the NAL active site through the modification of a cysteine residue at the targeted position (Figure 3). This required the cloning and characterisation of a cysteine-free NAL from *S. aureus* and development of unfolding/refolding conditions to allow for efficient chemical modification and production of native proteins. Non-natural amino acid incorporation was achieved through the conversion of a cysteine residue to dehydroalanine using 2,5-dibromohexan-1,6-diamide (diBr). Conjugate addition of a thiol then converts the dehydroalanine to the corresponding non-natural amino acid. NAL variants containing chemically incorporated non-natural amino acids at crucial active site residues have been characterised by mass spectrometry and also been shown to retain catalytic activity.

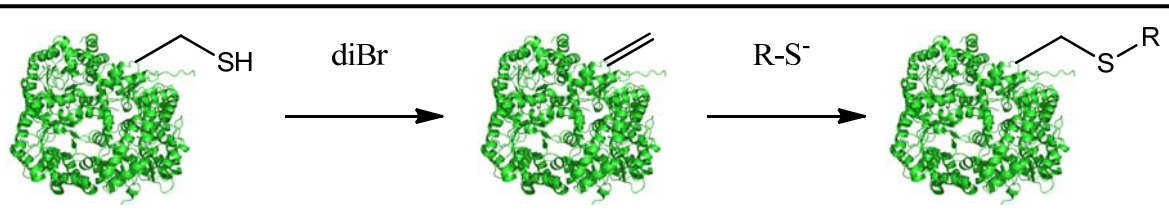

Figure 3: a schematic of non-natural amino acid incorporation *via* the conversion of a cysteine residue to dehydroalanine and subsequent addition of a thiol.

Furthermore, we have been able to crystallise and solve the 3D structures of a number of non-natural amino acid-containing NAL variants, including enzyme-substrate complexes (Figure

4). We now have the tools available to incorporate a range of non-natural amino acids throughout the NAL active site. This allows new routes to the alteration of substrate specificity or even the introduction of novel catalytic activity in NAL and potentially many other enzymes.

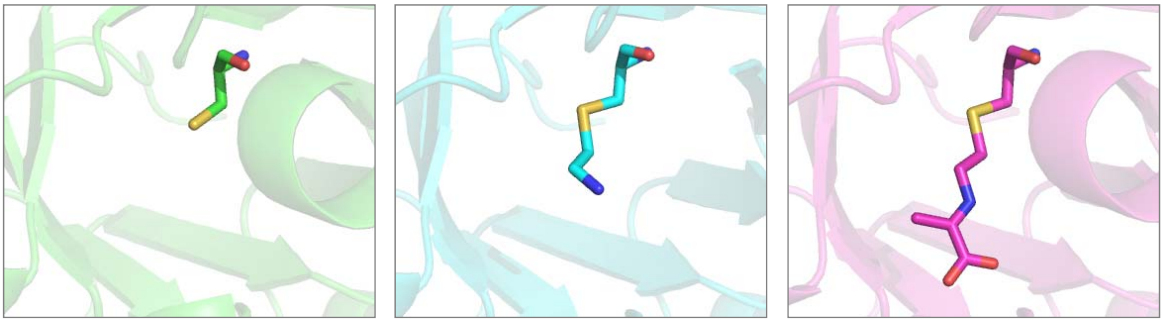

Figure 4: crystallographically-solved 3D structures of the NAL variant K165C (left) and the chemically modified variants K165thialysine (middle) and K165thialysine in complex with pyruvate (right).

Funding
Our work is funded by BBSRC, EPSRC, the Wellcome Trust and AstraZeneca.

Collaborators
We thank Dr Marc van der Kamp and Prof. Adrian Mulholland at the University of Bristol for their collaboration and expertise in computational modelling. We also thank Justin Chalker and Prof. Ben Davis at the University of Oxford for their help with chemical modification experiments.

Label-free electrochemical detection of enzymatic activity using microarrays

James Murray, Steven Johnson and Robin Bon

Introduction

In the past decades, microarray technologies have enabled the analysis of thousands of biochemical interactions simultaneously, leading to new biological insights. The immobilisation of nucleic acids, proteins and small molecules on microarray surfaces commonly relies on dot-printing techniques, whereas detection of binding is typically based on (direct or indirect) fluorescent labelling of target proteins. Recently, immobilisation of peptide aptamers on gold electrode microarrays and detection of their binding to proteins in cell lysates by label-free electrochemical spectroscopy have been demonstrated. We are investigating the use of this technology to construct substrate microarrays for the detection of activity and substrate specificity of enzymes responsible for post-translational modification of proteins. The concept is illustrated in Figure 1: Individual electrodes will be selectively functionalised with substrates via a self-assembled monolayer (SAM), and the conversion of the immobilised substrates will be detected by label-free electrochemical spectroscopy.

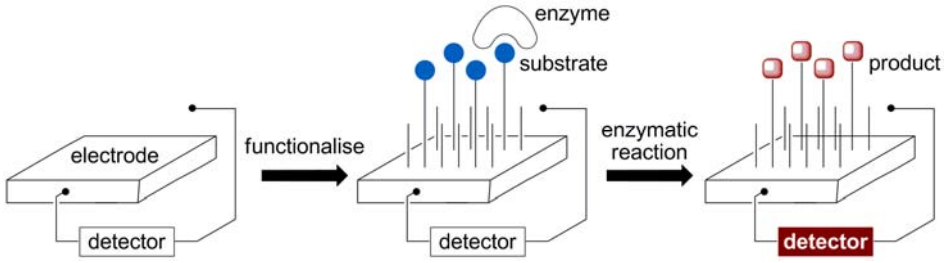

Figure 1: label-free electro-chemical detection of enzymatic activity. Substrates will be chemoselectively immobilised on electrodes. Upon enzymatic processing, the change of their size and/or charge will be measured using label-free electrochemical spectroscopy.

Results

Synthesis of labelled small molecules: We have now established the synthesis of azide- and amine-terminated linker systems **6** and **7**, which are necessary for the immobilisation of substrates on electrodes, using a combination of solution phase and solid phase chemistry (Scheme 1). Currently, we are attaching to these linkers a range of substrates, and evaluating the resulting constructs using biochemical and biophysical assays.

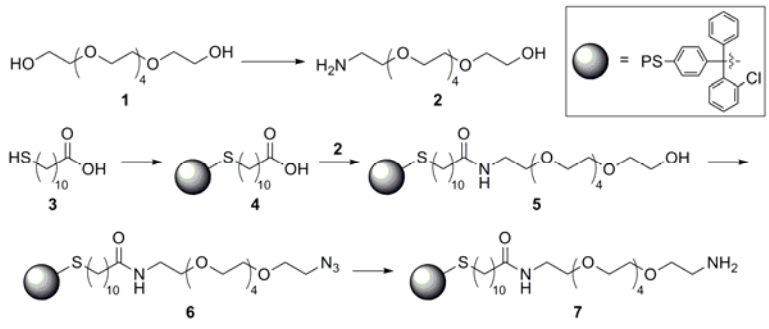

Scheme 1: solid phase synthesis of the linker systems used for the immobilisation of substrates,as established by JM. The thiol group is used for immobilisation on gold electrodes; the alkane chain ensures SAM formation; the PEG chain ensures compatibility with aqueous environments; the azide group (in **6**) or amine group (in **7**) is used for attachment of small molecules and peptides.

Funding

We thank the Biomedical and Health Research Centre for funding.

Breaking apart protein complexes by force

Oliver Farrance, Chris Wilson, Sheena Radford and David Brockwell

Introduction

Colicins are protein antibiotics synthesised by *E.coli* strains to target and kill related bacteria during environmental stress. E-type colicins such as colicin E9, exert their toxicity via nuclease activity. Colicins are multi-domain proteins contain a receptor (R) domain required for the initial binding event to the outer membrane of the victim bacterium (via the BtuB protein), a translocation (T) domain used to bring about translocation via interaction with OmpF and a cytoplasmic (C) DNase domain (termed E9, herein) that results in death of the competing cell subsequent to its translocation to the victim's cytoplasm (Figure 1). To prevent host suicide, colicins are expressed alongside specific immunity proteins (Im9 in the case of E9) which inactivate colicin enzymatic activity by binding to an exo-site adjacent to the active site.

Colicin:immunity protein complexes are amongst the strongest protein complexes known with a lifetime of weeks. Despite this, immunity protein release is a pre-requisite of colicin intoxication which occurs on a timescale of minutes. Colicin intoxication results in linkage of the colicin bound on the outer membrane to the energised inner membrane via formation of a 'translocon' whereupon immunity protein is jettisoned (Figure 1). Here we investigate whether force-induced conformational changes that may occur upon translocon formation can explain the disparity between the timescales of E9:Im9 dissociation and colicin intoxication.

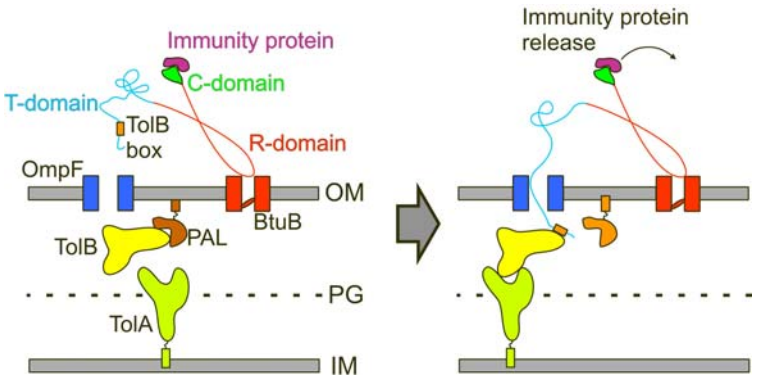

Figure 1: summary of the intoxication pathway for colicin E9. **Left:** colicin E9 comprises three domains, the R-domain (red), an unstructured T-domain (light blue) and the C-domain (a nuclease, light green). Colicin E9 is co-expressed alongside an immuty protein (Im9, pink) that inactivates E9, protecting the host. When exported to the excellular medium, the R-domain of colicin E9 binds to a competing bacterium via interaction with BtuB. The unstructured T-domain then threads through the lumen of OmpF and the TolB box binds to TolB. This in turn binds to TolA, indirectly linking colicin E9 to the energised inner membrane. **Right:** upon formation of this translocon Im9 is released by unknown mechanism. The C-domain is then translocated to the victim's cytoplasm by an unknown mechanism.

Results

To investigate how force affects the dissociation rate of E9:Im9 we used an atomic force microscope (AFM) to form and then break apart the E9:Im9 complex. This is depicted schematically in Figure 2(a). Briefly, Im9 is specifically immobilized onto the AFM tip and E9 onto a suitably derivatised inert surface. If the tip is brought into contact with the surface and a complex forms, retraction of the tip will load the complex with force until it breaks apart at a characteristic force. This force is dependent upon the intrinsic off-rate of the complex (measured by ensemble methods) and the speed at which the tip is retracted. By measuring the unbinding force many times at many different speeds it is possible to calculate the off-rate in the absence of force. This technique is called dynamic force spectroscopy (DFS).

Measuring the rupture forces between E9 and Im9 by DFS revealed that this very strong interaction is surprisingly labile to the application of force. Under application of only 20 pN force (at most) the rate of complex dissociation was found to be a million-fold faster than that measured by ensemble methods (Figure 2(a)). Consequently under low levels of force, Im9 is jettisoned on a timescale of seconds, commensurate with the timescale of colicin intoxication. By analyzing the effect of mutations and the effect of changing the pulling points on E9 and Im9 we identified partial unfolding of the N-terminal region as a position-

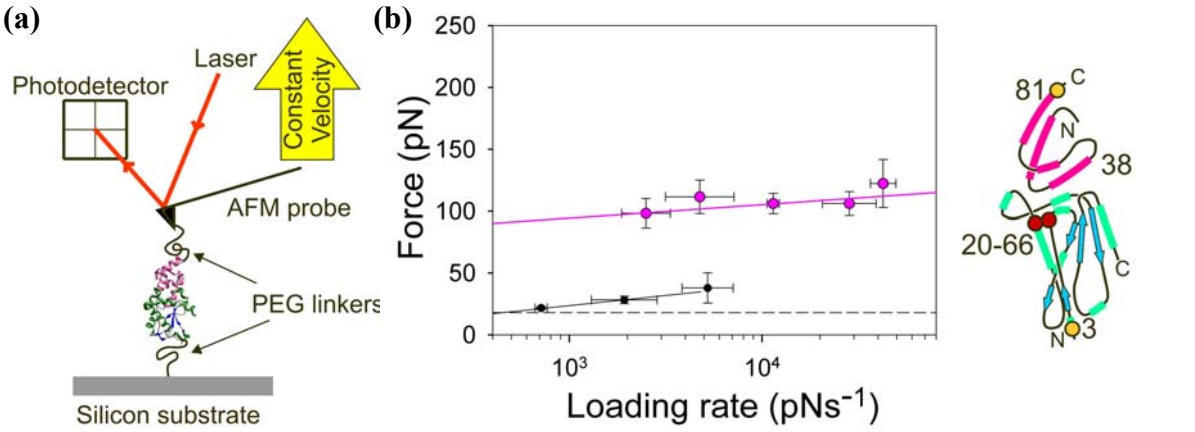

Figure 2: (a) measuring the strength of protein-protein interactions using an AFM. Im9 and E9 are immobilsed onto a derivatised AFM tip and silicon substrate at a defined site (via unique cysteine residues) using heterobifunctional polyethylene glycol linkers. After complex formation, the tip is moved away from the substrate and the force at which the complex breaks apart is quantified. **(b) left -** DFS of E9:Im9 (black) and $E9_{ds}$:Im9 (pink). The former complex is exceedingly force labile (dissociates at <20 pN) while the latter is mechanically strong. Accordingly, the extrapolated intrinsic off-rate of the former is a million-fold faster than the latter (5 and 5×10^{-6} s^{-1}, respectively). **Right -** a simplified topology diagram showing how formation of a disulfide bond on E9 (residues 20-66) insulates the binding interface from force induced remodeling when extended from residues 3 and 81 on E9 and Im9 respectively.

specific force-triggered, allosteric activator of immunity protein release. We term this novel, catastrophic force-triggered increase in off-rate as a 'trip bond'. Importantly, controls in which the trigger cannot be pulled, created by disulfide bond engineering yielded a mechanically strong complex ($E9_{ds}$:Im9) that dissociated at high force and gave k_{off} values that equate precisely with those measured using ensemble methods (Figure 2(b)).

For colicin function, a trip bond allows bipartite complex affinity whereby force induces a switch from a highly stable complex that is necessary to protect the host cell, to a rapidly dissociating, unstable complex able to trigger colicin intoxication. More generally, trip bonds allow an all-or-none mechano-transduction of a specific signal, adding to the emerging richness of the response of biomolecules and their complexes to force.

Publications

Crampton, N., Alzahrani, K., Beddard, G., Connell, S. & Brockwell, D. Mechanically unfolding protein L using a laser-feedback controlled cantilever (2011) *Biophys. J.* **100:**1800-1809.

Funding

We thank Nasir Khan for technical support and the BBSRC for funding.

Collaborators

External: Prof. C. Kleanthous (University of Oxford).
Leeds: Prof. G. Beddard (School of Chemistry), Emanuele Paci (Instititute of Molecular and Cellular Biology).

Manipulating the interaction of pH-responsive polymers with lipid membranes for intracellular drug delivery

Shengwen Zhang, Andrew Nelson, Zachary Coldrick and Rongjun Chen

Introduction

Biopharmaceuticals represent a powerful new class of medicines with potential for the treatment of a wide variety of previously intractable human diseases. One of the major obstacles to screening, development and commercialisation of biopharmaceuticals is the development of robust intracellular delivery platforms.

We have developed a class of efficient, non-toxic, scalable and adaptable polymeric carriers, which were desgined to to mimic the activity of viruses both in cell entry and endosomal escape mechanisms. The parent polymer is a biodegradable polyamide, poly(L-lysine isophthalamide) (PLP). It can be grafted with hydrophobic amino acids including phenylalanine (PP) or hydrophilic methoxy poly(ethylene glycol) amine (PA) to manipulate its amphiplicity and structure. The polymers can be tailored to have efficient cell entry. It has aslo been demonstrated *in vitro* and *in vivo* that the polymers can have a profound pH triggerability, which enables substantial intracellular delivery of drug agents (small molecule and biopharmaceutical agents) to cytoplasmic/nuclear targets for therapy.

Results

The work described in this report was focused on the fundamental mechanism of the interaction of the PLP-derived polymers with lipid membranes to explore the key factors, which enables them to traverse across membrane barriers.

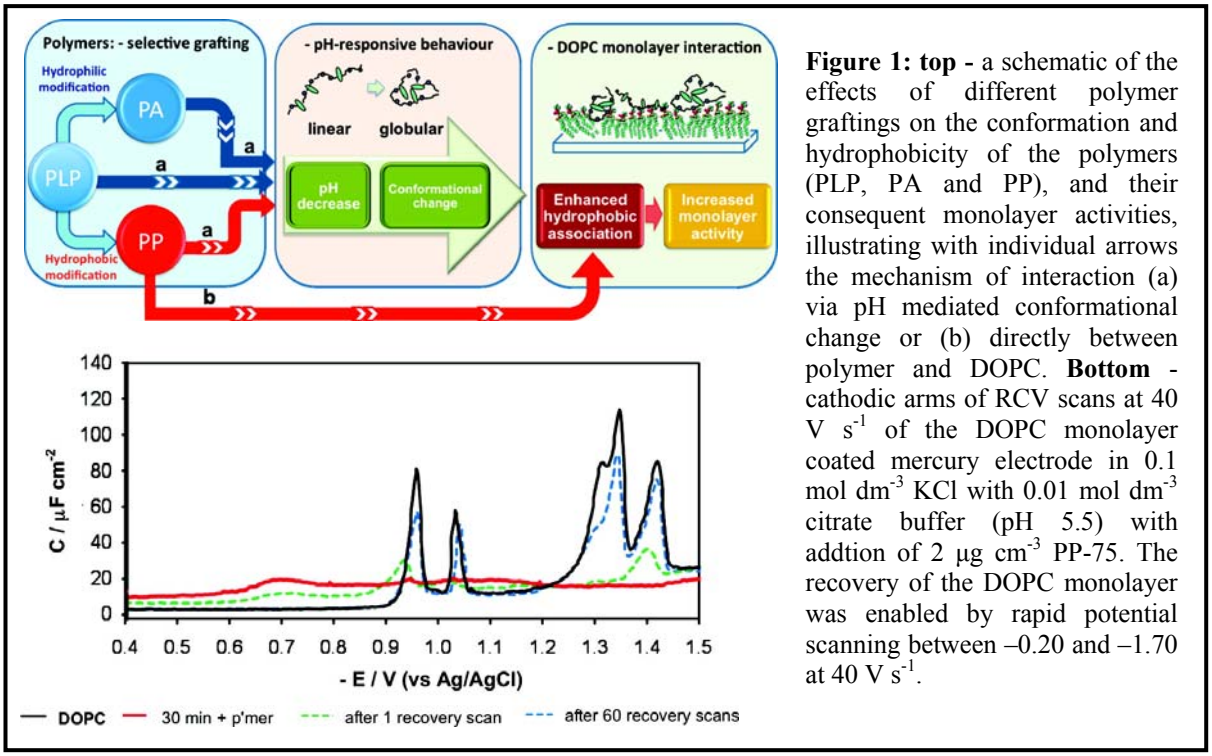

Figure 1: top - a schematic of the effects of different polymer graftings on the conformation and hydrophobicity of the polymers (PLP, PA and PP), and their consequent monolayer activities, illustrating with individual arrows the mechanism of interaction (a) via pH mediated conformational change or (b) directly between polymer and DOPC. **Bottom** - cathodic arms of RCV scans at 40 V s^{-1} of the DOPC monolayer coated mercury electrode in 0.1 mol dm^{-3} KCl with 0.01 mol dm^{-3} citrate buffer (pH 5.5) with addtion of 2 µg cm^{-3} PP-75. The recovery of the DOPC monolayer was enabled by rapid potential scanning between –0.20 and –1.70 at 40 V s^{-1}.

The interaction of the pH-responsive polymers, i.e. PLP, PA and PP, with phospholipid monolayers adsorbed on mercury electrodes have been studied (Figure 1). The polymers interact reversibly with the monolayer shown by altering the monolayer capacitance and inhibiting the phospholipid reorientation in electric field. Polymer grafting enhances the pH-mediated conformational change of the polymers which in turn increases their phospholipid monolayer activity. The most significant monolayer interactions have been observed with the

polymer grafted with hydrophobic phenylalanine. A low level of PEGylation of the backbone also increases the monolayer activity. The cell membrane activities of these amphiphilic polymers have been successfully mirrored in this supported DOPC monolayer model membrane system, isolating the key parameters for biomembrane activities and giving insight into the mechanism of the interactions.

The membrane interaction of the polymers has been further investigated using human erythrocytes. As presented in Figure 2, PP-50 adsorption on the surface of erythrocytes leads to thinning of the membrane. Cross-sectional AFM data shows depressions of the membrane around regions of polymer buildup. These depressions reach approximately 3 nm, 35-40% of the human erythrocyte bilayer thickness. The membrane thinning would contribute to the enhanced membrane permeability, and entensive bilayer thinning would lead to cell membrane collapse.

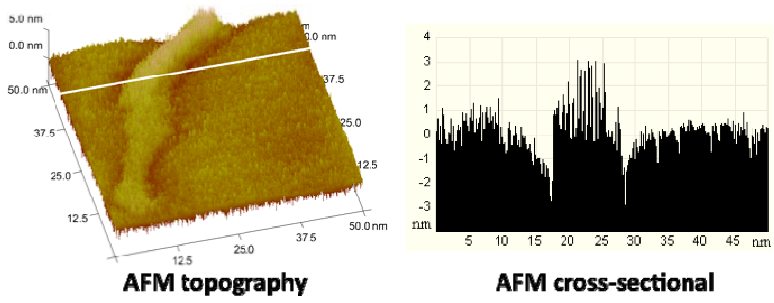

Figure 2: the topographic AFM micrograph and the AFM cross-sectional imaging along it white line of the surface of the erythrocyte membrane in the presence of polymer PP-50 adsorption. Cells were incubated at 37 ^{o}C in PBS pH 7.05 containing 400 mg mL^{-1} PP-50 for 9 h. Prior to imaging, cells were immobilized on a polylysine coated microscope slide, cross linked in glutaraldehyde (1%) for 5 min, washed three times with PBS and then air dried.

It has been demonstrated that the pH-responsive polymer was able to penetrate efficiently into the three dimensional multicellular spheroids, reach almost all the cells (~93%) in the spheroids, and achieve a high cell entry. When the polymers were internalised, they were able to disrupt endosomal membranes for effective intracellular release of endocytosed payloads.

Publications

Ho, V., Slater, N. & Chen, R. (2011) pH-responsive endosomolytic pseudo-peptides for drug delivery to multicellular spheroids tumour models. *Biomaterials* **32**:2953-2958.

Lynch A., Chen, R. & Slater, N. (2011) pH-responsive polymers for trehalose loading and desiccation protection of human red blood cells. *Biomaterials* **32**:4443-4449.

Metanawin, T., Tang, T., Chen, R., Vernon D. & Wang, X. (2011) Cytotoxicity and photocytotoxicity of structure-defined water-soluble C60/micelle supramolecular nanoparticles. *Nanotechnology* **22**:235604.

Zhang, S., Nelson, A., Coldrick Z. & Chen, R. (2011) The effects of substituent grafting on the interaction of pH-Responsive polymers with phospholipid monolayers. *Langmuir* **27**:8530-8539.

Funding

This work was supported by the Brian Mercer Award for Innovation (from the Royal Society), EPSRC and BBSRC.

Collaborators

Prof N. Slater, University of Cambridge. Prof X. Wang, University of Waterloo.

Understanding the cryoprotective action of glycerol

James Towey and Lorna Dougan

Introduction

Cryopreservation is an effective process in which molecules, cells or whole tissues are preserved by cooling to sub-zero temperatures. This method is widely utilized in industry, medicine and nanotechnology to prolong the storage life of specific components. This important process is possible due to molecules called cryoprotectants, such as glycerol. The molecular mechanisms by which these cryoprotectants stabilize and protect molecules and cells, while suppressing the formation of ice, are incompletely understood. Elucidating such molecular mechanisms is crucial to improve cryopreservation protocols, as well as to identify and formulate more efficient cryoprotectant solutions.

A structural approach

We use state-of-the-art equipment at the ISIS facility within the Rutherford Appleton Laboratories to complete structural studies on glycerol-water mixtures in the liquid state. Over the past decade, significant advances have been made in the methods of neutron diffraction with isotopic substitution and in the development of more powerful computational tools. Neutron diffraction is an ideal probe for the structural study of liquids providing a full atomistic-level, structural examination of glycerol-water solutions.

Molecular mixing as a cryoprotection method

We find that in a concentrated glycerol-water solution, there is a preference for isolated water molecules that goes beyond that expected for the mixture. We find that glycerol and water molecules mix very effectively, hindering the formation of an extended water network in the solution and hence the formation of ice. Furthermore, given the efficiency of water molecules to take the place of glycerol molecules in the hydrogen-bonded network, an extended glycerol network is impeded. Thus, we propose that it is the good mixing of this solution and the preference of water monomers that prevent ice, formed by water networks, from penetrating and disrupting biological systems. Given glycerol can be found in high concentrations in biological systems, the mixing of aqueous glycerol and the preference for water monomers could offer an attractive structural mechanism for protecting organisms under extreme cold conditions. Further studies on dilute and intermediate concentrations of aqueous glycerol solutions will help to elucidate whether this structural picture is valid across the concentration regime.

Potential impact and future work

These results highlight the importance of preferential hydrogen bonding in aqueous solutions and suggest a mechanism for cryoprotection. We find that glycerol effectively hydrogen bonds with water, resulting in a disrupted hydrogen-bonded water network. In future work we plan to examine the thermodynamic, structural, and dynamical properties of common cryoprotectant solutions in the supercooled liquid state. These are the thermodynamic conditions where these systems are yet to be explored in microscopic structural detail. Such detailed insight may lead to the development of optimized strategies to utilize these components in industrial applications, leading to the next generation of solution conditions for formulation and bioprocessing. These results will be important not only for cryopreservation applications, but to improve our understanding of life at low-temperatures. The characterization of target cryoprotectant solutions and their effect on biomolecules are also relevant to sustainable chemistry. Glycerol and propylene glycol are sustainable solvents

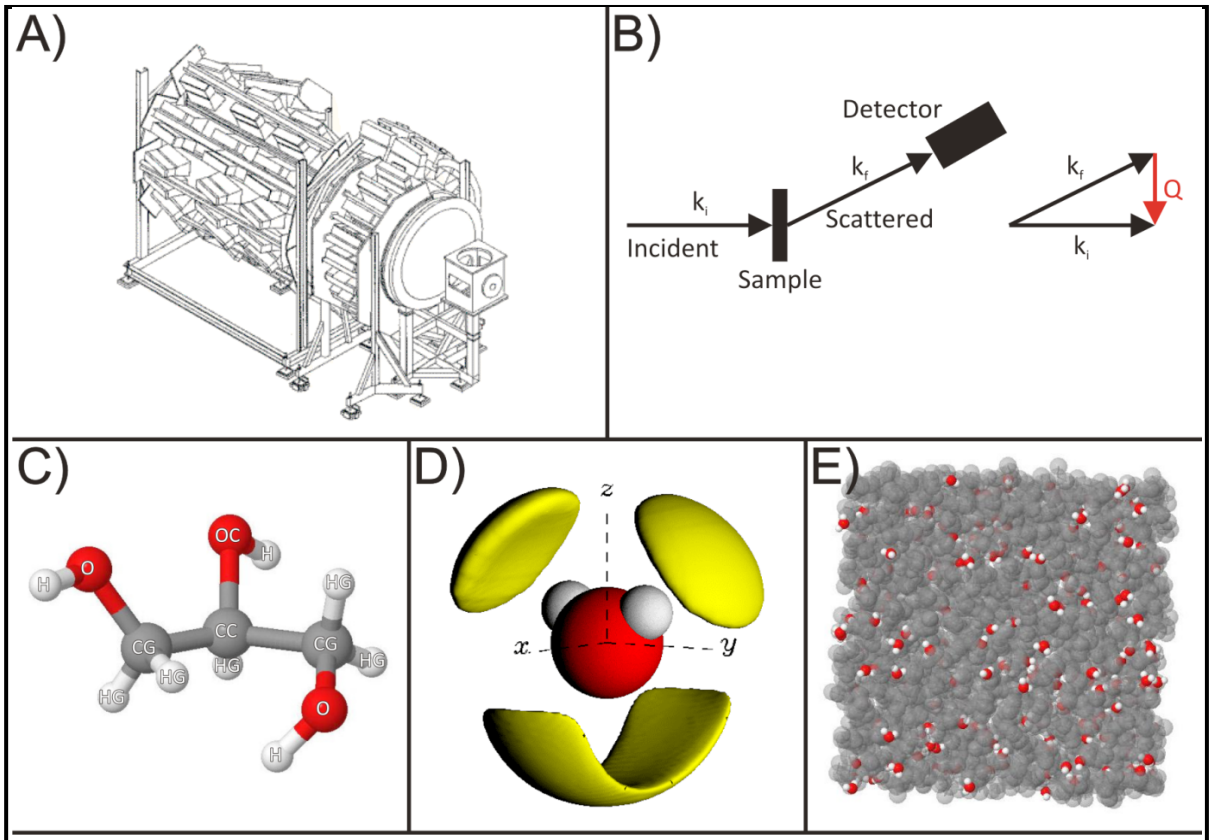

Figure 1: (a) schematic of the SANDALS neutron diffractometer at ISIS where the experiments were completed. **(b)** the measured quantity in the experiments is the difference between the incident k_i and scattered k_f wave vectors of the neutrons, known as Q. From the scattering data detailed structural information can be found accessed. For example, **(c)** molecular scale geometry such as intra-molecular bond angles in the molecule glycerol, **(d)** hydrogen bonding arrangements (the most probable region for nearest neighbour water molecules are shown in yellow around a central water molecule). **(e)** large scale mixing can also be investigated to detect the presence (or lack of) preferential interactions between molecule types, here glycerol (grey) and water (red).

for green chemistry, with excellently suitable properties for catalysis, organic synthesis, separations and materials chemistry, and pharmaceutical applications. Thus, these results form the foundation for a study that could have wide-reaching impact in many areas of research, industry and medicine.

Publications

Towey, J., Soper, A. & Dougan, L. (2011) Preference for isolated water molecules in a concentrated glycerol-water mixture. *J. Phys. Chem. B* **115:**7799-7812.

Towey, J., Soper, A. & Dougan, L. (2011) The structure of glycerol in the liquid state: a neutron diffraction study. *Phys Chem Chem Phys* **12:**9397-9445.

Funding

This work is being funded by EPSRC (2010-EP/H020616/1)

Collaborators

Prof. A. Soper, Rutherford Appleton Laboratories, UK

Kinked β-strands mediate high-affinity recognition of mRNA targets by the germ-cell regulator DAZL

Huw Jenkins, Miriam Walden, Bara Malkova and Tom Edwards

Introduction

A defect in germ cell (sperm and oocyte) development is the leading cause of male and female infertility. Control of translation through the binding of Deleted in Azoospermia-like (DAZL) to the 3'-UTRs of mRNAs, via a highly conserved RNA recognition motif (RRM), has been shown to be essential in germ cell development.

Results

Crystal structures of the RRM from murine Deleted in Azoospermia-like both alone and in complex with RNA sequences from the 3'-UTRs of mRNAs regulated by Dazl reveal high-affinity sequence-specific recognition of a GUU triplet involving an extended, kinked, pair of β-strands. Recognition of the GUU triplet is maintained whilst the identity and position of bases flanking this triplet varies. The Dazl RRM is thus able to recognise GUU triplets in different sequence contexts. Together with the demonstration that multiple Dazl RRMs can bind to a single RNA containing multiple GUU triplets, these structures suggest that the number of DAZL molecules bound to GUU triplets in the 3'-UTR provides a method for modulating the translation of a target RNA. The conservation of RNA binding and structurally important residues between members of the Deleted in Azoospermia (DAZ) family indicates that the mode of RNA binding revealed by these structures is conserved in proteins essential for gamete development from flies to humans.

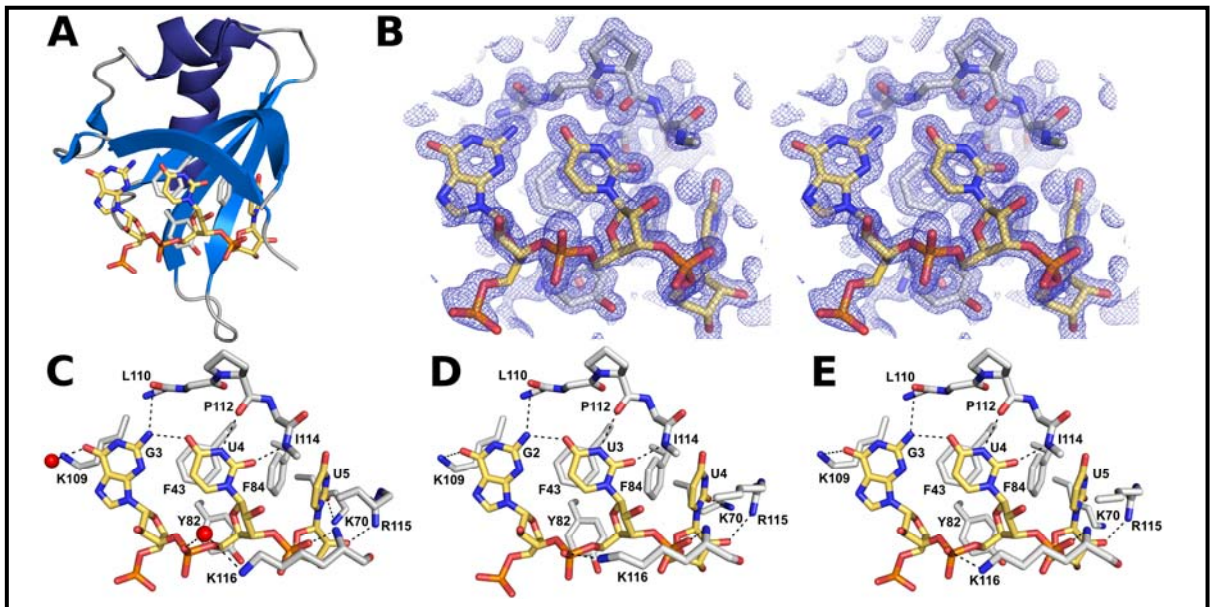

Figure 1: GUU triplet recognition by the Dazl RRM. **(a)** overview showing orientation of Figs 1*C-E*; for clarity Fig. 1*B* is rotated slightly. **(b)** stereo view of initial zinc-SAD phased electron density map contoured at 2σ. **(c)** recognition of the GUU triplet in the 32-132:8-nt structure **(d)** recognition of the GUU triplet in the 32-117:Mvh structure. **(e)** recognition of the GUU triplet in the 32-117:Sycp3 structure. Hydrogen bonds are shown as dashed lines.

Publications

Jenkins, H., Malkova, B. & Edwards, T. (2011). Kinked β-strands mediate high-affinity recognition of mRNA targets by the germ-cell regulator DAZL. *Proc. Natl. Acad. Sci. USA* **108:**18266-71.

Walden, M., Jenkins, H. & Edwards, T. (2011) Structure of the *Drosophila melanogaster* Rab6 GTPase at 1.4 Å resolution. *Acta Crystallogr. Sect. F* **67:**744-8.

Additional 2011 publications from the Edwards group:

East, D., Sousa, D., Martin, S., Edwards, T., Lehman, W. & Mulvihill, D. (2011) Altering the stability of the Cdc8 overlap region modulates the ability of this tropomyosin to bind co-operatively to actin and regulate myosin. *Biochem J.* 438:265-73.

Funding

We gratefully acknowledge funding for this work from the BBSRC, along with additional funding for the Edwards group from ERC, EPSRC and Astra Zeneca, Yorkshire Cancer Research, and The Wellcome Trust. We thank Sue Matthews for technical support.

Collaborators

External: D. Mulvihill (University of Kent), J. Trincao (Universidade Nova de Lisboa), R. Elliott (University of St Andrews).

Leeds: A. Wilson, A. Nelson, S. Warriner, J. Barr, A. O'Neill, S. Burgess, M. Peckham, P. Knight, N. Ranson, J. Hiscox, S. Harris and S. Homans.

de novo ligand design of novel bacterial RNA polymerase inhibitors

Martin McPhillie, Rachel Trowbridge, Katherine Mariner, Alex O'Neill, Peter Johnson, Ian Chopra and Colin Fishwick

Introduction

Bacterial RNA polymerase (RNAP) catalyses the synthesis of RNA from a DNA-template. Since this enzyme is essential for the growth and survival of bacteria, inhibition of bacterial RNAP is an established strategy for antibacterial therapy; for example the rifamycin antibiotics (known RNAP inhibitors) are used in the frontline treatment of tuberculosis. RNAP is considered an attractive antibacterial drug target since it is well conserved across bacterial genera but has distinct structural differences from eukaryotic RNAP. This qualifies bacterial RNAP as a target for broad-spectrum antibacterial therapy and permits the design of selective inhibitors. Despite the number of known inhibitors of bacterial RNAP, the rifamycins are currently the only class of bacterial RNAP inhibitor approved for clinical use, highlighting the challenge of RNAP as a drug target. Combating the rise in bacterial resistance to antibiotics is an important strategy in drug discovery. Novel antibacterial agents with new modes of action offer the best possibility to overcome existing resistance mechanisms. New opportunities to explore bacterial RNAP as a target have arisen following the 2008 discovery of the Myxopyronin B (MyxB) binding site. MyxB is an antibiotic produced from the myxobacterium *Myxococcus fulvus* Mxf50, which inhibits bacterial RNAP and the growth of Gram-positive and some Gram-negative bacteria. MyxB binds to the switch region of RNAP, where its mode of action has been proposed to involve either inhibition of the opening and closing of the βsubunit, or stabilisation of the refolding of the β -subunit switch-2 region, leading to an inactive conformation that cannot bind to template DNA. As bacteria have become resistant to the rifamycins, the MyxB binding site presents itself as an excellent opportunity for the design of new RNAP inhibitors as the two antibiotic binding sites are distant from each other.

Results

Inspection of the available MyxB-RNAP co-crystal structures revealed that the MyxB binding site within RNAP is U-shaped and sandwiched between two hydrophobic pockets. MyxB fills this cavity via its lipophilic side chains flanking the central core deep into these pockets, with its core pyrone ring making key interactions with residues near the cavity entrance. Given the high logP (7.5) of MyxB, it appears that most of its binding interactions are hydrophobic, although the whole molecule is sensitive to change, as demonstrated in studies of synthetic analogues. Using the co-crystal structure of *T. thermophilus* RNAP-des-myxopyronin B complex (PDB ID 3EQL), the MyxB binding site was explored using SPROUT. Given the large volume of this cavity focus was placed on the region around the enecarbamate side chain, since it is narrow and offers a bound inhibitor the potential for making hydrogen-bonding interactions with residues Trp1039 and Glu1041. Using SPROUT, a substituted pyridyl-benzamide scaffold was predicted to fill this volume and make interactions with residues Trp1039, Glu1041 and Gln611. Compound **1** was synthesised and tested in an in vitro *E. coli* RNAP assay using a Kool NC-45TM RNA polymerase template (Epicentre Biotechnologies). This revealed compound **1** to be a weak inhibitor of *E. coli* RNAP (IC50 151 μM).

In order to probe the possible binding conformations of compound **1**, the molecular docking program AUTODOCK was used to generate and evaluate a range of potential binding poses of **1** within the MyxB binding region of *T. thermophilus* RNAP. From these studies, the picolyl group of **1** was predicted to be located near the solvent exposed entrance of the binding cavity and adopt a range of different conformations of comparable energy. It was

binding cavity and adopt a range of different conformations of comparable energy. It was reasoned that restricting the degrees of freedom of this moiety could increase the binding affinity of this type of inhibitor. Additionally, inclusion of functional groups that could maintain the polarity within this region of the inhibitor due to its exposure to solvent at the entrance to the binding cavity, appeared favourable. Therefore, compounds **2** and **3** were prepared where the picolyl group of **1** was substituted for nitrogen-containing heterocycles. As predicted by the modelling, compounds **2** and **3** exhibited a marked increase in potency. These compounds represent the first reported examples of de novo designed ligands for the MyxB site of RNAP and have yielded important information on the requirements for ligand binding to this therapeutically important antibacterial target.

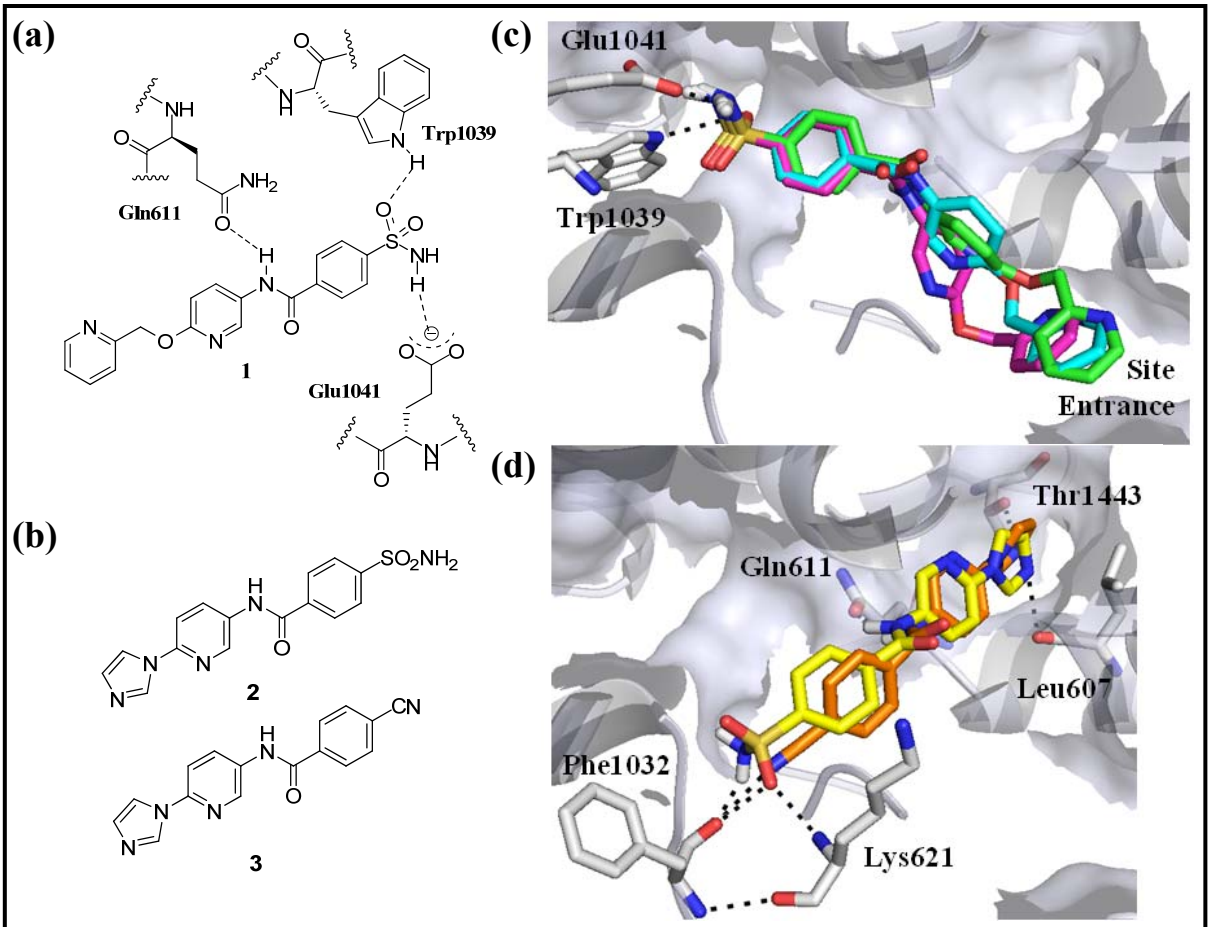

Figure 1: (a) compound 1 showing predicted interactions with RNAP. **(b)** AUTODOCK predicted docking poses of compound 1 (blue) within RNAP (grey): lowest energy pose (pink) and highest populated pose (green). **(c)** structures of compounds 2 and 3. **(d)** AUTODOCK predicted conformation of compounds 2 (yellow) and 3 (orange) within RNAP (grey).

Publications

Mariner, K., McPhillie, M., Trowbridge, R., Smith, C., O'Neill, A., Fishwick, C. & Chopra, I. (2011) Antibacterial activity and development of resistance to corallopyronin A, an inhibitor of RNA polymerase. *Antimicrob. Agents Chemother.* **55:**2413 – 2416.

McPhillie, M., Trowbridge, R., Mariner, K., O'Neill, A., Johnson, A., Chopra, I. & Fishwick, C. (2011) De novo ligand design of novel bacterial RNA polymerase inhibitors. *ACS Med. Chem. Lett.* **2:**729 – 734.

Funding

We thank the BBSRC and MRC for funding.

Identification and optimisation of small molecule modulators of protein targets as chemical probes and therapeutics

Ian Yule, Jeff Plante, Rachael Tennant, Jayakanth Kankanala, Rachel Trowbridge, Natalie Fisher, Richard Stilwell, Joseph Thompson, Adam Nelson, Colin Fishwick and Richard Foster

We are interested in the design, synthesis and optimisation of small molecules for therapeutic application or their use in the elucidation of biological function. By combining tools and techniques in medicinal chemistry, computer-aided drug design, high-throughput screening and combinatorial chemistry we aim to identify and optimise targeted small molecules as key modulators of specific biological function.

The group has capabilities in a number of areas for which bioactive molecules may be identified, optimised and/or targeted, including:

Medicinal chemistry, probe synthesis and chemical genetics

- Bio-targeted small molecules
- Targeted imaging agents
- Small molecule microarrays

Computational-aided drug design

- Ligand- and structure-based design
- Virtual screening
- *De novo* design

High-throughput screening

- 30k member diverse lead-like small molecule library
- Assay transfer/assay development

The activities are managed through the Medicinal Chemistry and Chemical Biology (MCCB) Technology group as part of the Biomedical Health Research Centre (BHRC) at Leeds. Several projects have been initiated during 2011. Most of these involve the design, synthesis and optimisation of small molecules as modulators of specific viral, cardiovascular and oncology targets, however we are also interested in the development of novel, label-free bio-screening technologies and targeted contrast imaging agents as tools to detect proteins which are causative in disease.

Selection of current projects:

1. Development of a novel anti-coagulant with minimal bleeding risk

We have identified potent and specific small molecule inhibitors of an enzyme involved in regulation of the coagulation cascade. These inhibitors have been identified by a number of complementary approaches incorporating virtual drug design, chemical synthesis, and HTS. Presently, we are optimising the inhibitors for potency, specificity and physicochemical properties using iterative optimisation *via* medicinal chemistry, virtual drug design and screening using a panel of orthogonal bioassays (project with Dr Helen Phillipou)

2. Identification of small molecule modulators of hepatitis C virus (HCV) p7 protein

The p7 viroporin has been proposed as a potential target for much needed new HCV therapies. Using rational design we have identified a number of small molecule modulators of p7 *in vitro* and in cell culture. Our present research is focussed towards optimising these 'hits' for potency, specificity and p7 genotype sensitivity. We are also determining the functional relevance of specific residues responsible for p7 channel activity (project with Dr Stephen Griffin)

3. Development and application of electrochemical microarrays for detection of small molecule–protein interactions

We are developing a small molecule electrochemical microarray for detection of protein-small molecule binding interactions. We are designing multiplexed small molecule microarrays to detect binding of proteins by electrochemical impedance. This approach constitutes a highly promising and flexible method towards the label-free detection of small molecule-protein interactions and has a number of potential therapeutic and translational applications, including micro-HTS and point of care diagnostic (project with Dr Steve Johnson)

4. Identification of novel small modulators of parkin activity as a treatment for Parkinson's disease

Parkin is an ubiquitin-protein ligase mutated in Autosomal Recessive - Juvenile Parkinsonism. We are using a series of rational approaches towards the identification of small molecule modulators of parkin activity in cell culture. Such molecules may offer a potential treatment for Parkinson's disease and other degenerative neurological conditions (project with Dr Phil Robinson)

5. Identification of small molecule modulators of TRP ion channels

We are adopting various approaches to the identification of small molecule modulators of various TRP channels using high-throughput screening and virtual drug design as a basis for 'hit' identification. Various inhibitor classes have been identified against various ion channels with significant sub-type specificity. The agents are being optimised for potency towards the possible treatment of various cardiovascular diseases (project with Prof David Beech)

6. Development of diversity-enriched screening libraries

We are using bespoke algorithms to identify accessible screening compounds with highly embedded diversity for incorporation into screening sets for HTS and for the generation of extensive virtual screening libraries. These bespoke, targeted collections will provide a rich source of small molecule ligands for future hit identification and development against an array of protein target classes.

Funding

This work was funded by the MRC, Parkinson's UK, CRUK and BHRC

Collaborators

Collaborators on the above projects: S. Griffin, H. Phillipou, R. Ariens, P. Robinson, E. Morrison, S. Johnson, D. Beech, L.-J. Jiang, Rao

Structure-guided drug design leads to highly potent inhibitors of the hepatitis C virus p7 ion channel

Toshana Foster, Arnout Kalverda, Gary S. Thompson, Joseph Thompson, Amy Barker, Arwen Pearson, David Rowlands, Steven Homans, Mark Harris, Richard Foster and Stephen Griffin

Introduction

Hepatitis C virus (HCV) infects over 170 million individuals, causing severe liver disease, and is the leading cause of liver cancer in the developed world. Current interferon-based therapy for HCV is inadequate and a new era of combination therapy with direct-acting antivirals (DAA) is fast approaching. We first discovered that the HCV p7 protein functions as a virus-coded ion channel, or "viroporin". Blocking p7 activity with prototype small molecule inhibitors prevented the production of infectious HCV particles. However, prototypes lack potency and are in need of significant improvement for drug development.

Results

We have undertaken a rational approach to developing novel p7-targeted compounds. Previous studies utilising *de novo* models had identified a peripheral binding site for adamantane class p7 inhibitors, validated through the identification of a specific resistance mutant, L20F.

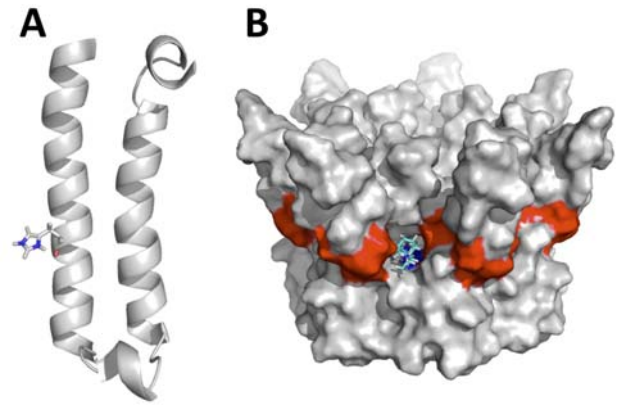

Figure 1: monomeric p7 NMR structure and structure-guided model of the p7 channel complex. **(a)** NOE-restrained solution structure generated from monomeric p7 protein in methanol. Hairpin confirmed by both PRE experiments and >60 long range NOEs. **(b)** channel model showing rimantadine docked into peripheral binding site. Relevant rimantadine-induced chemical shift changes shown in red.

Here, we solved the solution structure for monomeric p7 revealing a distinctive hairpin helical fold, validated by drug-specific chemical shift changes at the adamantane peripheral binding site absent for the L20F mutant. A structure-guided model of the heptameric p7 channel complex was then generated, where the peripheral binding site was clearly evident.

In silico screening of >250K compounds generated Lipinski-compliant molecules with high predicted binding affinities for the adamantane site. Several hits displayed nanomolar IC_{50} both *in vitro* and in virus culture, representing a significant (1000-fold) improvement over adamantanes. Structure-activity relationship studies led to yet further improved compounds, with IC_{50} <100 nM and activity against multiple HCV strains. Such inhibitor series represent significant progress towards identifying lead candidates for HCV drug development.

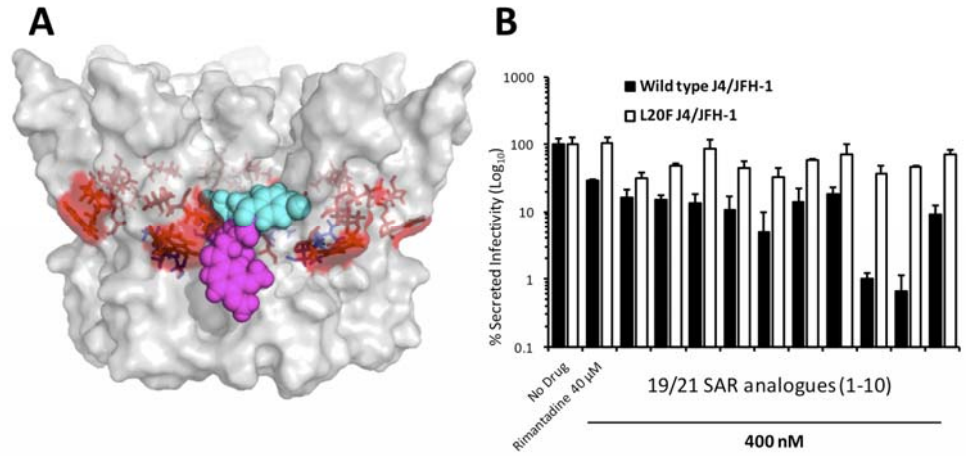

Figure 2: novel inhibitors of p7 channels. **(a)** channel model showing binding modes for initial hit compounds 19 and 21 (structures disguised for IP protection). **(b)** HCV infectious titres for wild-type and L20F viruses in the presence of 400 nM SAR analogues compared with the adamantine compound, rimantadine at 40 μM. Reversal of inhibition confirms compound specificity for adamantine site.

Publications

Foster, T Verow, M., Wozniak, A., Bentham, M., Thompson, J., Atkins, E., Weinman, S., Fishwick, C., Foster, R., Harris, M. & Griffin, H. (2011) Resistance mutations define specific antiviral effects for inhibitors of the hepatitis C virus (HCV) p7 ion channel. *Hepatology* **54:**79-90**.**

Ilett, E., Bárcena, M., Errington-Mais, F., Griffin, S., Harrington, K., Pandha, H., Coffey, M., Selby, P., Limpens, R., Mommaas, M., Hoeben, R., Vile, R. & Melcher, A. (2011) Internalization of Oncolytic Reovirus by Human Dendritic Cell Carriers Protects the Virus from Neutralization. *Clin. Cancer Res.* **17:**2767-2776.

Nandasoma, U., McCormick, C., Griffin, S. & Harris, M. (2011) Nucleotide requirements at positions +1 to +4 for the initiation of hepatitis C virus positive-strand RNA synthesis. *J. Gen. Virol.* **92:**1082-6.

Tedbury, P., Welbourn, S., Pause, A., King, B., Griffin, S. & Harris, M. (2011) The sub-cellular localisation of the hepatitis C virus non-structural protein NS2 is regulated by an ion channel-independent function of the p7 protein. *J. Gen. Virol.* **92:**819-30.

Funding

We gratefully acknowledge funding from YCR, CRUK, the LTHT Charitable Trust and the UoL Biomedical Health Research Centre.

Collaborators

External: Weinman (Kansas), Russell (Newfoundland), Gretch (Seattle), Yu (GSK), Hyser (Houston), Rose (NIBSC), Barclay (Imperial), Tuthill (IAH Pirbright), McCormick (Southampton), Targett-Adams (Medivir).
Leeds: Foster, Harris, Melcher, Macdonald, Rowlands, Cook, Fishwick, Homans, Barr, Tomlinson, Speirs.

High performance computer simulations of biomacromolecules

Sarah Harris

Introduction

Computational models have huge potential to provide insight into molecular biology by providing detailed animations of biomolecules and their interactions. In principle, these simulations act as a "computational microscope", so long as the results that are obtained can be validated against experimental data. Molecular simulation can show how the shapes of biomolecules change due to their thermal motion, how the structure of individual biomolecules is affected by subjecting them to mechanical stress and the possible biological consequences conformational diversity. However, the computational expense of the calculations, which require high performance supercomputer facilities, places serious limitations on the length and time-scales that can be accessed.

Results

Most recently, we have used atomistic molecular dynamics (MD) simulations of DNA minicircles to show how supercoiling can lead to writhing and local denaturation of the DNA, and have compared the results of simulations performed with implicit and explicit water models. We have used atomistic simulation of amyloid fibrils to aid in the interpretation of biochemical data, and we have also used steered molecular dynamics simulations of amyloid fibrils to show that their mechanical strength is dominated by the presence of defects. We are now developing a novel modelling algorithm which will enable us to model proteins at the mesoscale, in addition to at the fully atomistic level.

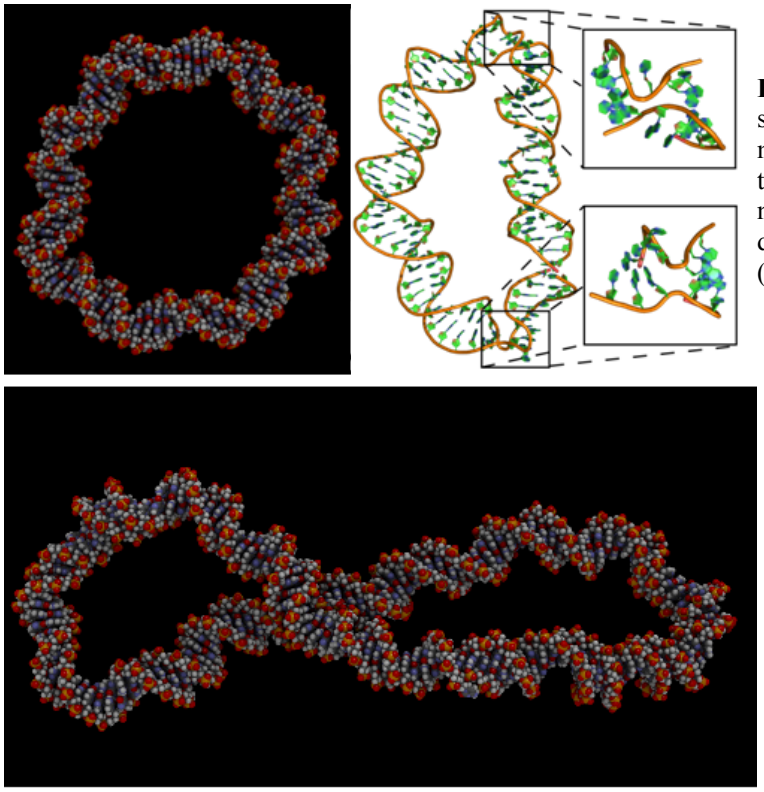

Figure 1: MD simulations of supercoiled DNA. A relaxed DNA minicircle remains circular after long timescale MD (top left), whereas a negatively supercoiled circle either denatures (top right) or writhes (bottom) depending on its size.

Publications

Berryman, J., Radford, S. & Harris, S. (2011) A systematic examination of polymorphism in amyloid fibrils by molecular dynamics simulation. *Biophys. J.* **100:**2234-2242.

Mitchell, J., Laughton, C. & Harris, S. (2011) Atomistic simulations reveal kinks, bubbles and wrinkles in supercoiled DNA. *Nucleic Acids Res.* **39:**3928-3938.

Funding

We would like to thank the BBSRC and EPSRC for funding. We thank the UK National Grid service and the ARC1 and HECToR teams for computational resources and support.

Collaborators

External: J. Harding (Sheffield), C. Laughton (University of Nottingham), E. Hyde (University of Birmingham), T. Maxwell (John Innes Centre, Norwich), A. Bates (University of Liverpool), L. Zechiedrich (Baylor College of Medicine, Texas), P. van der Schoot, A. Lyulin (Eindhoven University of Technology), A. Voityuk (University of Girona), S. Homans (University of Newcastle), S. Levene (University of Texas in Dallas), E. Snell (Hauptman-Woodward Medical Research Institute, Buffalo), G. Weber (University of Minas Gervais, Brazil), E. Drigo Filho (Universidade Estadual Paulista, Sao Paulo), D. Mulvihill (University of Kent), J. Sponer (Masaryk University, Czech republic) and J. Maddocks (Swiss Federal Institute of Technology, Lausanne).

Leeds: D. Read and O. Harlen (Maths), A. Scott (Engineering), M. Hardie and Julie Fisher (Chemistry). Within the Astbury Centre we are collaborating with S. Radford, A. Ashcroft, P. Stockley, A. Pearson, S. Warriner, N. Thomson, N. Stonehouse, E. Edwards, P. Olmsted, S. Burgess, J. Trinick, P. Knight and B. Turnbull.

Novel ligands for the Na^+-hydantoin membrane transport protein, Mhp1

Scott Jackson, Katie Simmons, Simon Patching, Ekaterina Ivanova, David Sharples, Jocelyn Baldwin, Stephen Baldwin, Colin Fishwick, Peter Johnson and Peter Henderson

Introduction

The Na^+-hydantoin membrane transport protein, Mhp1, is a member of the nucleobase-cation-symport, NCS1, family of secondary transport proteins (Figure 1). It is the first secondary active transport protein for which crystal structures of outward-open, occluded and inward-open conformations are all available, providing a structural basis for the alternating access mechanism of membrane transport. Transport proteins with a similar structural fold play important roles in human physiology. We describe the outcomes of a collaboration to design, synthesise and evaluate new ligands for the Mhp1 protein. Comparison of their relative effectiveness yields insights into the origins of specificity and molecular mechanism of the transport process.

Results

Starting from the coordinates of a novel closed structure of Mhp1 containing bound indolylmethylhydantoin (IMH), chemists at Leeds have employed *in silico* design and screening to devise a prioritised list of compounds likely to bind to Mhp1. Some of these are commercially available and some have been synthesized. Over 60 compounds have then been screened for their ability to inhibit the transport of radioisotope-labelled IMH and ranked in order of their effectiveness (Figure 1).

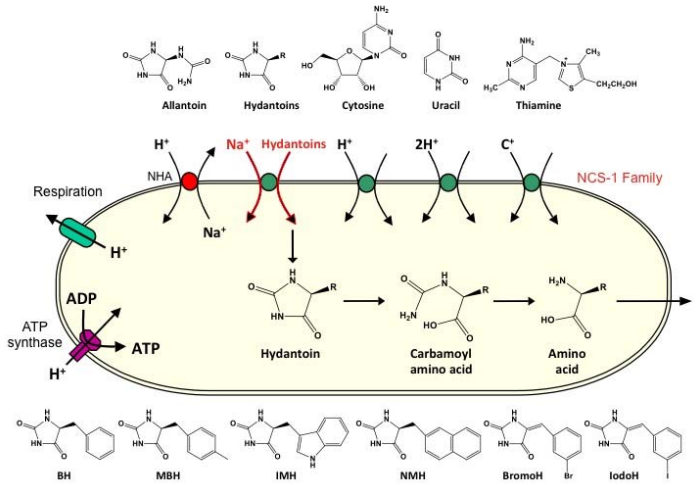

Figure 1: scheme for the energised transport of substrates by the NCS-1 family proteins. The large oval represents the cytoplasmic membrane of a microorganism. In bacteria a transmembrane electrochemical gradient of protons is generated by respiration or ATP hydrolysis, as shown on the left. The gradient may be used to drive proton/sodium antiport, sodium-nutrient symport, and substrate/substrate antiport secondary active transport systems NCS-1 family members are shown along the top. Each is a single protein indicated by a circle with its substrate's structure above. The metabolic pathway for hydantoins is illustrated in the cytoplasm. Underneath are structures and abbreviations for alternative ligands of the Na^+-hydantoin symporter, Mhp1, indicated in red. In higher organisms a transmembrane gradient of sodium ions would be generated by a Na^+,K^+-ATPase.

Nine of these compounds were then selected for further investigation on the basis that they bound to Mhp1 with an apparent affinity greater than that previously observed for the weakest-binding known substrate, D-benzylhydantoin. Using non-systematic names for the structures shown in Figure 2 their descending order of potency was D-=L-naphthylmethylhydantoin (NMH) > bromobenzylmethylenehydantoin (BromoH) > iodobenzylmethylenehydantoin (IH) > methylbenzylhydantoin (MBH) > D-=L-indolylmethylhydantoin (IMH) > L-benzylhydantoin (BH) > D-benzylhydantoin (BH). This order was substantiated by stop-flow spectrophotofluorimetric measurements of the binding parameters for each of the compounds.

Redetermination of crystal structures of Mhp1 in complex with D,L-NMH, bromoH, iodoH, or L-BH showed the ligands in poses consistent with location of the hydantoin moiety in an aromatic 'cage' provided by two tryptophan residues Trp117 and Trp220 with possible H-bonds to neighbouring protein Gln/Asn residues. In addition, the increasing bulky and hydrophobic substituents were comfortably accommodated in an adjacent hydrophobic cavity allowing for introduction of the extra halogens in a side pocket. The positions of the halogens were particularly clear in the electron density maps. Single residue mutations in residues surrounding the ligand binding site and their effects on the binding of ligands have been characterised.

The L- and D-indolylmethylhydantoins were themselves crystallised and their Xray structures shown to fit well into the pose suggested in the crystal structure of the IMH-Mhp1 complex. Molecular dynamics simulations of solution structures of L-IMH, L-NMH, D-NMH, L-BH, and D-BH revealed alternative stable poses of these molecules in solution, at least one of which in each case was sufficiently abundant to authenticate the validity of the pose modelled in to the protein binding site.

Two of the new crystal structures showed a novel conformation of Mhp1 in which the ligand was bound but the external gate remained open. All these data are revealing the nature of ligand recognition and the molecular mechanism of transport of the Mhp1 hydantoin transport protein.

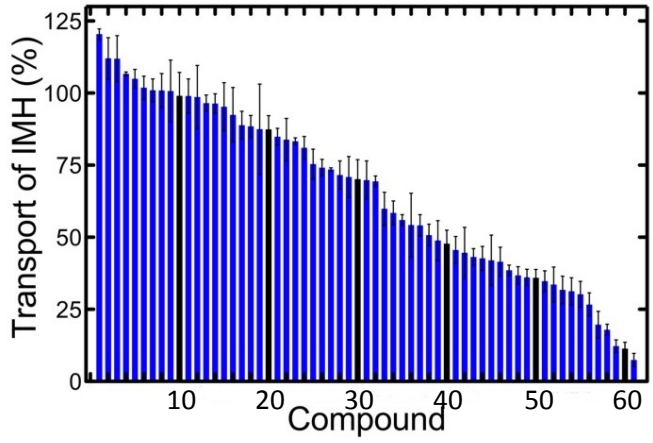

Figure 2: potency of all compounds assayed by inhibition of IMH transport. *E. coli* BL21 cells were grown and expression of the Mhp1 protein was induced before washing and resuspension in 150 mM NaCl, 5 mM NaCl MES . L-[2-^{14}C]indolylmethylhydantoin (50 μM final concentration) was added and its uptake measured after 15 sec and 2 minutes in the absence or presence of 500 μM unlabeled competing compound added 3 minutes beforehand. At least triplicate measurements were made using at least two batches of cells. Only results from the 15 sec time points are represented here. The identities of the numbered compounds may be obtained from the authors.

Publications

Bill, R., Henderson, P., Iwata, S., Kunji, E. Michel, H., Neutze, R., Newstead S., Poolman, B., Tate, C. & Vogel, H. (2011) Overcoming barriers to membrane protein structure determination. *Nat. Biotechnol.* **29:**335-340.

Robichaud, T., Appleyard , A., Herbert, R., Henderson, P. & Carruthers, A. (2011) Determinants of ligand binding affinity and cooperativity at the GLUT1 endofacial site. *Biochemistry* **50:**3137-3148.

Funding

BBSRC and the EU EDICT consortium.

Collaborators

A. Cameron, S. Iwata, T. Shimamura and S. Weyand (Diamond Light Source and Imperial College London. O. Beckstein and M. Sansom (University of Oxford).

Deuteration of solid-state NMR samples for structural measurements with weakly-binding ligands and membrane proteins

Simon Patching and Peter Henderson

Introduction

Solid-state NMR is unique for its ability to observe directly the binding of ligands to membrane proteins in their native membranes or purified and reconstituted in detergent micelles or lipids. This is made possible by using an isotope-labelled ligand (usually containing ^{13}C, ^{15}N, ^{19}F or ^{31}P) with the cross-polarisation magic-angle spinning (CP-MAS) experiment. Dipolar recoupling experiments can then be used to measure ligand-protein interactions with isotope labels incorporated at specific positions in the protein or precise intra-molecular distances and torsion angles within the ligand to elucidate its protein-bound structure. These experiments are more challenging when there is a significant non-specific component to the ligand signal. For a system that has a weakly-binding (high μM to mM affinity) ligand, the principal potential source of a non-specific component comes from excess unbound ligand frozen in solution, as structural measurements are usually performed with the sample at a temperature of less than -10 ºC. We have investigated deuteration as a novel way to suppress or eliminate this non-specific signal as demonstrated with the *E. coli* sugar transport protein GalP and its substrate D-glucose.

Results

The principle of our approach for using deuteration to eliminate the non-specific components of ligand signals from CP-MAS solid-state NMR spectra is outlined in Figure 1 for a membrane protein sample with a ^{13}C-labelled ligand. **A.** Shows the pulse sequence for a ^{1}H-^{13}C cross-polarisation experiment, which transfers magnetisation from ^{1}H nuclei to nearby ^{13}C nuclei and then the magnetisation on ^{13}C nuclei is detected to give signals in the ^{13}C spectrum. **B.** Shows the potential sources of ^{1}H-^{13}C CP interactions that can contribute to the observed ligand signal when a ^{13}C-labelled ligand is used with a membrane sample in H_2O. The main sources of ^{1}H magnetisation are: (i) ^{1}H in the ligand backbone; (ii) ^{1}H in ligand hydroxyl groups (or other exchangeable groups); (iii) ^{1}H in water molecules that are frozen/immobilised (non-specific); (iv) protein non-exchangeable ^{1}H (specific binding); (v) protein exchangeable ^{1}H (specific binding); (vi) membrane non-exchangeable ^{1}H (non-specific) and (vii) membrane exchangeable ^{1}H (non-specific). **C.** Shows how the majority of

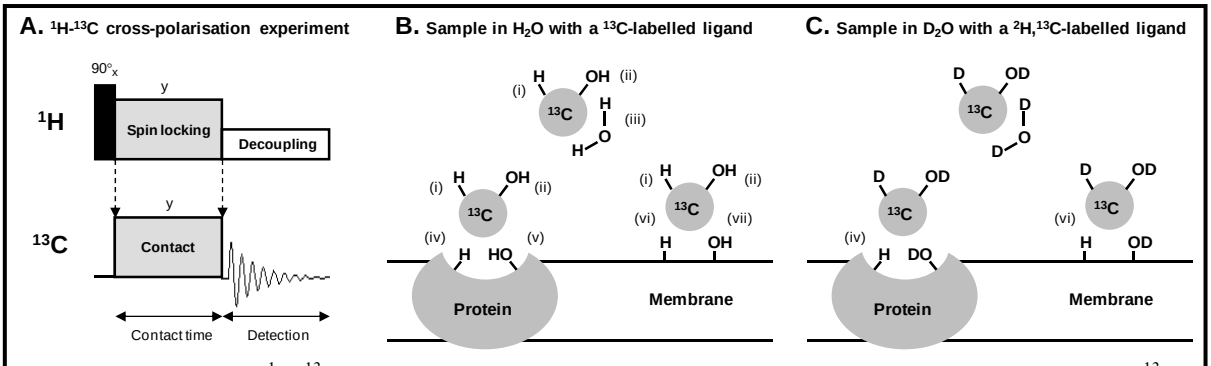

Figure 1: sources of ^{1}H-^{13}C CP interactions that can contribute to the signal for a weakly-binding ^{13}C-labelled ligand in a membrane protein sample under frozen conditions using solid-state NMR (see text above for details).

the ^{1}H-^{13}C pathways that can contribute a non-specific component to the ligand signal can be eliminated with the sample in D_2O and using a ^{2}H,^{13}C-labelled ligand. Notably this step includes removal of the interactions associated with unbound ligand.

We have investigated this experimentally by performing ^{1}H-^{13}C CP-MAS NMR measurements at a temperature of -15 ºC on samples of *E. coli* inner membranes containing the sugar transport protein GalP with its substrate D-glucose. This work has used samples in both H_2O and D_2O, using both D-[$^{13}C_6$]glucose and D-[$^{2}H_7$,$^{13}C_6$]glucose, and the GalP inhibitor forskolin (example spectra are shown in Figure 2). We have also performed 2D ^{13}C-^{13}C DARR and ^{1}H-^{13}C HETCOR dipolar recoupling experiments using these novel sample conditions.

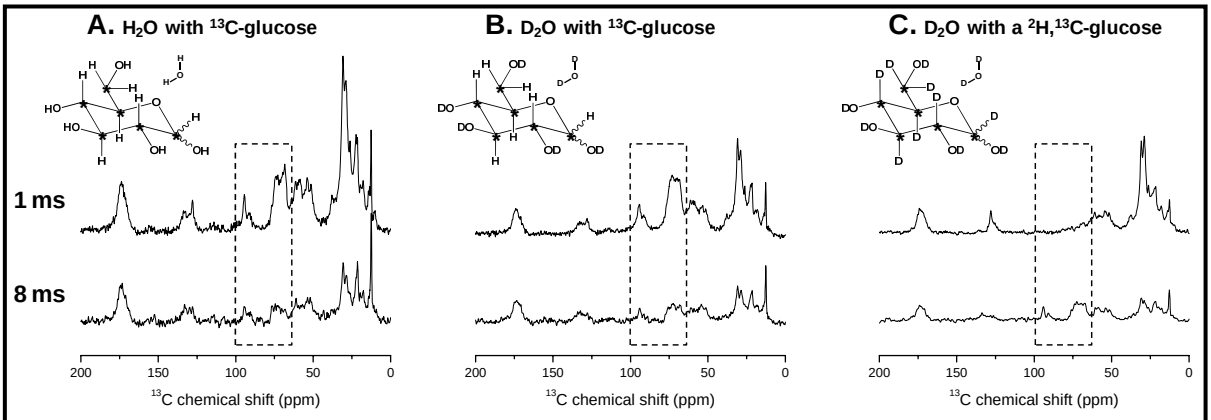

Figure 2: ^{13}C CP-MAS solid-state NMR spectra of *E. coli* inner membranes containing the sugar transport protein GalP and its substrate D-glucose at -15 ºC. **A.** is a sample in H_2O with D-[$^{13}C_6$]glucose. **B.** is a sample in D_2O with D-[$^{13}C_6$]glucose. **C.** is a sample in D_2O with D-[$^{2}H_7$,$^{13}C_6$]glucose. Spectra were acquired using CP contact times of both 1 ms and 8 ms. The dashed boxes highlight the signals for ^{13}C labels in D-glucose.

Publications

This work is being written up for publication.

Funding

This work was funded by grants from the EPSRC (EP/G035695/1) and the EU EDICT Consortium (contract FP7 201924).

Collaborators

This work was performed in collaboration with David Middleton at the University of Liverpool.

Investigating β_2m-amyloid associated cytotoxicity in primary monocytes and osteoarticular cells

Morwenna Porter, Katy Routledge, Sheena Radford and Eric Hewitt

Introduction

The formation of insoluble amyloid fibrils underlies a number of human diseases, many of which are characterised by cell loss and tissue damage. One such disease is dialysis-related amyloidosis (DRA), a debilitating osteoarticular disorder that affects patients on long-term haemodialysis. β_2-microglubulin (β_2m) is the non-covalent light-chain of cell surface major histocompatibility complex (MHC) class I molecules. Upon dissociation from MHC molecules, β_2m is normally degraded and excreted by the kidneys, however in patients with renal failure, neither the kidneys nor the dialysis membrane can remove β_2m and serum levels become highly elevated. At these concentrations β_2m forms amyloid deposits in the joints, which result in progressive bone and joint destruction. Whilst the mechanisms of amyloid formation have been well characterized, the cellular mechanisms by which amyloid deposition results in osteoarticular damage are unknown. We investigated the effect of β_2m-amyloid on primary human cells present in joints of subjects with DRA and found that amyloid-associated cytotoxicity is likely to be a major factor in bone and cartilage damage in DRA.

Characterizing the response of primary cells to β_2-microglobulin monomer and fibrils

Phagocytic macrophages infiltrate DRA joints and have been hypothesized to play a protective role in degrading amyloid deposits. However we found that primary human

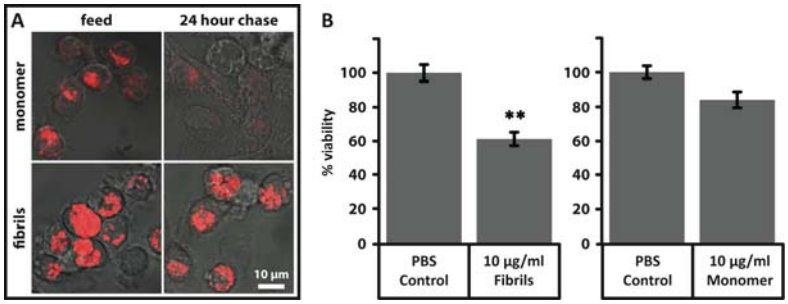

Figure 1: (a) Monocytes were incubated with TMR labelled monomer/fibrils (red) for 24 hours, washed, and degradation of internalized protein assessed after 24 hours. Monocytes degraded monomer but not fibrils. **(b)** monocytes were treated with fibrils/monomer for 24 hours and their effects on viability assessed using the MTT assay. Error bars represent SEM; ** =P≤0.001. Fibrils decreased monocyte viability.

macrophages, derived from peripheral blood monocytes, were unable to degrade β_2m-amyloid, and that this may be due in part to the cytotoxicity of β_2m-amyloid to these cells (figure 1). This explains why macrophages that infiltrate DRA amyloid deposits fail to halt the accumulation of β_2m-amyloid in the joints and allow the disease to progress

DRA is associated with the destruction of cartilage, and the weakening of bone leading to pathological bone cysts and fractures. We, therefore, investigated the effect of β_2m-amyloid on the cells that remodel bone (bone forming osteoblasts and bone resorbing osteoclasts) and make cartilage (chondrocytes).

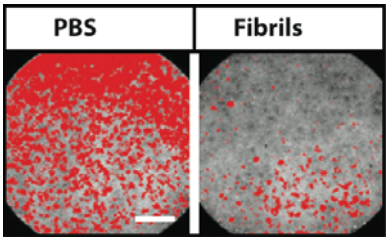

Figure 2: monocytic precursors were incubated on an artificial bone substrate, in the presence/absence of fibrils for 21 days. Resorption of the substrate, indicative of osteoclast activity, was then assessed. Resorbed areas are shown in red. Decreased resorption occurs in the presence of fibrils.

Osteoclasts, like macrophages, are derived from monocytic precursors and the cytotoxicity of β_2m-amyloid to this cell lineage may therefore be predicted to decrease osteoclast formation. Indeed, we found differentiation of monocytic precursors into functional osteoclasts is drastically reduced in the presence of β_2m-amyloid (Figure 2). In addition we found that β_2m-amyloid is cytotoxic to both osteoblasts and chondrocytes (Figure 3). Together these findings suggest a direct role for β_2m-amyloid toxicity in the disruption of normal bone homeostasis leading to decreased bone turnover and weakening of this tissue, as well as in the destruction of cartilage.

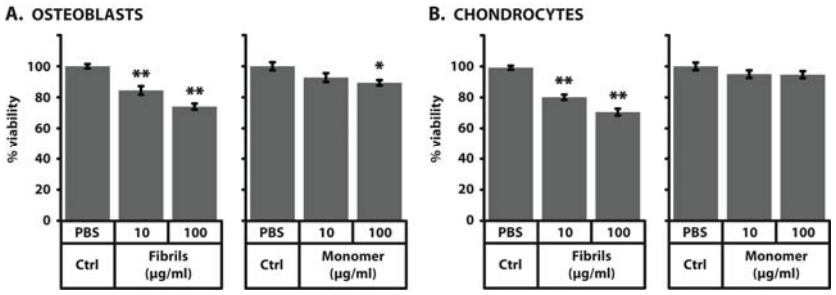

Figure 3: osteoblasts and chondrocytes were treated with fibrils/monomer for 24 hours and their effects on viability assessed using the MTT assay. Error bars represent the SEM; * =P≤0.01; ** =P≤0.001. Fibrils significantly decreased the viability of osteoblasts and chondrocytes.

In summary our findings provide new insights into how the joints are damaged in dialysis patients and provide a foundation for new research into the treatment of this debilitating disorder.

Publications

Porter, M., Routledge, K., Radford, S. & Hewitt, E. (2011) Characterization of the response of primary cells relevant to dialysis-related amyloidosis to β_2-microglobulin monomer and fibrils. *PLoS One* **DOI:** 10.1371/journal.pone.0027353.

Funding

We are grateful to the Yorkshire Kidney Research Fund for financial support.

TROSY solution-state NMR with a large α-helical membrane protein

Simon Patching, Arnout Kalverda, James Gowdy, Peter Henderson and Steve Homans

Introduction

Structure-determination with large α-helical membrane proteins by solution-state NMR spectroscopy is very challenging. The main challenges that have to be overcome before applying NMR experiments for structural measurements are as follows: **(i) Expression** - a suitable expression system that will produce milligram quantities of protein. **(ii) Purification and reconstitution** - a purification protocol that achieves milligram quantities of highly-pure protein reconstituted in a membrane mimetic that retains the native structure and function of the protein and that is compatible with NMR experiments. **(iii) Achieving high-resolution NMR spectra** - a prerequisite to applying experiments for assignment of signals and for solving structure. **(iv) Isotope labelling** - NMR-observable isotopes (usually ^{13}C and/or ^{15}N) have to be incorporated into the protein, uniformly or into specific amino acids, often combined with deuteration. **(v) Stability** - the NMR experiments are usually performed with the sample at a temperature of ≥ 20 ºC; the protein has to be stable at this temperature over days to weeks of NMR acquisition time.

For several years we have been developing labelling and sample preparation strategies to achieve high-resolution solution-state NMR spectra of the 12-helix (464 residues, 52 kDa) *E. coli* sugar transporter GalP, which is homologous with the human glucose transporter GLUT1, and is an ideal system to make significant progress on large systems. We have now shown that this is possible by combining selective amino acid labelling with TROSY-type NMR experiments.

Results

In its unlabelled form, we can routinely express GalP up to levels of 50% of total protein in *E. coli* inner membrane preparations, from which it can be purified with the aid of a genetically-engineered C-terminal His-tag to give protein yields of up to 10 mg/litre. This is a good starting point for applying isotope-labelling strategies, which can have a significant effect on lowering protein yield. We have now developed labelling and sample preparation methods with GalP that have allowed successful acquisition of both [^{15}N-^{1}H]-TROSY and [^{13}C-^{1}H]-methyl-TROSY spectra of the protein reconstituted in DDM detergent micelles. Examples are shown below.

[^{15}N-^{1}H]-TROSY spectra of [$^{15}N_2$]tryptophan-labelled GalP. The twelve tryptophan residues in GalP were selectively labelled with ^{15}N combined with uniform deuteration by expression using a tryptophan-auxotrophic host strain of *E. coli* combined with a modified minimal medium that contained [U-^{2}H,$^{15}N_2$]-*L*-tryptophan and [U-^{2}H]-*D*-glucose in D_2O. The protein was purified in the presence of [U-^{2}H]glycerol and reconstituted into [^{2}H]DDM micelles. [^{15}N-^{1}H]-TROSY spectra of the [U-^{2}H,$^{15}N_2$-Trp]GalP sample acquired on a 900 MHz NMR magnet at 25 ºC produced signals from both the side-chain and backbone positions of tryptophan residues in the protein (Figure 1).

[^{13}C-^{1}H]-methyl-TROSY spectra of [^{13}C-ILV]-labelled GalP. The methyl groups of isoleucine, leucine and valine residues of GalP were selectively labelled with ^{1}H,^{13}C combined with uniform deuteration and ^{15}N-labelling (specifically [U-^{2}H, U-^{15}N, Ile-$^{13}CH_3$, Leu/Val-$^{13}CH_3$,$^{12}CD_3$]GalP) by expression in *E. coli* using a modified minimal medium that contained ^{1}H,^{13}C-labelled precursors to Ile/Leu/Val residues, [U-^{2}H]-*D*-glucose and [^{15}N]ammonium chloride in D_2O. The protein was purified in the presence of [U-^{2}H]glycerol and reconstituted into DDM micelles. [^{13}C-^{1}H]-methyl-TROSY spectra of the [^{13}C-ILV]-

labelled GalP sample acquired on a 750 MHz NMR magnet at 20 ºC showed that we can detect and resolve signals that represent ~ 25-30 out of 36 Ile residues and ~ 60 out of 60 + 34 Leu and Val residues (Figure 2).

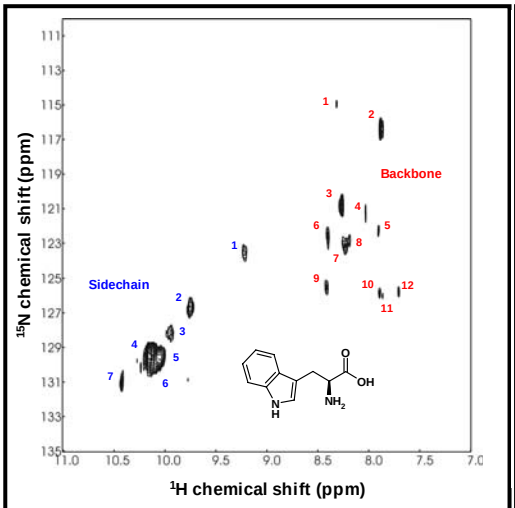

Figure 1: [^{15}N-^{1}H]-TROSY spectrum of [U-^{2}H,^{15}N$_2$-Trp]GalP in [^{2}H]DDM micelles at 25°C. Acquired at 900 MHz at HWB-NMR.

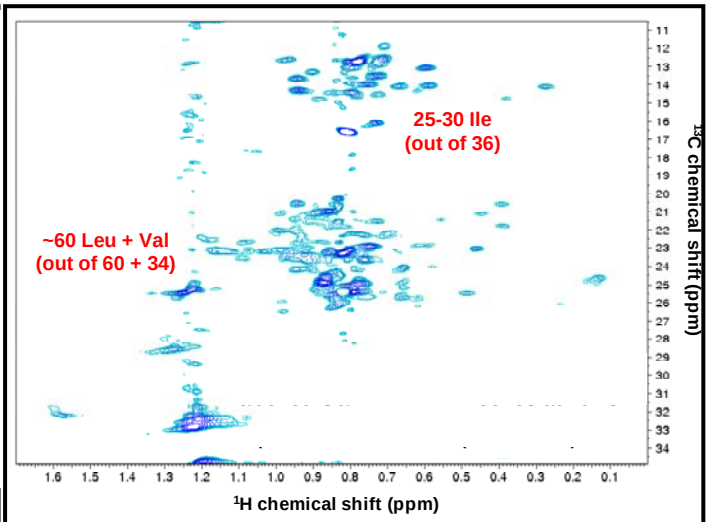

Figure 2: [^{13}C-^{1}H]-methyl-TROSY spectrum of ILV-labelled GalP in DDM micelles at 20°C. Acquired at 750 MHz at Leeds over 17 hours.

We are currently investigating the effects of inhibitors of GalP (forskolin and cytochalasin B) on the spectra and acquiring [^{13}C-^{1}H]-methyl-TROSY spectra on a higher field magnet (900 MHz).

Funding

This work was funded by grants from the EPSRC (EP/G035695/1) and the EU EDICT Consortium (contract FP7 201924).

Role of prion protein in the production and mechanism of action of amyloid-β oligomers in Alzheimer's disease

Lizzie Glennon, Heledd Griffiths, Kate Kellett, Harry King, Jo Rushworth, Andrew Tennant, Nicole Watt, Isobel Whitehouse and Nigel Hooper

Introduction

Alzheimer's disease (AD) is the commonest neurodegenerative disease of old age. Currently, there are no drugs available to halt or slow the progression of this devastating disease which is placing a huge burden on patients and carers. AD is characterised by the deposition in the brain of senile plaques that are composed of the amyloid-β peptide (Aβ). Through mechanisms that are poorly understood, Aβ oligomers, fibrils and/or aggregates are toxic to nerve cells. Aβ is derived from the larger transmembrane amyloid precursor protein (APP) through proteolytic cleavage by the β- and γ-secretases. The β-secretase (BACE1) cleaves within the APP sequence at the N-terminus of the Aβ peptide, with the γ-secretase complex cleaving the resulting membrane-bound stub at the C-terminus of the Aβ sequence.

The prion protein is probably best known for its role in the transmissible spongiform encephalopathies or prion diseases, such as Creutzfeldt-Jakob disease in humans and bovine spongiform encephalopathy in cattle. In these diseases the normal cellular form of the prion protein (PrP^{C}) undergoes a conformational conversion to the infectious form, PrP^{Sc}. We have shown that PrP^{C} inhibits the β-secretase cleavage of APP, lowering the amount of Aβ produced and, therefore, potentially protecting against AD. More recently, PrP^{C} was identified as a high affinity receptor for Aβ oligomers.

Regulation of Aβ production by prion protein

Cleavage of APP by the β-secretase BACE1 is the rate-limiting step in the production of Aβ. We reported previously that PrP^{C} inhibited the action of BACE1 towards wild type human APP (APP_{WT}) in cellular models and that the levels of endogenous murine Aβ were significantly increased in PrP^{C} null mice brain. We have investigated the molecular and cellular mechanisms underlying this observation. Through the use of recombinant proteins in ELISA and surface plasmon resonance experiments, along with the expression of mutants of BACE1 in cells, we found that PrP^{C} interacted directly with the pro-domain of the immature Golgi-localised form of BACE1. By monitoring BACE1 localisation in cells by confocal immunofluorescence microscopy and FACS, we found that this interaction decreased BACE1 at the cell surface and in endosomes, where it preferentially cleaves APP_{WT}, but increased it in the Golgi, where it preferentially cleaves APP with the Swedish mutation (APP_{Swe}). In transgenic mice expressing human APP with the Swedish familial AD mutation, PrP^{C} deletion had no influence on APP proteolytic processing, Aβ plaque deposition, levels of soluble Aβ or Aβ oligomers. In cells, although PrP^{C} inhibited the action of BACE1 on APP_{WT}, it did not inhibit BACE1 activity towards APP_{Swe}. The differential subcellular location of the BACE1 cleavage of APP_{Swe} (in the Golgi) relative to APP_{WT} (in endosomes) provides an explanation for the failure of PrP^{C} deletion to affect Aβ accumulation in APP_{Swe} mice. Thus, while PrP^{C} exerts no control on cleavage of APP_{Swe} by BACE1, it has a profound influence on the cleavage of APP_{WT}.

Regulation of Aβ toxicity by the prion protein

Soluble Aβ oligomers are one of the major culprits responsible for the neurodegeneration observed in AD but the mechanisms underlying this toxicity remain elusive. Various proteins have been identified as potential receptors for Aβ oligomers, including AMPA, NMDA, mGluR5 and α-7-nicotinic acetylcholine receptors. In addition, the GPI-anchored PrP^{C} was

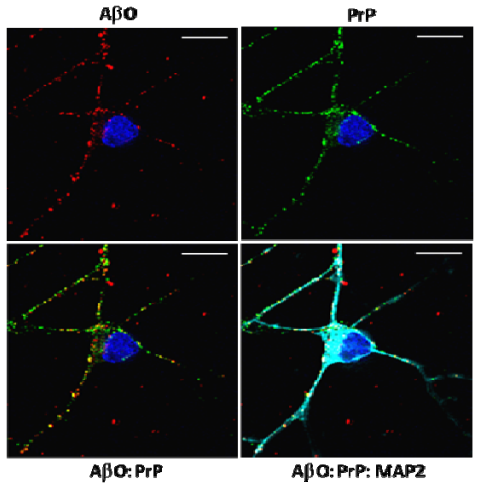

Figure 1: Binding of Aβ oligomers (AβO) to rat primary hippocampal neurons expressing PrP^C (PrP).

identified as a cell surface receptor for Aβ oligomers mediating their synaptotoxicity. Other studies have confirmed this, although the role of PrP^C in mediating Aβ neurotoxicity is controversial. Reasons for these conflicting results include the use of different and often poorly characterized preparations of oligomers, different toxicity measurements on divergent target cell populations under different conditions, and the use of different transgenic AD mouse models. It has been hypothesized that a putative PrP^C-associated transmembrane co-receptor may have a central role in mediating the effects of Aβ oligomers. We have confirmed that PrP^C is the major cell surface receptor for Aβ oligomers on neuronal cells (Fig. 1) and have identified that the transmembrane low-density lipoprotein receptor related protein 1 (LRP1) is required for both the cytotoxicity and endocytosis of Aβ oligomers following their binding to PrP^C.

Publications

Griffiths, H., Whitehouse, I., Baybutt, H., Brown, D., Kellett, K., Jackson, C., Turner, A., Piccardo, P., Manson, J. & Hooper, N. (2011) Prion protein interacts with BACE1 protein and differentially regulates its activity toward wild type and swedish mutant amyloid precursor protein. *J. Biol. Chem.* **286:**33489-33500.

Kellett, K., Williams, J., Vardy, E., Smith, D. & Hooper, N. (2011) Plasma alkaline phosphatase is elevated in Alzheimer's disease and inversely correlates with cognitive function. *Int. J. Mol. Epidemiol. Genet.* **2:**114-121.

Funding

This work was funded by the MRC, Wellcome Trust, Alzheimer's Research UK and BBSRC.

Collaborators

Tony Turner, Colin Fishwick, Chris Peers.

Novel spectroelectrochemical methods to study redox enzymes

Nikolaos Daskalakis, Lukasz Krzeminksi, Steve Evans, Peter Henderson and Lars Jeuken

Introduction

An overwhelming number of chemical reactions in nature, both in the living cell and in the inanimate world, are redox reactions. In biology, these reactions are catalysed by redox enzymes, many of which reside in the lipid membrane. Redox enzymes play a major role in almost all metabolic processes, including photosynthesis and biochemical processes such as the nitrogen cycle. By electrically connecting redox enzymes to electrodes, a powerful sensing platform is constructed that is able to characterise details of the catalytic mechanism of these enzymes. A method we have been exploring over the last 2 years is to combine fluorescence spectroscopy with electrochemistry. The fluorescence is used to monitor conditions such as pH or the redox state of a metal site in a multi-centre enzyme and the electrochemistry directly reports on the turn-over rate of the enzyme.

Proton-pumping enzymes

Two novel spectroelectrochemical approaches have been reported by us in 2011. In the first, surface adsorbed vesicles were used to study a proton-pumping enzyme, cytochrome bo_3, which is a terminal oxidase and proton-pumping enzyme in *Escherichia coli*. Cytochrome bo_3 was reconstituted in lipid vesicles, which were subsequently 'loaded' with a pH-responsive fluorescent dye. Proton-pumping is concurrent with the oxidation of lipophylic ubiquinol to ubiquinone and the reduction of molecular oxygen to water. In our system, the membrane-bound ubiquinone is electrochemically re-reduced to ubiquinol. Thus, ultimately, a proton gradient is formed across the immobilised vesicles as schematically indicated in Figure 1. In nature, transmembrane proton gradients are formed using energy supplied by light or chemical reactions, but in our biomimetic or hybrid organic–inorganic systems we have, for the first time, shown that surface-applied electrochemical potentials can also be used as an energy source. Analysis of the spectroelectrochemical data shows that the proton pumping activity is dependent on the pH gradient formed. Using a recently obtained ERC starting grant, this research will be continued within Astbury in collaboration with Dr. Roman Tuma. Single vesicles reconstituted with (less than) one cytochrome bo_3 enzyme will be used to study the proton-pumping mechanism at the single-molecule level.

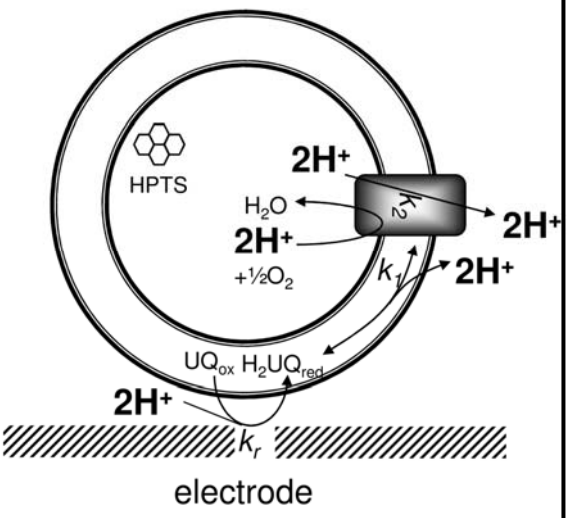

Figure 1: illustration of the experimental setup used and the four protons removed from the intravesicular compartment per 2 electrons required to reduce ubiquinone to ubiquinol. This illustration assumes a single orientation of the enzyme in the vesicles.

Copper-containing nitrite reductase

Simultaneous fluorescence and electrochemical measurements have also been applied to the study of a copper-containing enzyme, nitrite reductase (NiR). NiR is a homotrimer that contains two copper sites per monomer. One copper site (a type-1 copper site) functions solely in transferring electrons from NiR's protein partner, pseudoazurin, to the second copper (a type-2 copper site), where nitrite is reduced. Previous electrochemical studies of

NiR could not fully describe the catalytic mechanism of NiR, because the intramolecular and intermolecular (i.e., interfacial) electron transfer steps could not be resolved. The new method employed in 2011 simultaneously monitored the type-1 copper oxidation state and the nitrite turnover rate of a NiR from *Alcaligenes faecalis* S-6, thereby resolving these steps (Figure 2). The catalytic activity of NiR is measured electrochemically by exploiting a direct electron transfer to fluorescently labelled enzyme molecules immobilized on modified gold electrodes. The redox state of the type-1 copper site is determined from fluorescence intensity changes caused by Föster resonance energy transfer (FRET) between a fluorophore attached to NiR and its type-1 copper site. The homotrimeric structure of the enzyme is reflected in heterogeneous interfacial electron transfer kinetics with two monomers having a 25-fold slower kinetics than the third monomer. The intramolecular electron-transfer rate between the type-1 and type-2 copper site changes at high nitrite concentration (> 520 μM), resulting in an inhibition effect at low pH and a catalytic gain in enzyme activity at high pH. The results show that under certain conditions, the intramolecular rate is significantly reduced in turnover conditions compared to the enzyme at rest. This study provides a dire warning to previous studies in which rates are measured under non-turn over conditions (the enzyme at rest) and used to characterise the enzyme mechanism, as these rates might not reflect to true kinetics of the enzymes under turn-over conditions.

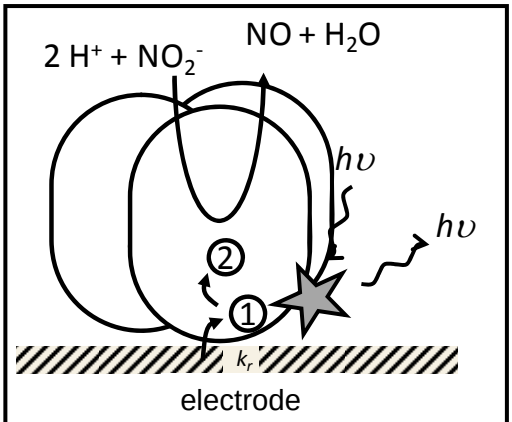

Figure 2: schematic representation of the spectroelectrochemical approach used to study NiR. The '1' and '2' represent the type-1 and type-2 copper sites, respectively. The star represents a fluorescent dye, which fluorescence is dependent on the oxidation state of the type-1 copper site.

Publications

Cheetham, M., Bramble, J., McMillan, D., Krzeminski, L., Han, X., Johnson, B., Bushby, R., Olmsted, P., Jeuken, L., Marritt, S., Butt., J & Evans, S. (2011) Concentrating membrane proteins using asymmetric traps and AC electric fields. *J. Am. Chem. Soc.* **133:**6521-6524.

Daskalakis, N., Muller, A., Evans, S. & Jeuken, L. (2011) Driving bioenergetic processes with electrodes. *Soft Matter* **7:**49 - 52.

Daskalakis, N., Evans, S. & Jeuken, L. (2011) Vesicle-modified electrodes to study proton-pumping by membrane proteins. *Electrochim. Acta* **56:**10398-10405.

Krzeminski, L., Cronin, S., Ndamba, L., Canters, G., Aartsma, T., Evans, S. & Jeuken, L. (2011) Orientational control over nitrite reductase on modified gold electrode and its effects on the interfacial electron transfer. *J. Phys. Chem B* **115:**126070-12614.

Krzeminski, L., Ndamba, L., Canters, G., Aartsma, T., Evans, S. & Jeuken, L. (2011) Spectroelectrochemical investigation of intramolecular and interfacial electron-transfer rates reveals differences between nitrite reductase at rest and during turnover. *J. Am. Chem. Soc.* **133:**15085-15093.

Funding

This work is funded by an ITN (FP6), EU (FP7), BBSRC and EPSRC.

Structural studies of the Vacuolar ATPase

Michael Harrison, Clair Phillips, John Trinick and Stephen Muench

Introduction

The vacuolar H^+-ATPase (V-ATPase) is a large transmembrane ATP driven proton pump which is essential in eukaryotic cells. It contains ~30 subunits of up to 14 different types separated into an ATP hydrolysing V_1 domain and proton translocating V_0 domain. Previous work within the group have shown that these subunits are arranged in a complex manner with the V_1 and V_0 domains containing the subunit stoichiometry A_3,B_3,C,D,E_3,F,G_3,H and a,c_{10},d,e, respectively. The AB subunits within the V_1 domain are responsible for ATP hydrolysis which drives the rotation of a central axle (subunits D,d,F) which in turn rotates the c-ring relative to the a subunit, transporting protons over the membrane. The a subunit is fixed relative to the c-ring through a complex stator network made up of subunits C,H,E,G (Figure 1a).

Miss-regulation, miss-localisation and point mutations within the V-ATPase have been shown to play a role in a number of disease states including osteopetrosis, kidney disease and Alzheimers. Structural and biochemical studies within my laboratory are focused on understanding the way in which the V-ATPase is regulated and localised within the cell and how this can be used to design novel therapeutics.

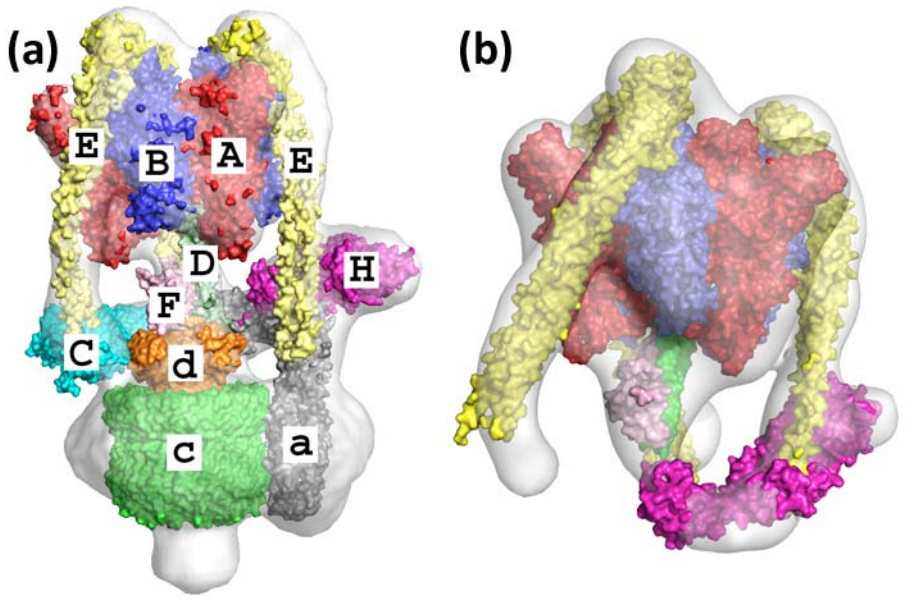

Figure 1: known crystal structures fitted within the cryo-EM reconstructions of the V-ATPase **(a)** and V_1 domain **(b)**. The subunits are coloured red, blue, cyan, light green, yellow, pink, magenta, orange, green and grey for subunits A, B, C, D, E, F, H, d, c, a, respectively. Subunit A is based on modelling data and not a known crystal structure.

Current research

Single particle electron microscopy has been used to study the structure of the V_1 domain that is isolated upon controlled dissociation of the V-ATPase. The isolated V_1 domain is unable to turnover ATP and we have been able to show a proposed mechanism of ATP silencing involving domain re-arrangements within the V_1 domain (Figure 1(b0). The isolated V_1 structure has also given us insights into the structural changes that bring about dissociation allowing us to propose a mechanism for V_1 dissociation. Understanding the mode of dissociation has important implications for the development of novel therapeutics (*e.g.*

alexidine dihydrochloride) which can turn off the V-ATPase in disease states such as invasive cancer cells and osteoporotic patients.

Mis-localisation has been shown to play a role in a number of disease states, for example Alzheimers and cutis laxis disease. The glycosylation of several V-ATPase subunits has been shown to be important in the correct localisation of the V-ATPase within the cell. By using negative stain electron microscopy and biochemical techniques we have been able to show that the V-ATPase displays significant glycosylation at the base of V_0 and that this glycosylation is likely to be on the e subunit. Moreover deglycosylation of the V-ATPase complex results in no change in activity or stability, re-enforcing the belief that this is a feature of signalling and not mechanism.

This work has been done in collaboration with Prof Wieczorek's group who provide us with *Manducca sexta* V-ATPase and some biochemical analysis.

Funding
This work was funded by the MRC and BBSRC.

Development and applications of methods for the synthesis of collections of diverse small molecules

Sushil Mauyra, Sarah Murrison, Christian Einzinger, Catherine Joce, Rebecca White, Martin Fisher, Mark Dow, Francesco Marchetti, Thomas James, Paolo Tosatti, Bruce Turnbull, Peter Stockley, Stuart Warriner and Adam Nelson

Introduction

Historically, chemists have explored chemical space in an uneven and unsystematic manner. An analysis of the scaffolds of the 25 million known cyclic small molecules (in 2008) revealed that one sixth of the compounds are based on just 30 (out of the 2.5 million) known molecular scaffolds! To address this historic uneven exploration, we have developed synthetic methods that allow the scaffolds of small molecules to be varied combinatorially and systematically. Here, we report an approach to the synthesis of skeletally-diverse small molecules that are broadly inspired by the alkaloid class of natural products.

An approach based on two three-component reactions

We have exploited two consecutive three-component reactions in the synthesis of skeletally-diverse alkaloid-like small molecules. The outcome of the reaction between amines **1**, carbonyl compounds **2** and triazines **3** depended on the substituents (Scheme 1). Following formation of a 2-aza-diene **4**, further cyclisation – to give either **5** or **6** – was observed with appropriate unsaturated substituents; further decoration with a Joullié-Ugi reaction was also possible (→ **7**, **8** or **9**). In addition, with an appropriately appended nucleophilic group, direct cyclisation to products of general structure **10** was also possible. We used this overall approach to prepare 43 alkaloid-like molecules based on 28 distinct frameworks. Crucially, each of the molecules was, in general prepared from 5 components; the substituents in these components determined the final scaffolds of each small molecule.

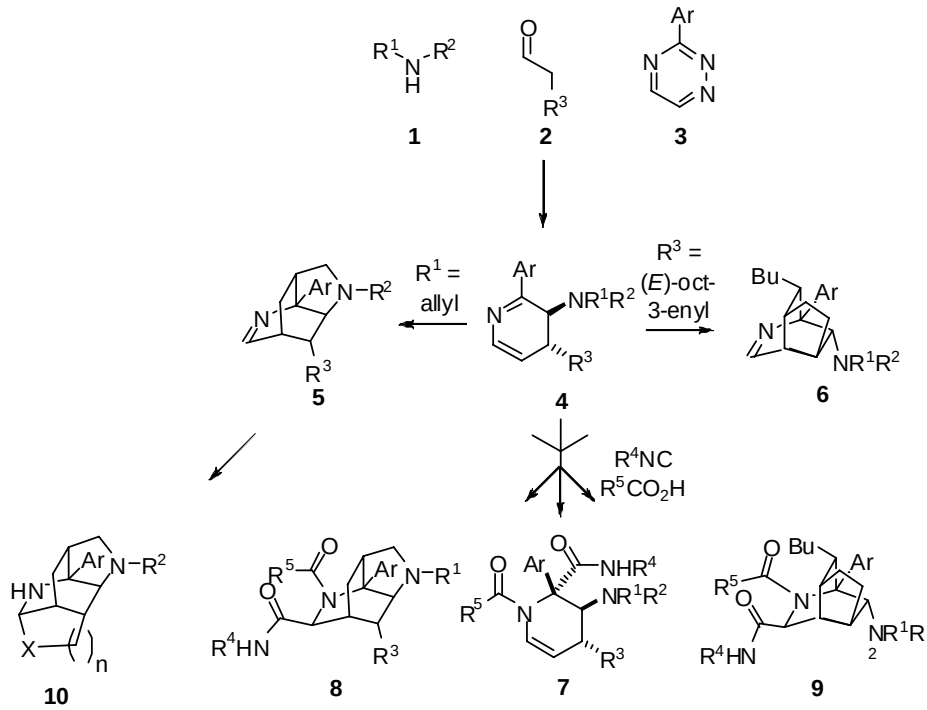

Figure 1: synthetic approaches to skeletally-diverse alkaloid-like compounds based on two three-component reactions.

Extension to lead-like chemical space
A strongly developing theme within the Nelson group is to develop diversity-oriented synthetic approaches that map onto the requirements of drug discovery programmes. Established diversity-oriented approaches have tended to focus on small molecules that lie well outside drug-like space. It is now generally accepted that attrition rates are strongly linked to molecular properties such as molecular weight, lipophilicity, the number of aromatic rings, and the fraction of sp^3-hybridised carbon atoms. Optimisation almost always leads to increases in both molecular weight and lipophilicity. So it is essential to have good starting points for optimisation, and, therefore, to control the properties of initial leads. The development of general strategies that are able to deliver skeletally diverse compounds – but within the boundaries of lead-like chemical space – is likely to be extremely demanding. But this goal is, nonetheless, an important challenge for synthetic chemists in the twenty-first century.

Summary
We have developed a range of approaches for the synthesis of skeletally-diverse small molecules. We are now exploiting these synthetic methods in the discovery and optimisation of ligands for a range of protein targets. This year, we have described bivalent bivalent *S*-adenosylmethionine (SAM) analogues that were designed to interact with the MetJ dimer in a bivalent sense. In addition, our collaborators have exploited GSK-3 inhibitors, discovered within the Nelson group, as tools for the chemically-directed differentiation of human embryonic stem cells. Further details of research within the Nelson group may be found at www.asn.leeds.ac.uk.

Publications
Bone, H., Nelson, A., Goldring, C., Tosh D. & Welham, M. (2011) A novel chemically directed route for the generation of definitive endoderm from human embryonic stems cells based on inhibition of GSK-3. *J. Cell. Sci.* **114:**1992-2000.

Murrison, S., Mauyra, S., Einzinger, C., McKeever-Abbas, B., Warriner, S. & Nelson, A. (2011) Synthesis of skeletally-diverse alkloid-like small molecules. *Eur. J. Org. Chem.* **12:**2354-2359.

Tosatti, P., Campbell, A., House, D., Nelson, A. & Marsden, S. (2011) Control in sequential asymmetric allylic substitution: stereodivergent access to *N,N*-diprotected unnatural amino acids. *J. Org. Chem.* **76:**5495-5501.

Funding
We thank EPSRC, BBSRC, the Wellcome Trust, the EU and AstraZeneca for support.

Collaborators
Dr Ben McKeever-Abbas, AstraZeneca, Professor Steve Marsden, University of Leeds, and Professor Melanie Welham, University of Bath.

Biophysical theory and simulation of stratum corneum lipid bilayers

Chinmay Das, Simon Connell and Peter Olmsted

Introduction

Lipid bilayer membranes are an essential component of all biological systems, forming a functional barrier for cells and organelles from the surrounding environment. The advent of new experimental techniques has led to an explosion in understanding the basic physical mechanisms behind membranes.

Stratum Corneum Bilayers

Stratum corneum (SC), the outermost layer of skin, consists of keratin-filled rigid non-viable corneocyte cells surrounded by multilayers of lipids; it is responsible for the barrier properties of skin. The composition (ceramide NS-24:0, free fatty acid 24:0 and cholesterol) plays a key role in determining the SC membrane structural properties, such as high density, low permeability, and the nature of the gel phase of these bilayers. One important result is that the bilayer phase is probably most likely to form (rather than a disordered inverse micellar phase) in the presence of external fields or templating effects, such as the keratin protein that takes up a large fraction of the SC. Our simulations suggest that the composition ratio in native SC lipid layers is responsible for both the good barrier properties and the stability of the lipid structure against mechanical stresses.

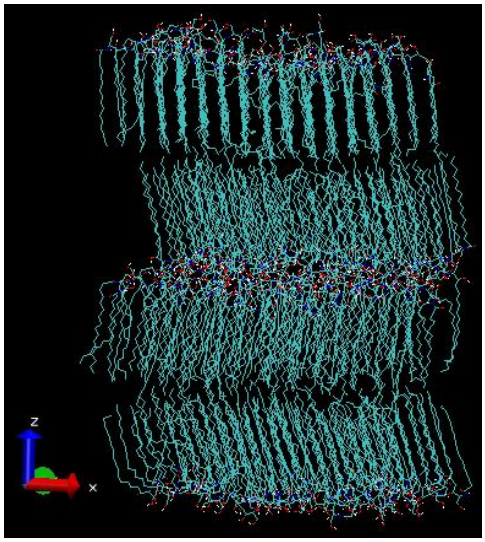

Figure 1: simulation of a ceramide bilayer showing tight hydrogen bonding between opposing leaflets.

We have developed a method to use AFM to extract the local stretching modulus of lipid bilayers. This is the first technique that can measure the mechanical properties of different regions of the same membrane, and we have demonstrated the technique on a three component mixture (DOPC, cholesterol, sphingomyelin) that exhibits liquid-liquid phase separation analogous to lipid rafts. We have shown that mechanical force can induce a transition from the liquid-ordered to liquid-disordered phases, and we have interpreted this in terms of the breaking of hydrogen bonds that stabilize the cholesterol-rich liquid-ordered phase.

We are in the second round of funding, in collaboration with Unilever, and the Universities of Bradford and Hull. This has provided a number of further insights and new findings about the design principles behind skin lipid membranes. The lipid compositions are highly hydrophobic, with the opposing leaflet head groups often strongly hydrogen-bonded. This helps with impermeability, and a layered structure can be maintained by the templating effect of the keratin bodies. The membranes are typically in the gel phase, but the asymmetric ceramide tails lead to an unusual soft amorphous layer between the stiffer leaflets. This seems to play an important role in flexibility and mobility, despite being in the gel phase, and allows facile membrane reorganization during swelling of keratin by water, or when under “normal” mechanical stresses.

Funding
This work was funded by the EPSRC, Yorkshire Forward, the EU (FP7 Network of Excellence SOFTCOMP), and Unilever.

Collaborators
This work was carried out in close collaboration with Massimo Noro and colleagues at Unilever Research Port Sunlight, as well as with groups at the Universities of Hull and Bradford.

Structural and mechanistic insights into the FusB family of fusidic acid resistance proteins

Georgina Cox, Gary Thompson, Huw Jenkins, Jennifer Tomlinson, Steve Homans, Thomas Edwards and Alex O'Neill

Introduction

A major focus in the O'Neill laboratory is on understanding the mechanisms by which bacteria resist the effects of antibiotics that are used to treat the infections they cause. Fusidic acid (FA) is a clinically-important antibiotic that inhibits bacterial protein synthesis by blocking release of the translocase, elongation factor G (EF-G), from the ribosome. In the bacterial pathogen *Staphylococcus aureus*, resistance to FA is usually mediated by members of the FusB family of proteins (FusB or FusC). These proteins bind to EF-G and protect bacterial translation from FA-mediated inhibition. Until recently, the interaction of FusB-type proteins with EF-G was poorly characterised, their structure had not been elucidated, and it was unknown how protection from FA might be mediated. Using a combination of biochemical and biophysical techniques, we have recently gained structural and mechanistic insights into this novel antibiotic resistance mechanism.

X-ray crystallographic studies of FusB-type proteins

The three-dimensional structure of FusC was determined by X-ray crystallography to 2.1 Å. The structure of FusC revealed that the FusB family are two-domain metalloproteins (Figure 1A), the C-terminal domain of which comprises a C4 (four cysteine)-type zinc finger which appears to represent a novel zinc-binding fold (ZBF).

Interaction between FusB-type proteins and EF-G

Using isothermal titration calorimetry (ITC), we established that FusB-type proteins bind EF-G with 1:1 stoichiometry and high affinity (K_d in the nM range). Binding studies performed with FusB and fragments of EF-G mapped the FusB binding site to the C-terminal domains (3, 4 and 5) of EF-G. To define the regions of FusB involved in the interaction with EF-G, nuclear magnetic resonance (NMR) chemical shift mapping was employed. The residues of FusB involved in the interaction between FusB and EF-G were found to reside almost exclusively in the ZBF (Figure 1B).

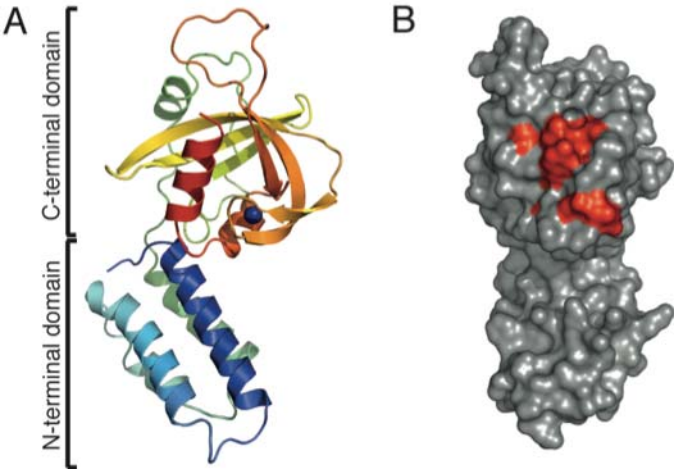

Figure 1: crystal structure of FusC, and the location of the EF-G binding site. **(a)** Ribbon diagram of FusC, with the zinc ion shown as a purple sphere. **(b)** Surface representation of FusC displaying the predicted EF-G binding site in red.

Modeling the FusC•EF-G complex

Computational docking predicted interaction between the ZBF of FusC and domains 3 and 4 of EF-G, consistent with the experimental data, and provided a model of the FusC•EF-G complex. Modeling of the FusC•EF-G complex on the ribosome revealed that owing to its size and location of binding on EF-G, bound FusC would cause steric clashes with the 30S subunit of the ribosome, which would probably inhibit EF-G from making the normal ribosomal contacts.

The effect of FusB-type proteins on EF-G function

Using a series of steady-state and transient kinetic assays, the effect of FusB on the function of EF-G on the ribosome was assessed. FusB-type proteins were found to accelerate release of EF-G from the ribosome, probably as a consequence of competition with the ribosome for EF-G-binding. Destabilization of EF-G binding to the ribosome in the absence of FA likely represents the cellular house-keeping function of FusB-type proteins, i.e. to facilitate release of EF-G from the ribosome following translocation, thereby clearing stalled ribosomes and allowing translation to resume. In the presence of FA, the effect of FusB-type proteins on the dissociation of stalled ribosome•EF-G complexes was particularly striking, and provides an explanation for the mechanism of FA resistance mediated by this family of proteins.

Publications

McLaws, F., Larsen, A., Skov, R., Chopra, I. & O'Neill, A. (2011) Distribution of fusidic acid resistance determinants in methicillin-resistant *Staphylococcus aureus. Antimicrob. Agents Chemother*. **55:**1173-1176.

Funding

This work was funded by the BBSRC.

Collaborators

Frank Peske, Marina Rodnina and Wolfgang Wintermeyer (Max Planck Institute for Biophysical Chemistry, Goettingen, Germany).

Free energy landscapes for disordered polypeptides, proteins under mechanical force and molecular machines

Zu Thur Yew, Kostas Papachristos, Richard Malham, Gael Radou, Supreecha Rimratchada, James Ross, James Gowdy, Briony Yorke, Matt Batchelor and Emanuele Paci

Introduction

Our goal is to describe in rigorous physical terms a large number of phenomena involving biological macromolecules with relevance in life science. To this end, we use theory, computational models and experimental measurements from advanced experimental probes available through collaborations at Astbury.

Everything that polypeptides do can be explained in terms of diffusion on a free-energy landscape. Such landscape, sculpted by evolution, cannot be directly probed by experimental techniques. Our understanding of biomolecules is highly biased towards ordered states such as native proteins.

Molecular dynamics uses computers to provide information on any suitably modelled molecular system, such as polypeptides, with unlimited time and spatial resolution, the main limitations being the timescale that can be studied, the size of the system under study and the accuracy of the model, the three being mutually connected.

Single molecule experimental techniques, and atomic force spectroscopy in particular, provide a validation tool for simulations, and are ideal to test hypotheses deriving from simulation and theoretical models. The application of a mechanical force to individual proteins affects the free landscape, providing valuable information on the landscape itself. We have demonstrated that the intrinsic multidimensionality of the free energy landscape is responsible for extraordinary mechanical properties of some proteins in force regimes, which are experienced by proteins *in vivo*. Such properties are responsible for mechano-transduction, force-sensing, force-bearing etc. Simpler models, which assume that the free-energy can be represented as a one dimensional function (typically with two minima, one for the folded and one for the unfolded state) are always a rough approximation of reality and often misleading.

Results

In an effort to understand the thermodynamic and kinetic origin of proteins' mechanical properties we dissected simple structures such as random coils, beta hairpin, helices, and highly charged, long, extended helices, which are naturally occurring and have been recently identified. We have demonstrated while their response to force moderate is not very dependent on the sequence, the spectral density of extension fluctuations, also in principle measurable using atomic force spectroscopy, provide one of the most detailed experimental probes on the free energy landscape of the sequences, providing also a fingerprint for highly disordered sequences.

Ground-breaking tools developed by Sergei Krivov at Leeds to determine free energy landscapes can be used to characterise all the essential features of complex free energy surfaces in simple terms, and predict the force dependence of folding and unfolding rates, to predict and explain in terms of microscopic variables the effect on cooperativity of a circular permutation on T4 lysozyme.

The study of very large systems such as molecular motors and machines in general is complicated by the low resolution of experimental information available and thus by the impossibility to model them at atomistic details. Starting from low-resolution cryo EM

images of vacuolar ATPase coarse-grain models have been obtained, which correspond, on a simplified free-energy landscape, to populated states or local minima.

One other challenge is to rationally re-design a naturally occurring homo-pentameric protein to assemble with icosahedral symmetry; this corresponds to sculpting a minimum in the free energy surface for the icosahedral form, together with a pathway that make the association kinetically possible. In more practical terms, we optimise the interactions between subunits while simultaneously avoiding destabilisation of subunits. Experimental validation is strictly necessary. The overall goal is to determine rules, which will point to the strategy employed by evolution to achieve the design of assemblies with specific geometries.

Current projects include the development of methods to interpret terahertz spectra of proteins, with the aim of characterising dynamical changes, which are not easily observable with other techniques (simulation is necessary to relate the global changes measured spectroscopically with localised dynamical changes.

Publications

Glowacki, D., Paci, E. & Shalashilin, D. (2011) Boxed molecular dynamics: decorrelation time scales and the kinetic master equation. *J. Chem. Theory Comput.* **7:**1244-1252.

Ricchiuto, P., Brukhno, A., Paci, E. & Auer, S. (2011) Communication: conformation state diagram of polypeptides: a chain length induced alpha-beta transition. *J. Chem. Phys.* **DOI:** 10.1063/1.3624928.

Collaborators

Our theoretical biophysics group thrives thanks to many collaborators within Astbury, Leeds and elsewhere.

External: J. Clarke (Cambridge), M. Rief (Munich), M. Kawakami (Japan), B. Khatri (Mill Hill), T. McLeish (Durham), S. Vazquez (Santiago de Compostela), M. Enciso (Madrid).

Leeds: A. Pearson, S. Muench, D. Brockwell, M. Webb, B. Turnbull, M. Peckham, P. Knight, L. Dougan, R. Tuma, D. Donnelly and A. Burnett.

Funding

This work is funded by the Wellcome Trust and BBSRC.

Dynamic structural science: Developing tools to probe molecular mechanism

Briony Yorke, James Gowdy, Michael Webb, Emanuele Paci and Arwen Pearson

The fundamental aim of physical and life scientists engaged in structural studies is to understand how structure leads to function. To truly understand how biological systems function it is vital to be able to observe structural changes as they occur. X-ray crystallography is a powerful tool, able to provide atomic resolution information, that has played an major role in determining how the structure relates to their function. For example, many enzymes are active in the crystalline state and this has enabled our group and others to determine the structures of the intermediate species that exist during enzymatic catalysis. However, the traditional application of X-ray crystallography yields structures that are averaged over both time and space, meaning that any dynamic behaviours that occur on timescale faster than data collection (i..e sub second) cannot be observed. Pump-probe Laue time-resolved crystallographic methods can image these dynamic changes in real time, but this methodology is currently limited to reversible systems that represent only a small subset of reactions of biological interest.

We are developing a time-resolved X-ray crystallographic method that will enable us to visualise the dynamic behaviour of irreversible systems. Using a pump-probe approach we will initiate the reaction in a crystal using light (pump), and then probe the structure after at a specific time along the reaction pathway by collecting a single diffraction image. This process can be repeated on many crystals (10^2-10^3) until a complete structural dataset is obtained. The time-delay between the pump and probe is then increased until structures at a suitable number of points along the reaction pathway have been obtained.

To develop our multi-crystal approach we are using L-Aspartate-α-decarboxylase as a test system. This enzyme is not inherently light sensitive and so a 'photocaged' substrate has been developed and characterised. The photocage is a large photolabile group which, when bound to the substrate, prevents catalytic activity but can be removed using a short laser pulse. Software has been developed to enable rapid detection and screening of microcrystals as well as an automated approach to the early stages of data processing, including merging data from many crystals.

Our early results show that the photocaged substrate binds in the correct position in the active site and can be uncaged using a laser pulse. We have been able to successfully obtain high resolution structures at cryo temperatures of the photocaged-ligand complex, the uncaged ligand complex and an early intermediate on the reaction pathway by combining data from many microcrystals. In collaboration with Robin Owen at beamline I24 of Diamond Light Source we are now beginning a series of experiments at room temperature to demonstrate that we can follow the decaging and reaction turnover by X-ray crystallography. If successful, these experiments will open the door for the detailed time-resolved studies of any macromolecular system that can be crystallized and for which a photoactivation strategy can be implemented.

We also use molecular simulation as a tool to both interpret our crystallographic measurements and to perform numerical realisations of *Gedankexperimente* that can help the design of future time resolved experiments. Combined QM/MM (Quantum mechanics / Molecular mechanics) simulations can provide a real time picture of the chemistry occurring at the active site, while the protein's overall conformational dynamics are modeled classically. The QM system can be modeled using *ab inito* calculations or more approximately with

semi-empirical and density-functional theory (DFT) based methods in order to predict reaction pathways.

One effective approach to simulate pathways between specified reactants and products is to use QM/MM together with empirical valence bond (EVB) simulations. This describes the potential energy surface of proteins as a combination of a classical force fields (to describe the non-reacting protein region) with a linear combination of multiple diabatic electronic resonance forms – the valence bond Hamiltonian – which describes the active site region. Such an approach is efficient, provides an estimation of the changes to be expected in the diffraction patterns being observed, and is a crucial tool in interpreting such changes. Simultaneously the fluctuations and correlated motions in the enzyme can be analysed and their effect on the rate, time distribution or pathway of the reaction determined and in the most interesting cases experimentally tested.

In parallel with these studies, we have an ongoing research programme aimed at monitoring and understanding the structural changes that occur when a macromolecular sample is exposed to X-rays. Due to the ionising nature of X-radiation, rapid chemical changes can occur within the sample after only a single diffraction image is recorded. Knowing what these changes are and the timescales on which they occur is vital for us to be able to confidently distinguish functionally related structural changes from changes due to radiation damage in our time-resolved studies. We have used visible absorption spectroscopy to monitor changes in heme centres during X-ray exposure, demonstrating that the heme centres undergo rapid reduction in the X-ray beam. Recently we have begun to investigate the phenomenon of X-ray excited optical luminescence (XEOL) as a possible probe for both global and site specific radiation damage. We have identified the amino acids which are the major contributors to the XEOL signal and have begun to characterise the bleaching of the XEOL signal that occurs with prolonged X-ray exposure.

Publications

Gumiero, A., Metcalfe, C., Pearson, A., Raven, E. & Moody, P. (2011) The nature of the ferryl heme in compounds I and II. *J. Biol. Chem.* **286:**1260-1268.

Owen, R., Yorke, B., Gowdy, J. & Pearson, A. (2011) Revealing low dose radiation damage using single crystal spectroscopy. *J. Synch. Rad*. **18:**367-373.

Funding

This work is funded by the BBSRC, Wellcome Trust and EPSRC.

A new experimental approach to probe global protein dynamics

Kasia Tych, Andrew Burnett, Richard Malham, Emanuele Paci, John Cunningham and Arwen Pearson

Functionally-related dynamics of protein molecules, such as those involved in ligand binding and signalling, are associated with the fast thermal fluctuations of amino acid side chains occurring on time-scales between ~100 femtoseconds and several picoseconds. These time-scales are exactly those probed by terahertz (THz) spectroscopy and there have been several reports in recent years of the application of THz time-domain spectroscopy to the study of proteins. These have demonstrated that THz spectroscopy is sensitive to conformational changes linked to function. Despite this increasing interest, our understanding of the fundamental basis for the THz response of proteins, and hence our ability to link changes in the THz spectra to specific regions of the protein remains extremely poor.

We have developed an experimental set-up that, for the first time, has permitted us to record THz spectra from protein crystals. Using this instrument, we have demonstrated that THz spectroscopy is sensitive to the solvent content of the crystal and have investigated how dehydration alters the THz response. Such hydration studies, as well as other studies of global protein dynamics are usually carried out using inelastic or quasi-elastic neutron scattering, a technique that typically requires long measurement times, large amounts of sample (>100mg) and, often, isotopic labelling. THz spectroscopy has allowed us to access similar information, with short acquisition times and using a fraction of the sample mass with no need for isotopic labelling.

Our ongoing experiments with this instrument are now focused on probing the dynamic transitions within proteins that occur with temperature, as well as using the THz response to probe functionally related dynamics linked to ligand binding and catalysis. In addition, we are investigating the sensitivity of THz spectroscopy to the long-range structural order that occurs in fibres, fibrils and crystalline material.

As well as our experimental studies, we use molecular modelling and simulation in order to link the functionally related spectral changes we observe with specific structural changes in the protein. While a number of challenges exist, this is essential is the information provided by THz measurements is to be related to residue-specific properties and translated into specific dynamical changes interpretable in terms of function and binding affinity.

Publications

Tych, K., Burnett, A., Wood, C., Cunningham, J., Pearson, A., Davies, A. & Linfield, E. (2011) Applying broadband terahertz time-domain spectroscopy to the analysis of crystalline proteins: a dehydration study. *J. Appl. Cryst.* **44:**129-133.

Funding

This work is funded by the Wellcome Trust , the Leverhulme Trust and EPSRC.

The cytoskeleton and molecular motors, from molecular mechanisms to super-resolution imaging

Kathryn White, Katarzyna Makowska, Marcin Wolny, Matthew Batchelor, Francine Parker Melanie Colegrave and Michelle Peckham

Introduction

All cells need a cytoskeleton to maintain shape, to move, and for movement of intracellular vesicles and proteins. In skeletal and cardiac muscles, the cytoskeleton is highly organised to facilitate the main function of these muscles, which is to contract and either generate movement or force. The two main proteins that interact to generate contraction are actin, which is organised into thin filaments, and myosin, which is organised into thick filaments.. The organisation of these cytoskeletal proteins is so precise that each thick filament has exactly 296 molecules of myosin in each thick filament. Thick and thin filaments inter-digitate and are organised into an almost crystalline array. Along the length of the muscle fibre, the filaments are organised into a repeating pattern of units, about 2 microns long, called the muscle sarcomere, and each muscle sarcomere is identical to the next. Building these precise structures in muscle, and precisely regulating the lengths and organisation of contractile proteins is a major feat, and still one that is only poorly understood.

In non-muscle cells, myosins and actin are less organised, but still interact to enable cells to crawl on a substrate, generate force, or to move substances around inside the cells. There is still much to learn about the 39 different types of myosin in humans and how they are specialised for their functions either in muscle, or in non-muscle cells.

Investigating mutations in cardiac myosin that cause disease

Mutations in sarcomeric proteins cause the disease hypertrophic cardiomyopathy. About 40% of these mutations occur in the β-cardiac myosin heavy chain (bMHC), the major component of the myosin molecule. Some of these mutations are found in the filament-forming tail domain of this myosin, and we have been investigating how these mutations affect the structure of this region of the myosin (funded by the British Heart Foundation). Intriguingly, we've discovered through this work that while myosin has a well-characterised coiled coil that dimerises this type of myosin, shorter peptide fragments up to 105 residues long do not necessarily dimerise by themselves, unless they contain a specific region of the coiled coil.

Novel 'single alpha-helical' domains

While that tail of cardiac myosin contains a well-characterised coiled coil, which is responsible for dimerising the myosin heavy chain, we recently showed that many other unconventional myosins originally thought to contain a region of coiled coil, actually contain a stable single alpha helix. We've also shown that this type of structure is stiff enough to contribute to the movement of a myosin lever. We have just recently begun to study this domain in more detail (funded by BBSRC), to try to understand why it is so stable, and how the residues found in this type of structure contribute to its stability.

Coiled coil or single alpha helix?

None of the prediction programs available are able to convincingly predict whether a sequence is coiled coil or single alpha helix. Programs that detect coiled coils such as Pepcoil or Coils, commonly fail to distinguish between these two distinct structures. Regions of coiled coil can show features of single alpha helices that may help in triggering formation of a region of alpha helix that helps to seed coiled-coil formation.

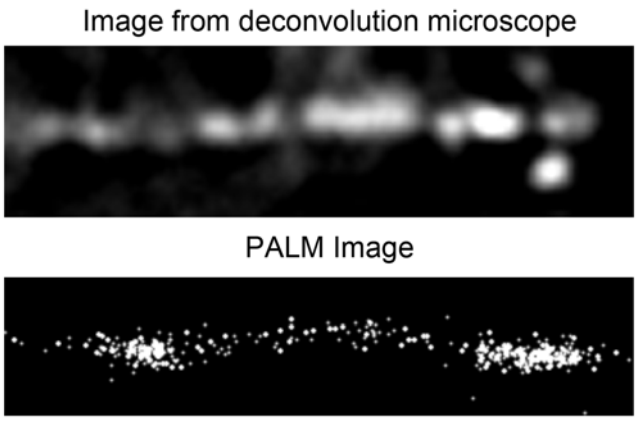

Figure 1: comparison of a typical high resolution light microscope image, obtained by deconvolution microscopy, of alpha-actinin in the Z-disc, with a PALM image of a Z-disc obtained using mEos2-tagged alpha-actinin.

Notice the large improvement in resolution in the PALM image.

Super-resolution imaging

Normally, the amount of detail that can be observed in a specimen in a light microscope is limited by the resolution of the instrument (~200nm). Various techniques have been developed in the last few years to overcome this limit, and I have been learning one of these; Photo-activated Light Microscopy (PALM) through visits to Hari Shroff's lab at NIH (USA), funded by a Wellcome Trust flexible travel award. I obtained high-resolution images of alpha-actinin in the Z-disc of adult cardiomyocytes (Figure 1), with a resolution of 20nm. Money has now been raised to build this type of microscope in Leeds in the next year.

Funding

This work was funded by the British Heart Foundation, BBSRC, and the Wellcome Trust.

Interactions of the intact FsrC membrane histidine kinase with its pheromone ligand GBAP revealed through synchrotron radiation circular dichroism (SRCD)

Simon Patching, Shalini Edara and Mary Phillips-Jones

Introduction

Enterococcus faecalis is a significant agent of hospital-acquired infection, accounting for over 20 % of cases in the UK. Adherence to host tissue and organs is a key feature of these infections and one of the most important virulence factors that contributes to the adherence properties is gelatinase (GelE) which is under the control of the quorum sensing Fsr signal transduction pathway. Quorum sensing has therefore been identified as a promising target for the design of novel antibacterial agents.

During the past year, we have been developing SRCD methods to stabilise and characterise intact FsrC, the membrane sensor kinase component of the FsrC pathway, including its molecular interactions with the activating pheromone signalling ligand, GBAP. Use of SRCD (rather than CD) permits low volume measurements which are important for studies of low abundance membrane proteins. The work has led to the determination of the first quantitative (k_d) binding data for any intact membrane protein using CD methods, and paves the way for obtaining binding data for other ligands including inhibitors. We suggest that SRCD may also serve as a useful method to confirm stability of FsrC and other membrane proteins purified within detergent micelles prior to undertaking other methodologies such as crystallisation which depend on stability for success.

Results

Using SRCD, we identified suitable conditions required to stabilise purified FsrC within detergent micellar complexes. Once these conditions were established, stabilised protein was used in SRCD studies in the far- and near-UV regions to investigate binding by its native quorum ligand, gelatinase biosynthesis-activating pheromone (GBAP). Whilst GBAP binding did not significantly affect FsrC secondary structure (as revealed by measurements in the far-UV region – Fig. 1), nor the thermal stability of FsrC (data not shown), measurements in the

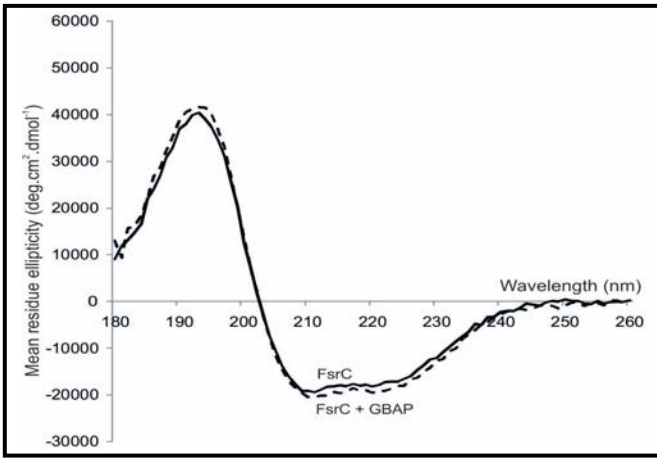

Figure 1: the effect of two-fold GBAP on FsrC revealed through SRCD in the far-UV region of the spectrum at 20 °C. Solid line, 6 µM FsrC (plus equivalent acetonitrile); dashed line, 6 µM FsrC in the presence of two-fold GBAP (dissolved in acetonitrile). Average of four scans.

near-UV region revealed that the tertiary structure in the regions of the Tyr and Trp residues was significantly affected (Fig. 2a). Titration experiments using several GBAP:FsrC molar ratios within the range of 0:1 and 5:1 revealed a calculated k_d value of 2 µM (Fig. 2b), indicative of relatively loose binding of GBAP to FsrC, which is consistent with its role in signal transduction in which rapid responses to changing GBAP levels are required.

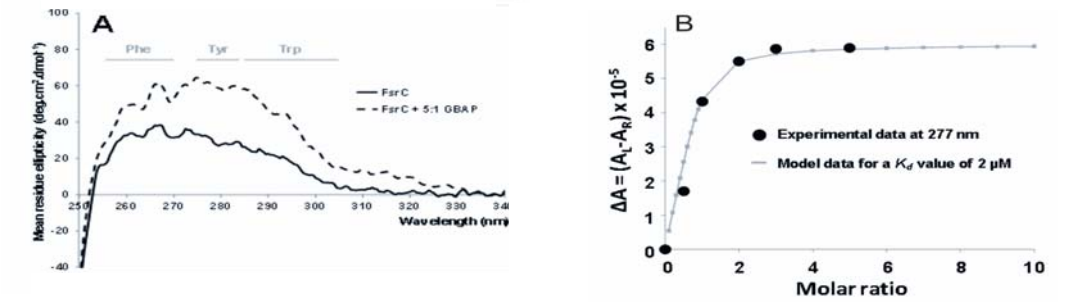

Figure 2: GBAP binding to FsrC revealed through SRCD measurements in the near-UV region at 20 ^{o}C. **(a)** 20 µM FsrC in the absence (solid line) and presence (dashed line) of five-fold GBAP. Data corrected for buffer/acetonitrile/GBAP signals by subtraction of control spectra; **(b)** Determination of binding affinity (K_d value) for GBAP binding using data from titration data analysed using the programme CD Titration v1.6.

Publications

Ma, P., Nishiguchi, K., Yuille, H.M., Davis, L.M., Nakayama, J. and Phillips-Jones, M.K. (2011) Anti-HIV siamycin I directly inhibits autophosphorylation activity of the bacterial FsrC quorum sensor and other ATP-dependent enzyme activities. *FEBS Lett*. **585:**2660-2664.

Funding

This work was funded by the BBSRC, Diamond Light Source and the University of Leeds. SGP acknowledges the EU EDICT Consortium (contract FP7 201924) for financial support on other projects.

Collaborators

This work was accomplished in collaboration with Dr P. Ma (ITQB, Portugal), Drs G. Siligardi and R. Hussain (Diamond Light Source, Oxfordshire) and Professor J. Nakayama (Kyushu University).

Exploring protein folding energy landscapes

Alice Bartlett, Gerard Huysmans, Lindsay McMorran, Arnout Kalverda, Gareth Morgan, Clare Pashley, Gary Thompson, Stephen Baldwin, David Brockwell and Sheena Radford

Introduction

Understanding the role of a protein's primary amino acid sequence in controlling the search for the native conformation is of fundamental importance. Progress towards this goal requires the structural and energetic characterisation of all species encountered on the folding energy landscape. Work in our laboratory focuses on using a range of biophysical approaches to examine the folding landscapes of the small four-helical colicin immunity protein, Im7, and the folding of β-barrel outer membrane proteins.

Conformational properties of the unfolded state of Im7 in nondenaturing conditions

Previous work in our laboratory has provided extensive insights into the folding of a four-helix protein, Im7 (immunity protein 7), which folds via an on-pathway intermediate. While the transition states and folding intermediate have been characterised in detail, knowledge of the unfolded ensemble under the same ambient conditions remained sparse. The unfolded ensemble in aqueous solution represents the starting point of protein folding. Characterisation of this species is often difficult since the native state is usually predominantly populated at equilibrium. To address this problem, we have introduced destabilising amino acid substitutions into the sequence of Im7, such that the unfolded state becomes predominantly populated at equilibrium in the absence of denaturant (Figure 1). Using far- and near-UV CD, fluorescence, urea titration and heteronuclear NMR experiments, we showed that three amino acid substitutions (L18A–L19A–L37A) are sufficient to prevent Im7 folding. Using measurement of chemical shifts, ^{15}N transverse relaxation rates and sedimentation coefficients, the results revealed that the unfolded species of L18A–L19A–L37A deviates significantly from random-coil behaviour. Specifically, we found that this unfolded species is compact ($R_h = 25$ Å) relative to the urea-denatured state ($R_h \geq 30$ Å) and contains local clusters of hydrophobic residues in regions that correspond to the four helices in the native state. Despite these interactions, there is no evidence for long-range stabilising tertiary interactions or persistent helical structure. The results reveal an unfolded ensemble that is conformationally restricted in regions of the polypeptide chain that ultimately form helices I, II and IV in the native state.

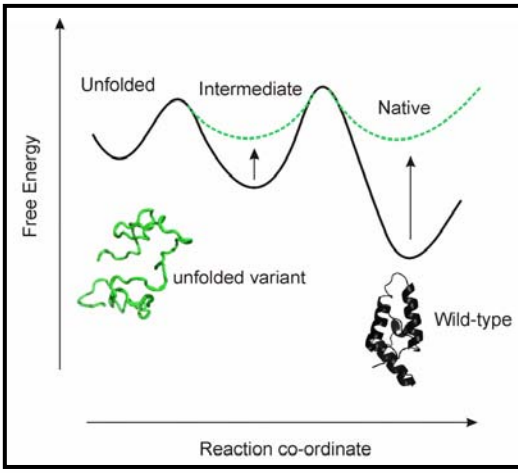

Figure 1: protein engineering was used to create an unfolded Im7 variant. Three leucine to alanine amino acid substitutions were introduced into the sequence of Im7 (L18A, L19A and L37A) to destabilise the native and intermediate state, so that the unfolded ensemble became the most stable species at equilibrium.

Current work

PagP, an integral outer membrane protein (OMP) from *E.coli*, has been shown to fold *via* a polarized transition state, with highly structured C-terminal β-strands, while the N-terminal

α-helix and β-strands remain largely disordered. Detailed kinetic studies of PagP revealed that the protein folds through parallel pathways, which can be modulated by changing the conditions under which folding is initiated (see Brockwell lab report). The homologous β-barrel outer membrane proteins, OmpT and OmpP, have also been studied and conditions found under which they can fold to the native state in synthetic liposomes *in vitro*. Their folding kinetics are being investigated and compared with those of PagP with a view to finding generic features in the folding mechanisms of bacterial OMPs. Our laboratory is also employing kinetic folding techniques to look at refolding of PagP in low concentrations of urea, to allow investigation of how the chaperone proteins found in the periplasm of *E.coli* can influence folding *in vitro*. By elucidating the mechanism of action of these proteins, which are essential for the correct trafficking, folding and insertion of OMPs *in vivo*, it is hoped to gain insights into the mechanisms of OMP folding in the cell.

Publications

Knowling, S**.**, Bartlett, A. & Radford S. (2011) Dissecting key residues in folding and stability of the bacterial immunity protein 7. *Protein Eng. Des. Sel.* **24:**517-523.

Funding and acknowledgements

This work is funded by the BBSRC and The Wellcome Trust. We thank Nasir Khan for technical support.

Collaborators

Immunity protein work performed in collaboration with Colin Kleanthous at the University of York.

Investigating the mechanisms of amyloid formation

Andrew Hellewell, Toral Jakhira, Theo Karamanos, , Aneika Leney, Eva Petrik, Maya Pandya, Morwenna Porter, Claire Sarell, Charlie Scarff, Alessandro Sicorello, Ricardo Tomé, Lucy Woods, Wei-Feng Xue, Alison Ashcroft and Sheena Radford

Introduction

Despite the large scientific interest the field of protein misfolding has gathered over the years, the mechanisms by which proteins self-assemble to form amyloid fibrils remain to be elucidated. Here we have used modern NMR and mass-spectrometry techniques to further understand the mechanism of amyloid formation by β_2-microglobulin (β_2m), a protein that assembles into amyloid fibrils in joints and whose deposits are associated with dialysis-related amyloidosis. Intriguingly, acid unfolded β_2m (at pH 2.5) converts into amyloid fibrils within hours, whereas under physiological conditions (pH 7) the protein remains soluble in the absence of additional factors. It has previously been reported that aggregation is initiated by a partially-folded species involving a non-native *trans* isomer of the peptidyl-proline bond at residue 32. Unravelling the structural properties of this on-pathway species and exploring the complex energy landscape of β_2m aggregation at low pH will improve our understanding about the mechanism of fibril formation and may aid the treatment of DRA.

Structure, dynamics and amyloid potential of an on-pathway intermediate

NMR experiments confirmed that a truncated variant of wild type (WT) β_2m (termed ΔN6) is an excellent mimic of the intermediate crucial for amyloid formation. By carefully adjusting experimental conditions the structure of ΔN6 was obtained using solution NMR, for the first time (Figure 1A). As expected, ΔN6 contains a *trans* prolyl bond at residue 32 and shows a remarkable rearrangement of side chains in the hydrophobic core in contrast with the minor differences in the main chain in comparison to WT β_2m.

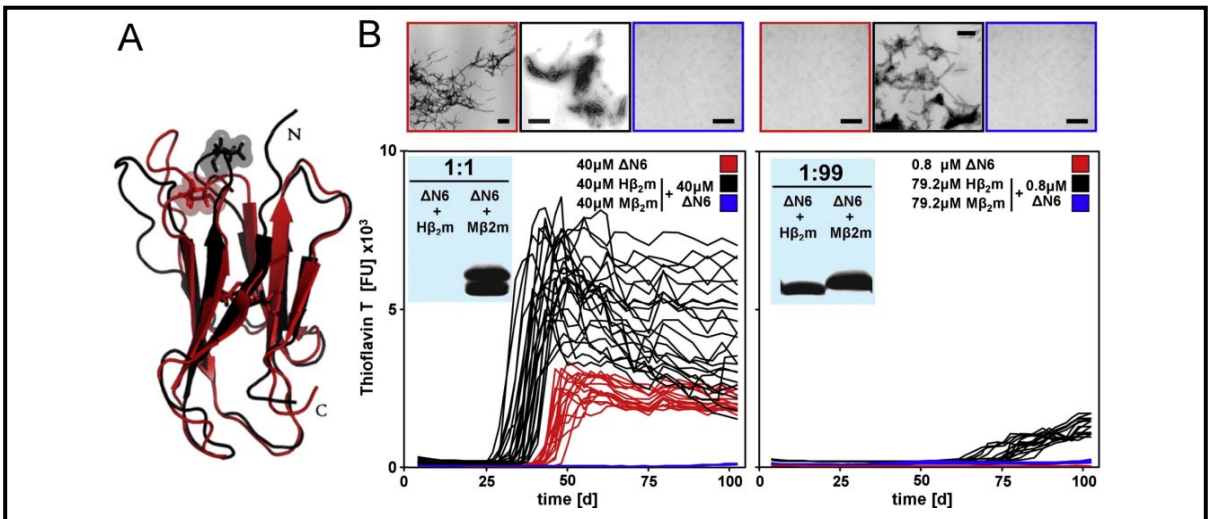

Figure 1: structure and amyloid potential of ΔN6. Overlay of the structures of WT β_2m (black) and ΔN6 (red) at physiological pH. Proline 32 is shown in sticks representation **(a)**. Prion-like conversion of WT β_2m by ΔN6 or inhibition of ΔN6 aggregation by murine β_2m in 1:1 and 99:1 ratio **(b)** monitored by ThT fluorescence (main panels), electron microscopy (top panels) and SDS-PAGE (insets).

The increased amyloidogenicity of ΔN6 compared with WT β_2m implies that it can populate more aggregation-prone species under these conditions. Investigation of protein dynamics by NMR revealed regions of the protein (BC and DE loops) which undergo significant motions under the most amyloidogenic conditions, suggesting that chemical exchange to more amyloid-prone states of the protein is taking place. More intriguingly, ΔN6 was found able to convert WT β_2m into a more amyloidogenic state(s) in a prion-like manner (Figure 1B).

Taken together, the structure, increased dynamics and effect of ΔN6 on the non amyloidogenic WT species highlight its role as a catalyst of fibril formation.

Ligand binding to distinct states diverts aggregation of an amyloid-forming protein

After an initial screen of a variety of small molecules, the antibiotic rifamycin SV was identified as an inhibitor of β_2m fibrillogenesis at pH 2.5. As shown by different biophysical techniques (ThT fluorescence, EM, CD, NMR) addition of rifamycin SV leads to the formation of spherical aggregates instead of long straight fibrils (Figure 2A). Most interestingly, electrospray ionisation-ion mobility spectroscopy-mass spectrometry (ESI-IMS-MS) revealed that the smallmolecule is able to bind to distinct conformers of β_2m at low pH (Figure 2B) and also dissociate already formed oligomers during the lag phase of fibril formation. The results demonstrate how ligand binding can disrupt the energy landscape of fibrillogenesis by driving aggregation through alternative pathways and highlight the power of ESI-IMS-MS to identify protein conformations that are on pathway to fibril formation.

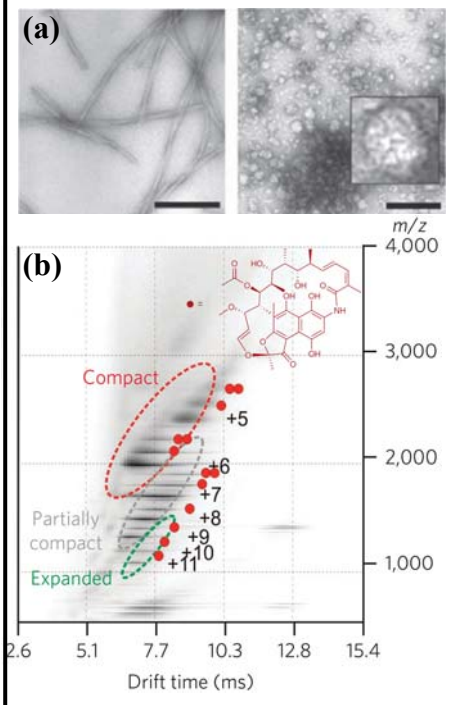

Figure 2: ligand binding disrupts protein aggregation. **(a)** binding of rifamycin SV drives the formation of spherical aggregates (right) instead of long straight fibrils (left). **(b)** the ESI-IMS-MS 3D driftscope plot shows that rifamycin binds to partially folded or unfolded conformers of β_2m (red dots). The molecular structure of rifamycin SV is shown as inset.

Publications

Eichner, T., Kalverda, A., Thompson, G., Homans, S. & Radford, S. (2011) Conformational conversion during amyloid formation at atomic resolution. *Mol. Cell* **41:**161–172.

Smith, D., Woods, L., Radford, S. & Ashcroft, A. (2011) Structure and dynamics of oligomeric intermediates in β_2-microglobulin self-assembly. *Biophys. J.* **101:**1238–1247.

Woods, L., Platt, G., Hellewell, A., Hewitt, E., Homans, S., Ashcroft, A. & Radford, S. (2011) Ligand binding to distinct states diverts aggregation of an amyloid-forming protein. *Nat. Chem. Biol.* **7:**730–739.

Funding

This work is supported by the BBSRC, Wellcome Trust, Yorkshire Kidney Research Fund, MRC and the University of Leeds.

Collaborators

External: R. Griffin (M.I.T.), S. Macedo-Ribeiro (Universidade do Porto), H. Saibil, (Birkbeck College), D. Middleton (University of Liverpool), M. Vendruscolo (University of Cambridge) and A. Rodger (University of Warwick).
Leeds: S. Harris, E. Hewitt, S. Homans, I. Manfield, P. Stockley and S. Warriner.

Biomimetic production of precise nanomagnetic particles using magnetic bacteria and their biomineralisation proteins

Johanna Galloway, Masayoshi Tanaka, Jonathan Bramble, Andrea Rawlings, Stephen Baldwin, Stephen Evans and Sarah Staniland

Introduction

Scientific and economic interest in nanotechnology has grown in recent years. Within this the quest to produce tiny and highly tailored magnetic particles or nanomagnets is crucial. Nanomagnets have a range of practical uses such as: the development of 3D information storage systems providing high density data storage; medical applications such as site specific targeted therapies and image enhancers for diagnostic medicine.

However, as nanotechnology grows, so too does the need to develop precisely engineered nanomagnets. Different applications demand different shapes and sizes of particles and different magnetic properties. Producing nanomagnets with highly controlled; composition, size and shapes, in large enough amounts to be of use to these industries, have therefore become a key goal of researchers.

Magnetotactic bacteria are the simplest organisms that perform biomineralisation (figure 1A). They take up iron ions from solution and produce nanoparticles of magnetite (Fe3O4) within lipid vesicles (called magnetosomes) with precise control, resulting in a strain specific uniform size and morphology. Interesting our recent TEM study has revealed how magnetic bacteria divide and what happens to the magnetosome chain within them during this process.

The aim of this group's research is to investigate, understand and then manipulate the biomineralisation process within these bacteria to enable the production of high-yields of customised nanomagnets for nanotechnological application using the genetic precision of nature.

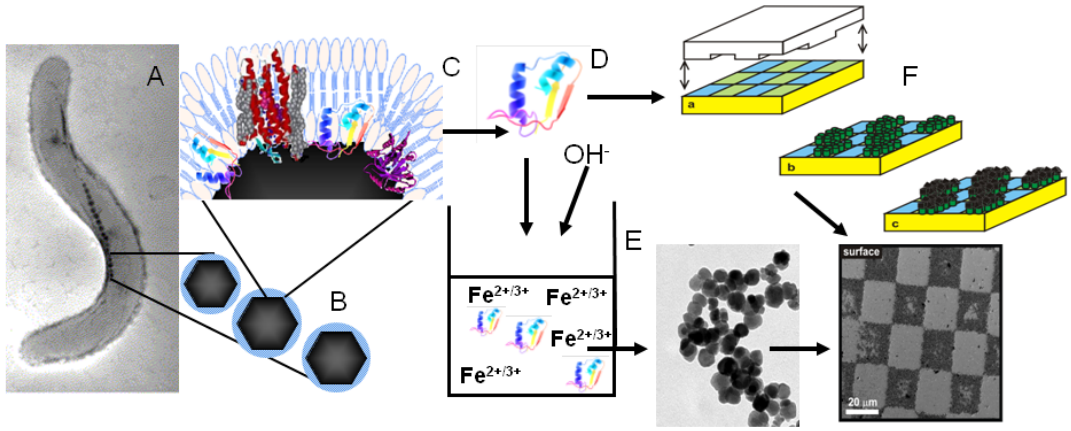

Figure 1: schematic of some research activity. **(a)** shows a magnetotactic bacterium and **(b)** shows enlarged magnetosomes with **(c)** showing a close-up of the magnetosome membrane representing magnetosome membrane specific (Mms) proteins. **(d)** represent Mms6 with **(e)** depicting the in vitro precipitation. F) shows how Mms6 can be used to both control magnetic nanoparticle morphology and locate them in a pattern on a surface.

The Research

The magnetic composition of magnetosomes as been successfully altered in vivo by doping the magnetosomes with cobalt resulting in magnetosomes with an increased magnetic coecivity compared to control magnetosomes. This was achieved with the addition of cobalt ions into the bacterial growth media which were taken up and incorporated into the magnetite mineral in approximately 1% quantities. More recently we have increased the doping levels of cobalt to 3% and also achieved in vivo magnetosome doping with Mn (2.7 %) and Cu (15.6%). This has been achieved by a systematic study of growth and magnetosome over a range of concentrations of various transition metals to find the minimum inhibitory concentration for the microbes and the optimum doping levels. Additionally, we induced the production of independent nanoparticles of Te and Se within the cell. It must be noted that doping concentrations are restricted when magnetosomes are modified *in vivo* due to poisoning of the organism. We thus sought an *in vitro* route to offer more flexibility and higher-yields. Here, in collaboration with the lab of Prof. Matsunaga we build on their original method to develop a biomimetic route to more precise nanomagnets synthesized at room temperature using protein mediated precipitation of magnetic nanoparticles. The protein used was Mms6 (magnetosome membrane specific, 6 KDa) which was found to be unique to the magnetosome membrane and tightly bound to the crystal (Figure 1C & D). When this protein was expressed and purified and used *in vitro* it was found to control particle size and shape (Figure 1E).

Research is now being conducted in two parallel and complementary directions

Firstly, the physical investigation of how Mms proteins interact with the forming mineral and control the magnetite's formation and morphology is being investigated (BBSRC funded). Several new proteins are being identified and expressed while their interaction with magnetite is being assessed using a range of spectroscopy, electron/force microscopy and neutron scattering techniques. Once key motifs, peptide and binding sites can be identified we could begin to design tailored additives for high-yield industrial nanomagnet production.

Secondly, we are developing a range of methods using the expressed Mms proteins *in vitro* for more advanced synthesis. We are enhancing this with the addition of membranes and vesicles to the systems (EPSRC funded). This is being furthered by experimenting with different proteins that affect the fucntionality of membranes. For example we are investigating novel metal ion transport proteins and vesicle deformation proteins which can be incorporation into vesicles along with Mms proteins to develop a range of novel, flexible biomimetic systems.

Finally, we have patterned a SAM surface with Mms6 and successfully mineralised morphologically controlled magnetic nanoparticles located in patterned on the surface (Figure 1F). This is currently been advanced further to form customised nanomagnetic arrays. This is just one of many biomimetic systems we are developing to create several novel mineral/membrane assemblies, some tethered/free and attached to surfaces.

Publications

Aljabali, A., Barclay, J., Cespedes, O., Rashid, A., Staniland, S., Lomonossoff, G. & Evans, D. (2011) Charge modified Cowpea mosaic virus particles for templated mineralization. *Adv. Func. Mater.* **21:**4137-4142.

Galloway, J., Arakaki, A., Masuda, F., Tanaka, T., Matsunaga, T. & Staniland, S. (2011) Protein from magnetic bacterial magnetosomes (Mms6) controls size, morphology and crystallinity of cobalt-doped magnetite nanoparticles *in vitro. J. Mater. Chem.* **21:**15244 – 15254.

Moisescu, C., Bonneville, S., Staniland, S., Ardelean, I. & Benning, L. (2011) Iron uptake kinetics and magnetosome formation by *Magnetospirillum gryphiswaldense* as a function of pH, temperature and dissolved iron availability.
Geomicrobiology J. **28:**590-600.

Funding
This work has been funded by the EPSRC (Overseas Postdoctoral Life-science Interface Fellowship Scheme 2005-2008 EP/C53204X/1) while Masayoshi Tanaka is funded as a Royal Society Newton Fellow under the Newton international fellowship scheme. Research is being funded by the BBSRC (2010-1014 BB/H005412/1) and the EPSRC (2011-2015 EP/I032355/1).

Collaborators
External: B. Ward (University of Edinburgh), A. Harrison (ILL, Grenoble), T. Matsunaga (Tokyo University of Agriculture and Technology), D. Cowan (University of the Western Cape), A. Roychoudhury (University of Stellenbosch, Stellenbosch). M. Edirisinghe, University College London), E. Stride, University College London).
Leeds: C. Moisescu and L. Benning, School of Earth and Environment.

Enhanced stability and activity of a truncated replication initiator protein

Lauren Mecia and Christopher Thomas

Introduction

Our previous studies of plasmid replication have used the model initiator protein RepD, encoded by staphylococcal plasmid pC221. RepD demonstrates sequence-specific DNA nicking and closing activity *in vitro*, but unlike many other plasmid-specified relaxases it does not employ a His-hydrophobic-His motif at the active site. Instead, an alternate motif is found, common to initiator proteins of the pT181 family of staphylococcal plasmids, bacteriophages of Gram-negative organisms and relaxases of Tn916-like conjugative transposons among others. This motif is identified as *Rep_trans* in the Pfam catalogue.

Our pursuit of structural prototypes of the *Rep_trans* motif has led us to the initiator protein of the *Geobacillus stearothermophilus* plasmid pSTK1. We previously found that the designated 269 aa reading frame encoding *Rep_trans* yielded no functional product. Instead, a longer translation product of 42 kDa (including purification tag) was required to show nicking-closing activity on the cognate *ori*STK substrate. Here we call this product RepSTK.

Recent findings

Partial proteolysis of RepSTK yields a stable fragment of ~31 kDa. Unexpectedly, peptide mass fingerprinting revealed digestion only at the C terminus of RepSTK. Based on these observations we have cloned, expressed and purified a series of C-terminal deletions of RepSTK; this report concerns a truncated, 33 kDa tagged product, RepSTK-b.

Although CD spectra of RepD, RepSTK and RepSTK-b at ambient temperature are similar (not shown), the thermal stability of RepSTK-b appears to be greater than either RepSTK or RepD (Fig. 1(a)). Moreover, in nicking-closing assays conducted at 65°C with the *ori*STK substrate, RepSTK-b is seen to convert more negatively-supercoiled substrate to relaxed, covalently-closed (RC) product at lower concentrations than RepSTK (Fig. 1(b)).

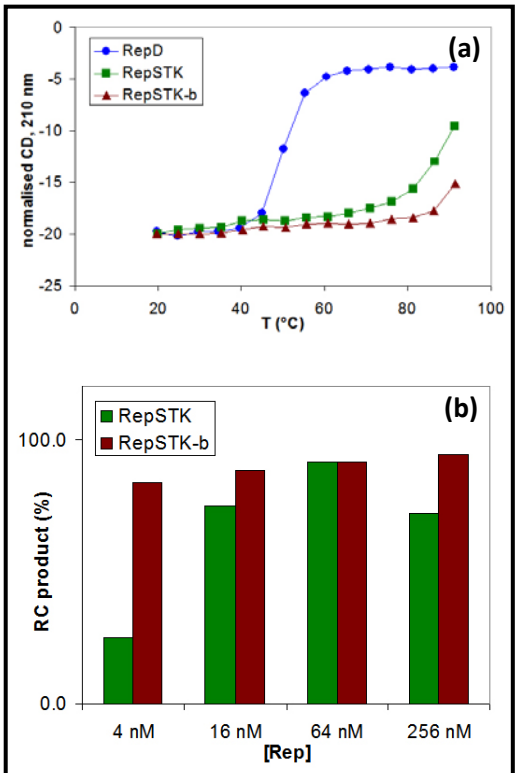

Figure 1: (a) thermal stability of Rep protein **(b)** topoisomerase activities.

Conclusions and future work

As a new and stable fragment representative of a *Rep_trans* initiator, RepSTK-b is now entering crystallisation trials. The results also raise the question of the function of the C-terminal domain of RepSTK. For RepD, this domain encodes both DNA-binding and dimerisation specificity. Unlike RepD, RepSTK shows no non-covalent DNA binding at the replication origin. Instead, the topoisomerase data suggests some inhibitory activity, perhaps required for regulation of the initiation of plasmid replication *in vivo*.

Acknowledgements

We thank Jeff Keen for peptide mass fingerprinting analysis. LBM was supported by the first-year undergraduate research placement scheme of the Faculty of Biological Sciences.

How does the size of the tip affect measurements in atomic force microscopy?

Sergio Santos and Neil H. Thomson

Introduction

The atomic force microscope (AFM) is a high resolution surface profilometer that uses a cantilever probe as a force sensor to feel the top surface of a sample. Since it measures forces, it is versatile and can image all kinds of samples, including biological molecules and materials. The integrated sharp tip at the end of the probe has a radius of curvature on the order of 10 nanometres, the absolute size of which affects the ultimate resolution. Probes are made in commercial batch fabrication, micro-machining techniques and in the last decade, the sharpness and reliability of the tips has improved. However, since the AFM operates in near contact or continuous contact with a surface, the tip may change in physical size or chemical state, due to wearing or contamination. The ability to know the size and state of the tip *in situ*, has restricted quantitative analysis and interpretation of AFM data to date, particularly on rough and mechanically heterogeneous samples, such as those biology presents. We have been focussing on characterising tip size *in situ* and understanding how this affects measurement outcomes.

Energy dissipation between AFM tip and sample

AFM is often run in a dynamic imaging mode, whereby the cantilever is vibrated, typically at kHz to MHz frequencies. The intermittent contact that the tip has with the sample eliminates shearing forces that are particularly damaging for biological specimens. In dynamic AFM, the presence of the surface is detected because energy is typically dissipated in the tip-sample junction which modulates both the amplitude and frequency of the cantilever oscillation. While we often try to minimise the force at which the tip interacts, this can be difficult to achieve in all situations. In particular, very sharp tips, which optimise resolution, lead to high pressures in the tip-sample junction, resulting in tip creep or wear. We have developed methods to determine how much energy is dissipated through the tip and how this affects the wearing of the tip. This has allowed us to develop a simple way to shape the tip to a stable size. While this limits resolution, it enables quantitative comparisons of mechanical response from one sample to the next. It has also helped to gain deeper understanding of the pressure profile between the tip and sample, leading to better interpretation of nanoscale interactions.

Apparent and true height in AFM

One of the main uses of the AFM is to measure the height of biomolecules, nanoparticles, the rugosity of the surface features, etc. The instrument, however, is notorious for always producing values which are lower the true ones. We have modeled the tip-sample interaction to show that this is due the area of interaction between the tip and the sample being finite. For example, even for the sharpest tip (i.e. an atom) the region of the sample interacting with it at relatively long distances is of the order of the size of atoms. This implies that there are certain limitations as to, for example, measure the true height of subatomic features even with a one atom tip. In terms of single molecular imaging (e.g. DNA), the finite geometry of the tip implies that there is a certain averaging between the height of the sample and the height of the supporting surface. Now that we have established the principle of height reconstruction is understood, recovering the true height is possible with reliable models of cantilever dynamics.

True non-contact imaging in ambient AFM

The AFM can be operated in ambient conditions where a water layer forms on hydrophilic surfaces. The water layer is of the order of several angstroms to 2nm in thickness, depending on relative humidity. Better understanding of the cantilever dynamics during imaging has

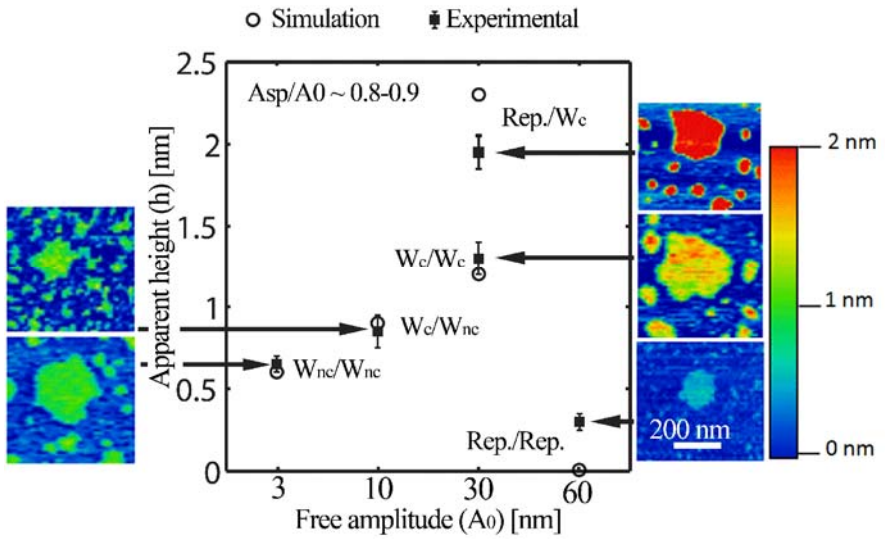

Figure 1: experimental and simulation data of water patches on a $BaF_2(111)$ surface. Only in the true non-contact scenario (W_{nc}/W_{nc}) does the modelling and experiment both give the expected water layer height of 0.6nm.

enabled us to produce a true non-contact imaging mode for ambient, where neither water layers on the tip or the surface are disturbed during imaging. This means that we can measure the true height of water layers on surfaces by using this imaging mode in conjunction with the development of the understanding of the geometrical basis of height reduction for nanoscale features. This will lead us to map local physical chemistry of biological systems down to the single molecule level, i.e. mapping of hydrophobic and hydrophilic regions of proteins and nucleic acids.

Publications

Santos, S., Verdaguer, A., Souier, T., Thomson, N. & Chiesa, M. (2011) Measuring the true height of water films on surfaces *Nanotechnology* **DOI:** 10.1088/0957-4484/22/46/465705

Santos, S., Barcons, V., Christenson, H., Font, J. & Thomson, N. (2011) The intrinsic resolution limit in the atomic force microscope: implications for heights of nanoscale features. *PLoS ONE* **6**: e23821.

Santos, S., Barcons, V., Verdaguer, A., Font, J., Thomson, N. & Chiesa, M. (2011) How local are energy dissipation processes in nanoscale interactions? *Nanotechnology* **DOI:**10.1088/0957-4484/22/34/345401

Santos, S. & Thomson, N. (2011) Energy dissipation in a dynamic nanoscale contact. *App. Phys. Lett.* **DOI:**10.1063/1.3532097

Funding

This work was funded by a BBSRC Doctoral Training Grant and a CASE award from Asylum Research Corporation.

Establishing novel non-antibody binding probe libraries

Christian Tiede, Sarah Deacon, Anna Tang, Michael McPherson and Darren Tomlinson

Introduction

Antibodies are the best-studied group of biological binding molecules to date. They are important in a wide variety of biological and medical applications, but for diagnostics and as detection reagents they are limited by their significant size, poor stability, production costs and batch-to-batch variation. To overcome these issues numerous alternative binding reagents have been developed, including non-antibody binding proteins (nABP). These can bind to epitopes on target proteins and so have potential as molecular biology tools, therapeutic agents and as diagnostic tools for detection and imaging of proteins in patient samples.

The BioScreening Technology Group (BSTG) has been established as a facility for nABP development and screening. We have engineered a range of small, soluble and stable proteins that provide scaffolds to present binding surfaces whose amino acid sequences are randomised to create large libraries of nABP's that are screened using phage display.

Results

To demonstrate effective expression and presentation of the nABP on phage, the myc-tag epitope was displayed as an nABP loop and expressed in a range of phage vectors. Phage ELISA, using anti-MYC tag antibody as bait, identified the most effective expression system (Figure 1A). After optimisation a library containing greater 10^{10} individual clones with randomised loops was created. Sequencing showed a good distribution of amino acids across the loops (Figure 1B).

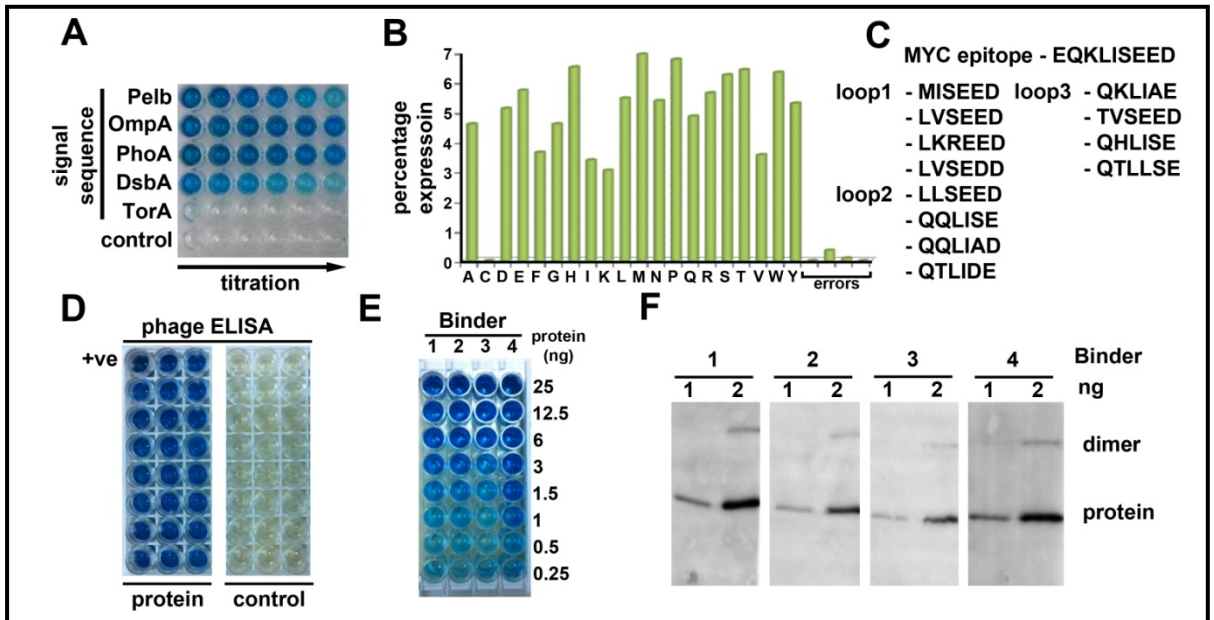

Figure 1: **(a)** expression of nABP by different signal sequences, the colour intensity indicates expression level. **(b)** 100 clones were sequenced to show amino acid distribution of the loop regions. **(c)** loop sequences similar to the MYC epitope found in the nABPs. **(d)** Positive phage ELISA of 23 clones against target protein compared with negative control wells **(e)**, four purified nABPs were labelled with biotin and used as reagents to detect target protein. All showed sensitive detection of target protein by ELISA. **(f)** biotin labelled nABPs used to detect target protein by Western blotting.

The nABP library was then used to identify binders to the anti-MYC antibody. After two panning rounds by phage ELISA every nABP selected contained a loop region with at least

one similar sequence to the myc-tag epitope, confirming all three loops are exposed and can interact with target proteins (Figure 1C). Next we performed phage display against a biotinylated target protein that was presented on plates or magnetic beads coated with streptavidin or neutravidin. After pan three phage clones showing specific binding to the target by phage ELISA were isolated (Figure 1D). Four nABPs were purified and used in ELISAs (Figure 1E) and Western blots (Figure 1F).

We have now generated reagents against twelve different proteins. The selected nABPs are being assessed for use in applications including electronic devices for diagnostics, reagents for molecular and cellular biology, reagents for inhibiting protein-protein interactions, and co-crystallisation to map binding sites for drug discovery. The BSTG works collaboratively on many projects, contact Darren Tomlinson or Mike McPherson if these types of reagents are of interest.

Publications

Deacon, S. & McPherson, M. (2011) Enhanced expression and purification of fungal galactose oxidase in *Escherichia coli* and use for analysis of a saturation mutagenesis library. *ChemBioChem* **12:** 593-601.

Lamont, F., Tomlinson, D., Cooper, P., Shnyder, S., Chester, J. & Knowles M. (2011) Small molecule FGF receptor FGFR-dependent urothelial carcinoma growth in vitro and in vivo inhibitor. *Br. J. Cancer* **104:**75-82.

Stadler, L., Hoffmann, T., Tomlinson, D., Song, Q., Lee, T., Busby, M., Nyathi, Y., Gendra, E., Tiede, C., Flanagan, K., Cockell, S., Wipat, A., Harwood, C., Wagner, S., Knowles, M., Davis, J. & Ko Ferrigno, P. (2011) Structure-function studies of an engineered scaffold protein derived from Stefin A. II: Development and Applications of the SQT variant. *Protein Eng. Des. Sel.* **24:**751-63.

Funding

Our group is supported by the Biomedical Health Research Centre, EPSRC, YCR and LLR.

Collaborators

Our collaborators include the WELMEC project, Ann Morgan, Andrew MacDonald, Michael Webb, Francesco Del Galdo, Stephen Griffin, Douglas Thompson, Richard Barton, Reuben Tooze, Gina Doody, Bruce Turnbull, Colin Johnson, Mark Hull, Kevin Critchley, Neil Smith (AstraZeneca) and Chris Ullman (Isogenica).

Structure and operation of the DNA-translocating type I DNA restriction enzymes

Christopher Kennaway, Chun Feng Song, William Nicholson and John Trinick

Introduction

Type I DNA restriction/modification (RM) enzymes (~250 kDa) are complex molecular machines found in the majority of bacterial species. Their early discovery paved the way for the development of genetic engineering using Type II enzymes. They control (restrict) the influx of foreign DNA via horizontal gene transfer into the bacterium while maintaining sequence-specific methylation (modification) of host DNA. The endonuclease reaction of these enzymes on unmethylated DNA is preceded by bidirectional translocation of thousands of base pairs of DNA toward the enzyme.

Results

The structures of two type I RM enzymes, EcoKI and EcoR124I, were studied using electron microscopy (EM), small-angle scattering (neutron and X-ray), and molecular modeling. The electron microscopy and image processing was done in Leeds. DNA binding triggers a large contraction of the open form of the enzyme to a compact form. The path followed by DNA through the complexes was revealed by using a DNA mimic anti-restriction protein. The structures reveal an evolutionary link between type I RM enzymes and type II RM enzymes.

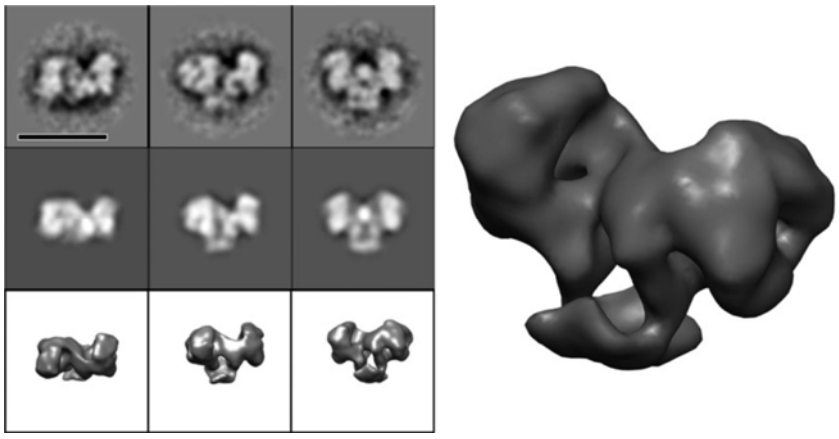

Figure 1: structure of the Type I RM enzyme EcoR124I (+DNA) determined by negative stain electron microscopy and single particle image processing. For the 3 × 3 panel, the top row is image averages, the middle row is the corresponding 3D reconstruction reprojections, and the bottom row is 3D surface views of the 3D reconstruction (bar, 200 A˚); on the right is a larger 3D surface.perspective view. The longest dimension is ~18 nm.

Funding

Supported by BBSRC.

Collaborators

David Dryden (University of Edinburgh), Geoff Kneale (University of Portsmouth) and Janusz Bujnicki (Adam Mickiewicz University, Poznan, Poland) .

Nucleic acid translocation by a hexameric molecular motor at single molecule level

Roman Tuma

Introduction

The viral packaging ATPase P4 is a cooperative molecular motor that translocates RNA into preformed capsids. P4 belongs to the ubiquitous class of hexameric helicases. The mechanisms proposed for action of P4 and other hexameric helicases assume that subunits cycle through discrete states with different affinities for the bound nucleic acid. P4 and other hexameric helicases load their nucleic acid substrates into the central channel via a ring opening mechanism which results in a stable topological enclosure of the bound strand. The bound nucleic acid in turn stimulates the ATPase activity and induces catalytic cooperativity. The cooperativity and nucleic acid affinity depend on the interactions between the topologically enclosed nucleic acid and the motor. However, the topological enclosure of the polynucleotide poses problems for quantitative assessment of these interactions. Commonly used ensemble assays (e.g. gel electrophoresis mobility shift, fluorescence) measure the coupled reaction consisting of the loading (ring opening) and the intrinsic binding inside the channel which in turn controls movement along nucleic acid strand. On the other hand, single molecule techniques permit study of intrinsic binding within the central channel separate of the loading process.

Results

Using a single molecule approach we have characterized translocation of P4 along ssRNA. P4 undergoes one-dimensional diffusion along the topologically bound RNA. The diffusion is hindered by activation energy barriers that depend on the nucleotide binding state of the motor. In the presence of ATP, net unidirectional movement is discernible in addition to reduced diffusive motion. At low ATP concentrations translocation is frequently interrupted by periods of fast diffusion. The results suggest that P4 grasps RNA using a clutch-like mechanism instead of cycling through stable, discrete RNA-binding states. During translocation, ATP hydrolysis-driven conformational changes are transmitted to RNA via electrostatic potential of the clutch (Fig. 1).

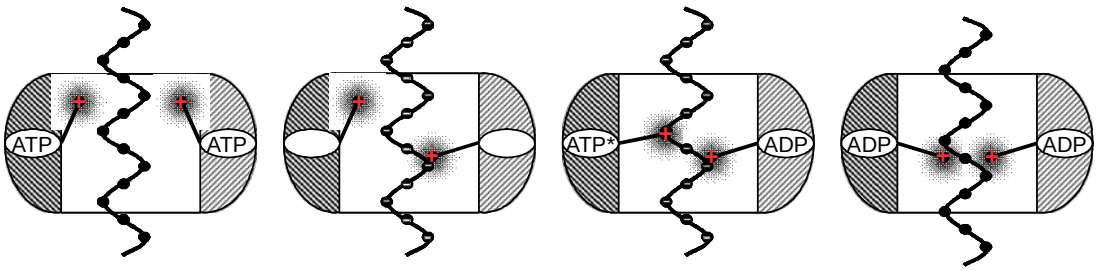

Figure 1: positively charged levers in P4 channel (red) enclose a negatively charged RNA (black) and form an electrostatic clutch. From left to right: In the presence of ATP the levers are withdrawn and weakly interact with RNA; stronger interaction with RNA is observed in the apo state in which the levers are free to adopt several conformations; during hydrolysis and in the presence of ADP the levers are clamped onto the RNA to prevent sliding.

Collaborators

Most of the work has been done by my former colleagues J. Lisal, T. Malinauskas and K. Hattula (University of Helsinki, Finland).

Synthesis and application of stable phosphohistidine analogues

Tom McAllister, Jeff Hollins, Katherine Horner, Nathalie Valette, Zhenlian Ling, Arwen Pearson, Michael Nix, Darren Tomlinson and Michael Webb

Introduction

Phosphorylation of histidine is central to regulation of bacterial two-component signalling and is frequently observed as in intermediate in enzymatic reaction mechanisms. Its importance in eukaryotic systems is however not known; the lability of the modification means that no immunochemical probes of the modified amino acids exist. Our interest in this modification stems from its presence in the substrate of the PPDK regulatory protein (PDRP) from plants and bacteria. PDRP only inactivates PPDK when the catalytic intermediate, phosphohistidine is present.

Results

We have recently reported an optimised synthesis of our analogues of phosphohistidine which is fully compatible with the Fmoc-strategy for solid-phase peptide synthesis. We are now using these analogues both to explore the mechanism of PDRP but also to identify antibodies and non-antibody binding proteins capable of specifically recognising the modification in the context of a protein.

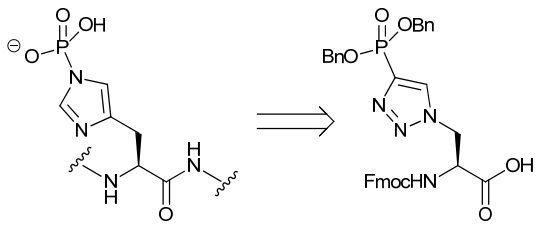

Figure 1: design strategy used the development of stable analogues of phosphohistidine.

Publications

Astley, H., Parsley, K., Aubry, S., Chastain, C., Burnell, J, Webb, M. & Hibberd, J. (2011) The pyruvate, orthophosphate dikinase regulatory proteins of Arabidopsis are both bifunctional and interact with the catalytic and nucleotide binding domains of pyruvate,orthophosphate dikinase *Plant J.* **68:**1070-1080

McAllister, T., Nix, M. & Webb, M. (2011) Fmoc-chemistry of stable analogues of phosphohistidine *Chem. Commun*. **47:**1297-1299

Funding

This work was funded by the BBSRC and the EPSRC

Collaborators

J. Hibberd (Cambridge) and C. Eyers (Manchester)

Identification of the ribonucleoprotein complex required for efficient viral RNA processing in oncogenic herpesviruses

Brian Jackson, Marko Norenberg, Sophie Schumann and Adrian Whitehouse

Introduction

Post-transcriptional events which regulate mRNA biogenesis are central to the regulation of gene expression. As a consequence, cells have evolved a 'gene-expression production line' that encompasses the routing of a nascent transcript through multimeric mRNA–protein complexes that mediate its splicing, polyadenylation, nuclear export and translation. Of these events it has become clear that splicing is particularly important for mRNA nuclear export, as recruitment of multiprotein complexes required for mRNA export are bound to mRNA in a splicing dependent manner. Two multiple protein complexes, namely, hTREX and the EJC bind at separate locations on spliced mRNA. hTREX, which comprises Aly, UAP56 and the multiprotein ThoI complex, is recruited exclusively to the 5' end of the first exon, providing 5'-polarity and therefore directionality observed in mRNA export.

However, in contrast to the majority of mammalian genes, analysis of herpesvirus genomes has highlighted that most lytically expressed viral genes lack introns. Herpesviruses replicate in the nucleus of the host mammalian cell, and therefore require their intronless mRNAs to be exported out of the nucleus to allow viral mRNA translation in the cytoplasm. This therefore leads to an intriguing question concerning the mechanism by which the viral intronless mRNAs are exported out of the nucleus in the absence of splicing. To circumvent this problem, and to facilitate viral mRNA export, γ-2 herpes viruses encode the ORF 57 protein. ORF 57 interacts with Aly, binds viral RNA, shuttles between the nucleus and the cytoplasm and promotes the nuclear export of viral mRNA.

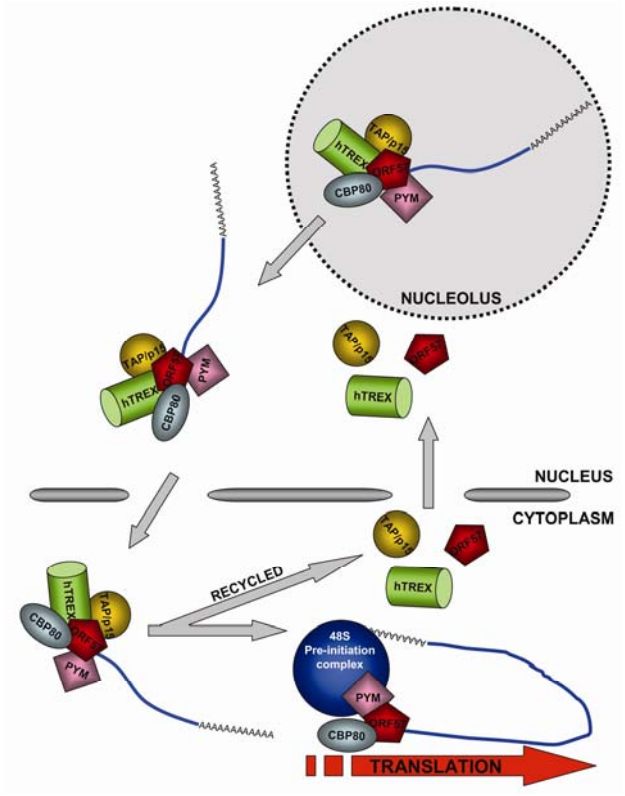

Figure 1: KSHV ORF57 mimics splicing to recruit the necessary nuclear export factors onto viral intronless transcipts and also mimics an EJC to enhance their translation.

We are currently investigating how an intronless viral mRNP is assembled in KSHV and what role ORF57 plays in that process. We have shown that ORF57 interacts with hTREX and is essential for the recruitment of hTREX onto intronless viral mRNA transcripts. Importantly, ORF57 does not recruit the EJC to intronless viral transcripts. Moreover, we are currently determining how ORF 57 recognises the viral mRNA and allows recruitment of hTREX. This is the first system that has distinguished between hTREX and EJC *in vivo* and demonstrates that recruitment of hTREX alone to mRNA transcripts is sufficient for their nuclear export. Therefore, we believe this viral system is an exciting model to further study mRNA export mechanisms. We propose a model for

herpesvirus mRNA export, whereby ORF57 mimics splicing in order to recruit the mRNA export machinery to intronless viral mRNAs.

We are now determining the structure of the interaction interface at atomic-resolution between ORF57 homologues and the hTREX proteins, such as Aly, In collaboration with Dr Alexander Golovanov (University of Manchester) and Professr Stuart Wilson (University of Sheffield). This will provide a detailed comparison of the binding interfaces between ORF57 homologues and Aly using solution-state NMR. The regions of HSV ICP27 and HVS ORF57 involved in binding by Aly have been mapped as residues 104-112 and 103-120, respectively. We have identified the pattern of residues critical for Aly recognition, common to both ICP27 and ORF57. The importance of the key amino acid residues within these binding sites was confirmed by site-directed mutagenesis. The functional significance of the ORF57-REF/Aly interaction was also probed using an *ex vivo* cytoplasmic viral mRNA accumulation assay and this revealed that mutants that reduce the protein-protein interaction dramatically decrease the ability of ORF57 to mediate the nuclear export of intronless viral mRNA. Together these data precisely map amino acid residues responsible for the direct interactions between viral adaptors and cellular REF/Aly and provide the first molecular details of how herpes viruses access the cellular mRNA export pathway. Future work will utilise these identified binding interfaces as possible new drug targets, to be used in the future for anti-viral drug design efforts, for the prevention or treatment of KSHV-related malignancies usinf rational-based drug design approaches.

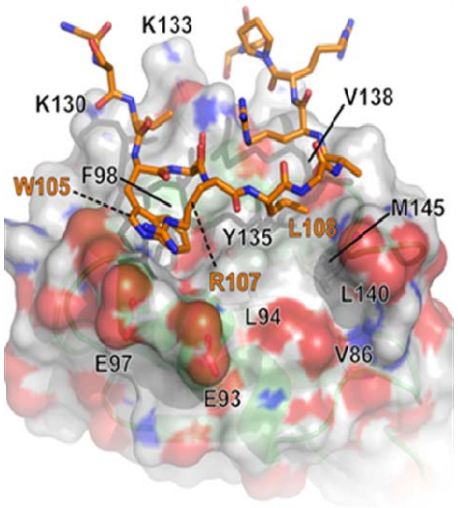

Figure 1: ORF57 homologue (HSV ICP27) recognizes and specifically binds to the surface of the RRM domain of cellular export factor REF/Aly.

Publications

Jackson, B., Boyne, J., Norenberg, M., Taylor, A., Hautbergue, G., Walsh, M., Wheat, R., Blackbourn, D., Wilson, S. & Whitehouse, A. (2011) An interaction between KSHV ORF57 and UIF provides mRNA-adaptor redundancy in herpesvirus intronless mRNA export. *PLoS Pathog.* **7:**e1002138.

Taylor, A., Jackson, B., Noerenberg, M., Hughes, D., Boyne, J., Verow, M., Harris, M. & Whitehouse, A. (2011) Mutation of a C-terminal motif affects KSHV ORF57 RNA binding, nuclear trafficking and multimerisation. *J. Virol.* **85:**7881-7891.

Tunnicliffe, R., Hautbergue, G., Kalra, P., Jackson, B., Whitehouse, A., Wilson, S. & Golovanov, A. (2011) Structural basis for the recognition of cellular mRNA export factor REF by herpes viral proteins HSV-1 ICP27 and HVS ORF57. *PLoS Pathog*. **7:**e1001244.

Funding

This project is funded by the BBSRC, YCR and Wellcome Trust.

Designed inhibitors of protein-protein interactions

Maria Filby, Panchami Prabhakaran, Valeria Azzarito, Kerya Long, Natasha Murphy, Alison Ashcroft, Thomas Edwards, Stuart Warriner, Adrian Whitehouse and Andrew Wilson

Introduction

Protein-Protein interactions (PPIs) play prominent roles in many biological processes and hence provide attractive opportunities for the design of small molecule based therapeutics. In this bottom-up approach, *'Proteomimetics'* - synthetic molecules that can mimic the spatial projection of key binding residues from a secondary structural motif have proven to be effective for generation of inhibitors of several PPIs. Similarly, '*Surface mimetics'* - molecules with recognition domains from a core scaffold in a multivalent manner can attain high affinity protein surface recognition. This report will summarise our group's efforts using these two methods.

α-helix mimetic inhibitors

Aromatic oligoamides functionalized with different side chains based on two scaffolds, reported from our group act as α-helix mimetic inhibitors of the oncogenic p53-hDM2 interaction. In order to probe how side-chain side-chain interactions might control/stabilise the active conformation, oligomers functionalized with different side-chains were synthesized. Solid-state and solution-state conformational analyses prove conformational pre-organization through hydrogen bonding. The studies also show that even with simple aromatic and aliphatic substituents, side chain orientation is subject to subtle steric and non-covalent effects (See Fig. 1). In the past year, we have developed a solid-phase synthesis method for these scaffolds that exploits a CEM™ automated microwave assisted peptide synthesizer. These results will help us in our ongoing research work to design libraries bioactive helix mimetics.

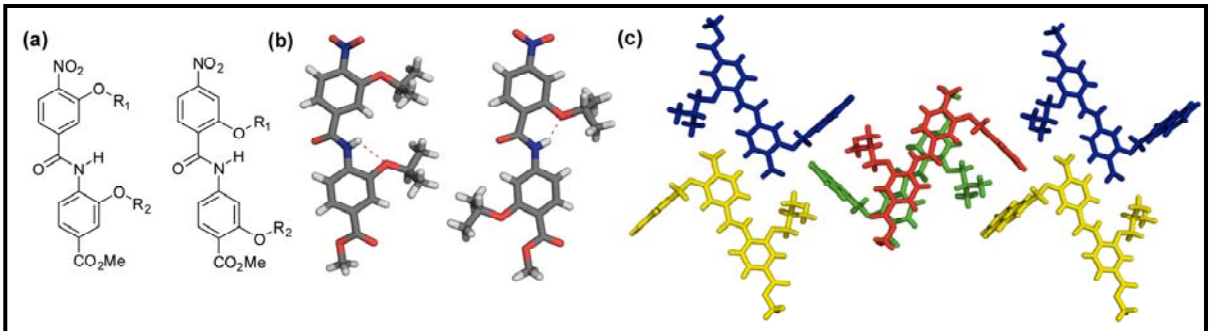

Figure 1: (a) structure of *O*-alkylated helix mimetic scaffolds (b) crystal structures of oligobenzamides (c) side-chain hydrophobic interactions observed in solid-state packing.

Surface mimetics

Our initial studies on highly functionalized ruthenium(II) tris-bipyridine complexes show that these compounds can as receptors for protein-surfaces and can be used as inhibitors of protein-protein interactions. As a part of this ongoing research, we assessed the cellular uptake of a series of ruthenium complexes possessing diverse functional groups. This will help us to understand the role of functional groups in modulating the cell-uptake, localisation and toxicity prperties. Complexes having molecular weight >3000 Da and multiple negative charges, are efficiently transfected into HEK-293T cells with 95% efficiency at low concentration (10 μM) and are generally not toxic, making them suitable for further elaboration as cellular probes. Localisation is to lysosomes and our results suggest endocytosis is the mechanism of cell uptake (Fig. 2). Our future studies are focused towards

modifying the compounds to promote endosomal release, so as to pursue the goal of developing cell permeable inhibitors of PPIs.

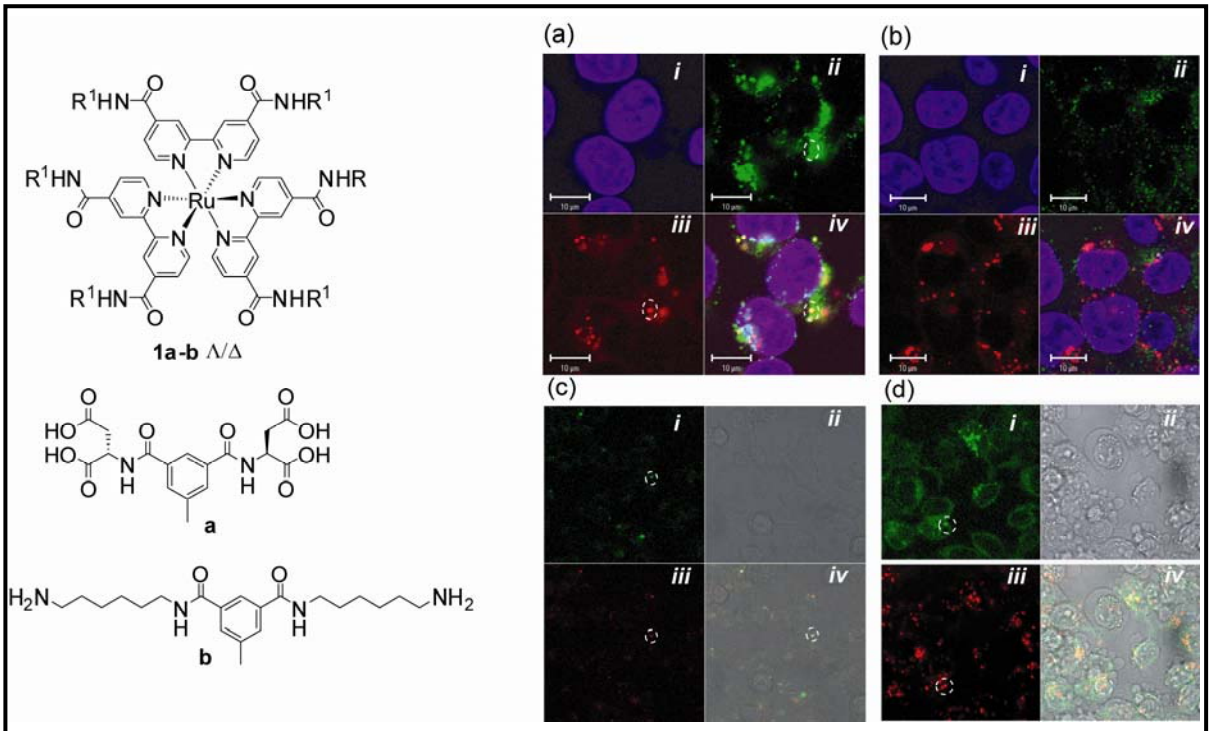

Figure 1: cell localization behavior of compounds 1a and 1b **(a)** 1b with antibody for LAMP1 in fixed cells and **(b)** 1b with antibody for MPR in fixed cells (i) nucleus staining with propidium iodide (ii) Lysosome (LAMP1) or golgi network (MPR) staining (iii) Ruthenium complex emits pink/red (iv) colocalization of all the panels.; **(c)** 1a with lysotracker in living cells and **(d)** 1b with lysotracker in living cells; colocalisation is denoted by white dashed circle.

Publications

Gooch, A., Barrett, S., Fisher, J., Lindsay, C. & Wilson, A. (2011) Ditopic triply hydrogen-bonded heterodimers *Org. Biomol. Chem.* **9:**5938-5940.

Gooch, A., McGhee, A., Pellizzaro, M., Lindsay, C. & Wilson, A. (2011) Substituent control over dimerization affinity of triply hydrogen bonded heterodimers *Org. Lett.* **13:**240-243.

Filby, M. Muldoon, J., Dabb, S., Fletcher, N., Ashcroft, A. & Wilson, A. (2011) Protein surface recognition using geometrically pure Ru(II) tris(bipyridine) derivatives. *Chem. Commun.* **47:**559-561.

McGhee, A., Plante, J., Kilner, C. & Wilson, A. (2011) Solid-state structures of ureidoimidazoles *Supramol*. *Chem*. **23:**470-479.

Pellizzaro, M., McGhee, A., Renton, L., Nix, M., Fisher, J., Turnbull, W. & Wilson, A. (2011) Conformer-independent ureidoimidazole motifs-tools to probe conformational and tautomeric effects on the molecular recognition of triply hydrogen-bonded heterodimers. *Chemistry* **17:**14508-14517.

Funding

We gratefully acknowledge EPSRC, the University of Leeds, The Wellcome Trust, Yorkshire Cancer Research and The European Research Council for financial support of this research.

ASTBURY SEMINARS 2011

13th January
Dr Gianfranco Gilardi , Division of Molecular Biosciences, Imperial College London
"Cytochrome P450: A versatile class of enzyme for environmental and pharmacological applications"

3rd February
Dr Tom Monie, Department of Biochemistry, Univeristy of Cambridge
"SNPing apart immune signalling - is it more than just a CARD trick?"

1st April
Prof Stephen Curry, Division of Cell and Molecular Biology, Imperial College London
"Your flexible foe: structure of 3C protease, a potential drug target from foot-and-mouth disease virus"

15th April
Prof Cristina Risco, National Center for Biotechnology, Madrid
"Studying virus factories and cell architecture with new high resolution imaging techniques"

3rd May
Prof Ken Taylor, Institute of Molecular Biophysics, Florida State University at Tallahassee
"Visualizing active contraction in insect flight muscle using electron tomography: novel thin filament attachments revealing the myosin power stroke and a mechanisms for stretch activation"

13th June
Dr Sarah Butcher, Institute of Biotechnology, University of Helsinki
"Secrets of an age-old plague revealed by electron cryo-tomography"

16th June
Annual Astbury Lecture
Prof Sir Alec Jeffreys, Department of Genetics, University of Leicester
"Genetic fingerprinting: past, present and future"

13th July
Prof Rohit Pappu, Washington University in St Louis
"Phase behaviour of intrinsically disordered proteins and implications for specificity in DNA binding"

18th July
Prof Juliet Gerrard, School of Biological Sciences, University of Canterbury, New Zealand
"Amyloid fibrils as useful materials?"

19th October
Dr Andrew Thomas, Hoffman-La Roche Ltd, Basel, Switzerland
"Discovery of RG1678: A potent and selective GlyT1 inhibitor (GRI) for the treatment of Schizophrenia"

3rd November
Dr Simon Webb, Manchester Interdisciplinary Biocentre, University of Manchester
"Mimicking membranes using molecular self-assembly"

10th November
Dr Liz Duke, Diamond Light Source
"Soft X-ray Cryo Microscopy: Opportunities for imaging intact biological cells"

8th December

Prof Stephen Evans, School of Physics and Astronomy, University of Leeds

"I Lose, You Lose, We Win: Implementing Simple Strategies for the Manipulation of Membrane Proteins"

PUBLICATIONS BY ASTBURY CENTRE MEMBERS 2011

Achalkumar, A., Bushby, R. and Evans, S. (2011) Synthesis of nitrilotriacetic acid terminated tethers for the binding of his-tagged proteins to lipid bilayers and to gold. *Tetrahedron* **67:** 6246-6251.

Adams, J., Fielding, S. and Olmsted, P. (2011) Transient shear banding in entangled polymers: A study using the rolie-poly model. *J. Rheol.* **55:** 1007-1032.

Aljabali, A., Barclay, J., Cespedes, O., Rashid, A., Staniland, S., Lomonossoff, G. and Evans, D. (2011) Charge modified cowpea mosaic virus particles for templated mineralization. *Adv. Func. Mater.* **21:** 4137-4142.

Astley, H., Parsley, K., Aubry, S., Chastain, C., Burnell, J., Webb, M. and Hibberd, J. (2011) The pyruvate, orthophosphate dikinase regulatory proteins of arabidopsis are both bifunctional and interact with the catalytic and nucleotide-binding domains of pyruvate, orthophosphate dikinase. *Plant J.* **68:** 1070-1080.

Auer, S. (2011) Phase diagram of polypeptide chains. *J. Chem. Phys*. **DOI:** 10.1063/1.3656764.

Beales, P., Bergstrom, C., Geerts, N., Groves, J. and Vanderlick, T. (2011) Single vesicle observations of the cardiolipin-cytochrome c interaction: Induction of membrane morphology changes. *Langmuir* **27:** 6107-6115.

Beales, P., Nam, J. and Vanderlick, T. (2011) Specific adhesion between DNA-functionalized "Janus" vesicles: Size-limited clusters. *Soft Matter* **7:** 1747-1755.

Belyaev, N., Kellett, K., Beckett, C., Makova, N., Revett, T., Nalivaeva, N., Hooper, N. and Turner, A. (2010) The transcriptionally active amyloid precursor protein (app) intracellular domain is preferentially produced from the 695 isoform of app in a beta-secretase-dependent pathway. *J. Biol. Chem*. **285:** 41443-41454.

Berryman, J., Radford, S. and Harris, S. (2011) Systematic examination of polymorphism in amyloid fibrils by molecular-dynamics simulation. *Biophys. J*. **100:** 2234-2242.

Blake, K., Randall, C. and O'Neill, A. (2011) In vitro studies indicate a high resistance potential for the lantibiotic nisin in staphylococcus aureus and define a genetic basis for nisin resistance. *Antimicrob. Agents Chemother*. **55:** 2362-2368.

Bon, R., Guo, Z., Stigter, E., Wetzel, S., Menninger, S., Wolf, A., Choidas, A., Alexandrov, K., Blankenfeldt, W., Goody, R. and Waldmann, H. (2011) Structure-guided development of selective rabggtase inhibitors. *Angew. Chem. Int. Ed. Engl.* **50:** 4957-4961.

Bone, H., Nelson, A., Goldring, C., Tosh, D. and Welham, M. (2011) A novel chemically directed route for the generation of definitive endoderm from human embryonic stem cells based on inhibition of gsk-3. *J. Cell Sci*. **124:** 1992-2000.

Bradley, H., Baldwin, J., Goli, G. R., Johnson, B., Zou, J., Sivaprasadarao, A., Baldwin, S. and Jiang, L.-H. (2011) Residues 155 and 348 contribute to the determination of p2x(7) receptor

function via distinct mechanisms revealed by single-nucleotide polymorphisms. *J. Biol. Chem*. **286:** 8176-8187.

Brown, L.-A., O'Leary-Steele, C., Brookes, P., Armitage, L., Kepinski, S., Warriner, S. and Baker, A. (2011) A small molecule with differential effects on the pts1 and pts2 peroxisome matrix import pathways. *Plant J.* **65:** 980-990.

Brukhno, A., Akinshina, A., Coldrick, Z., Nelson, A. and Auer, S. (2011) Phase phenomena in supported lipid films under varying electric potential. *Soft Matter* **7:** 1006-1017

Bunka, D., Lane, S., Lane, C., Dykeman, E., Ford, R., Barker, A., Twarock, R., Phillips, S. and Stockley, P. (2011) Degenerate RNA packaging signals in the genome of satellite tobacco necrosis virus: Implications for the assembly of a t=1 capsid. *J. Mol. Biol*. **413:** 51-65.

Cabriolu, R. and Auer, S. (2011) Amyloid fibrillation kinetics: Insight from atomistic nucleation theory. *J. Mol. Biol*. **411:** 275-285.

Cabriolu, R., Kashchiev, D. and Auer, S. (2011) Size distribution of amyloid nanofibrils. *Biophys. J.* **101:** 2232-2241.

Campos-Sandoval, J., Redondo, C., Kinsella, G., Pal, A., Jones, G., Eyre, G., Hirst, S. and Findlay, J. (2011) Fenretinide derivatives act as disrupters of interactions of serum retinol binding protein (srbp) with transthyretin and the srbp receptor. *J. Med. Chem.* **54:** 4378-4387.

Cheetham, M., Bramble, J., McMillan, D., Krzeminski, L., Han, X., Johnson, B., Bushby, R., Olmsted, P., Jeuken, L., Marritt, S., Butt, J. and Evans, S. (2011) Concentrating membrane proteins using asymmetric traps and ac electric fields. *J. Am. Chem. Soc*. **133:** 6521-6524.

Cheneler, D., Bowen, J., Evans, S., Gorzny, M., Adams, M. and Ward, M. (2011) Characteristics and durability of fluoropolymer thin films. *Polym. Degradation Stab.* **96:** 561-565.

Crampton, N., Alzahrani, K., Beddard, G., Connell, S. and Brockwell, D. (2011) Mechanically unfolding protein l using a laser-feedback-controlled cantilever. *Biophys. J.* **100:** 1800-1809.

da Costa, A., Keen, J., Wild, C. and Findlay, J. (2011) An analysis of the phosphoproteome of immune cell lines exposed to the immunomodulatory mycotoxin deoxynivalenol. *Biochim. Biophys. Acta* **1814:** 850-857.

da Costa, A., Mijal, R., Keen, J., Findlay, J. and Wild, C. (2011) Proteomic analysis of the effects of the immunomodulatory mycotoxin deoxynivalenol. *Proteomics* **11:** 1903-1914.

Dallas, M., Boyle, J., Milligan, C., Sayer, R., Kerrigan, T., McKinstry, C., Lu, P., Mankouri, J., Harris, M., Scragg, J., Pearson, H. and Peers, C. (2011) Carbon monoxide protects against oxidant-induced apoptosis via inhibition of K(v)2.1. *FASEB J.* **25:** 1519-1530.

Daskalakis, N., Mueller, A., Evans, S. and Jeuken, L. (2011) Driving bioenergetic processes with electrodes. *Soft Matter* **7:** 49 - 52.

Deacon, S. and McPherson, M. (2011) Enhanced expression and purification of fungal galactose oxidase in *Escherichia coli* and use for analysis of a saturation mutagenesis library. *ChemBioChem* **12:** 593-601.

Deville, K., Gold, V., Robson, A., Whitehouse, S., Sessions, R., Baldwin, S., Radford, S. and Collinson, I. (2011) The oligomeric state and arrangement of the active bacterial translocon. *J. Biol. Chem.* **286:** 4659-4669.

Dykeman, E., Grayson, N., Toropova, K., Ranson, N., Stockley, P. and Twarock, R. (2011) Simple rules for efficient assembly predict the layout of a packaged viral RNA. *J. Mol. Biol*. **408:** 399-407.

East, D., Sousa, D., Martin, S., Edwards, T., Lehman, W. and Mulvihill, D. (2011) Altering the stability of the cdc8 overlap region modulates the ability of this tropomyosin to bind co-operatively to actin and regulate myosin. *Biochem. J*. **438:** 265-273.

Eichner, T., Kalverda, A., Thompson, G., Homans, S. and Radford, S. (2011) Conformational conversion during amyloid formation at atomic resolution. *Mol. Cell* **41:** 161-172.

Elboray, E., Grigg, R., Fishwick, C., Kilner, C., Sarker, M., Aly, M. and Abbas-Temirek, H. (2011) X=y-zh compounds as potential 1,3-dipoles. Part 65: Atom economic cascade synthesis of highly functionalized pyrimidinylpyrrolidines. *Tetrahedron* **67:** 5700-5710.

Filby, M., Muldoon, J., Dabb, S., Fletcher, N., Ashcroft, A. and Wilson, A. (2011) Protein surface recognition using geometrically pure Ru(ii) tris(bipyridine) derivatives. *Chem. Commun*. **47:** 559-561.

Flatt, J., Guizouarn, H., Burton, N., Borgese, F., Tomlinson, R., Forsyth, R., Baldwin, S., Levinson, B., Quittet, P., Aguilar-Martinez, P., Delaunay, J., Stewart, G. and Bruce, L. (2011) Stomatin-deficient cryohydrocytosis results from mutations in slc2a1: A novel form of glut1 deficiency syndrome. *Blood* **118:** 5267-5277.

Foster, R., Bonner, M. and Ward, I. (2011) The use of nano and micron-sized particles to enhance the interlayer adhesion in self-reinforced, single-polymer composites. *Composites Sci. Technol*. **71:** 461-465.

Foster, T., Gallay, P., Stonehouse, N. and Harris, M. (2011) Cyclophilin a interacts with domain ii of hepatitis c virus ns5a and stimulates RNA binding in an isomerase-dependent manner. *J. Virol*. **85:** 7460-7464.

Foster, T., Verow, M., Wozniak, A., Bentham, M., Thompson, J., Atkins, E., Weinman, S., Fishwick, C., Foster, R., Harris, M. and Griffin, S. (2011) Resistance mutations define specific antiviral effects for inhibitors of the hepatitis c virus p7 ion channel. *Hepatology* **54:** 79-90.

Galloway, J., Arakaki, A., Masuda, F., Tanaka, T., Matsunaga, T. and Staniland, S. (2011) Magnetic bacterial protein mms6 controls morphology, crystallinity and magnetism of cobalt-doped magnetite nanoparticles in vitro. *J. Mater. Chem*. **21:** 15244-15254.

Garcia, J., Zhang, Y., Taylor, H., Cespedes, O., Webb, M. and Zhou, D. (2011) Multilayer enzyme-coupled magnetic nanoparticles as efficient, reusable biocatalysts and biosensors. *Nanoscale* **3:** 3721-3730.

Glover, C., Postis, V., Charalambous, K., Tzokov, S., Booth, W., Deacon, S., Wallace, B., Baldwin, S. and Bullough, P. (2011) Acrb contamination in 2-d crystallization of membrane proteins: Lessons from a sodium channel and a putative monovalent cation/proton antiporter. *J. Struct. Biol*. **176:** 419-424.

Glowacki, D., Paci, E. and Shalashilin, D. (2011) Boxed molecular dynamics: Decorrelation time scales and the kinetic master equation. *J. Chem. Theory Comput.* **7:** 1244-1252.

Gooch, A., Barrett, S., Fisher, J., Lindsay, C. and Wilson, A. (2011) Ditopic triply hydrogen-bonded heterodimers. *Org. Biomol. Chem*. **9:** 5938-5940.

Gooch, A., McGhee, A., Pellizzaro, M., Lindsay, C. and Wilson, A. (2011) Substituent control over dimerization affinity of triply hydrogen bonded heterodimers. *Org. Lett.* **13:** 240-243.

Goulet, A., Lai-Kee-Him, J., Veesler, D., Auzat, I., Robin, G., Shepherd, D., Ashcroft, A., Richard, E., Lichiere, J., Tavares, P., Cambillau, C. and Bron, P. (2011) The opening of the spp1 bacteriophage tail, a prevalent mechanism in gram-positive-infecting siphophages. *J. Biol. Chem.* **286:** 25397-25405.

Grant, C., Thomson, N., Savage, M., Woon, H. and Greig, D. (2011) Surface characterisation and biomechanical analysis of the sclera by atomic force microscopy. *J. Mech. Behav. Biomed.* **4:** 535-540.

Griffiths, H., Whitehouse, I., Baybutt, H., Brown, D., Kellett, K., Jackson, C., Turner, A., Piccardo, P., Manson, J. and Hooper, N. (2011) Prion protein interacts with bace1 protein and differentially regulates its activity toward wild type and swedish mutant amyloid precursor protein. *J. Biol. Chem.* **286:** 33489-33500.

Gumiero, A., Metcalfe, C., Pearson, A., Raven, E. L. and Moody, P. (2011) Nature of the ferryl heme in compounds i and ii. *J. Biol. Chem*. **286:** 1260-1268.

Hedberg, C., Dekker, F., Rusch, M., Renner, S., Wetzel, S., Vartak, N., Gerding-Reimers, C., Bon, R., Bastiaens, P. and Waldmann, H. (2011) Development of highly potent inhibitors of the ras-targeting human acyl protein thioesterases based on substrate similarity design. *Angew. Chem. Int. Ed. Engl.* **50:** 9832-9837.

Ho, V., Slater, N. and Chen, R. (2011) Ph-responsive endosomolytic pseudo-peptides for drug delivery to multicellular spheroids tumour models. *Biomaterials* **32:** 2953-2958.

Hoffmann, A., Nettels, D., Clark, J., Borgia, A., Radford, S., Clarke, J. and Schuler, B. (2011) Quantifying heterogeneity and conformational dynamics from single molecule fret of diffusing molecules: Recurrence analysis of single particles (rasp). *Phys. Chem. Chem. Phys.* **13:** 1857-1871.

Hollingworth, P. *et al.* (2011) Common variants at ABCA7, MS4A6A/MS4A4E, EPHA1, CD33 and CD2AP are associated with Alzheimer's disease. *Nat. Genet.* **43:** 429-435.

Hong, Y., Macnab, S., Lambert, L., Turner, A., Whitehouse, A. and Usmani, B. (2011) Herpesvirus saimiri-based endothelin-converting enzyme-1 shrna expression decreases prostate cancer cell invasion and migration. *Int. J. Cancer* **129:** 586-598.

Hooper, N. (2011) Glypican-1 facilitates prion conversion in lipid rafts. *J. Neurochem*. **116:** 721-725.

Ilett, E., Barcena, M., Errington-Mais, F., Griffin, S., Harrington, K., Pandha, H., Coffey, M., Selby, P., Limpens, R., Mommaas, M., Hoeben, R., Vile, R. and Melcher, A. (2011) Internalization of oncolytic reovirus by human dendritic cell carriers protects the virus from neutralization. *Clin. Cancer. Res.* **17:** 2767-2776.

Jackson, B., Boyne, J., Noerenberg, M., Taylor, A., Hautbergue, G., Walsh, M., Wheat, R., Blackbourn, D., Wilson, S. and Whitehouse, A. (2011) An interaction between KSHV ORF57 and UIF provides mRNA-adaptor redundancy in herpesvirus intronless mRNA export. *PLoS Pathog.* 7: e1002138.

Jenkins, H., Malkova, B. and Edwards, T. (2011) Kinked beta-strands mediate high-affinity recognition of mRNA targets by the germ-cell regulator DAZL. *Proc. Natl. Acad. Sci. USA* **108:** 18266-18271.

Jopling, H., Howell, G., Gamper, N. and Ponnambalam, S. (2011) The VEGFR2 receptor tyrosine kinase undergoes constitutive endosome-to-plasma membrane recycling. *Biochem. Biophys. Res. Commun*. **410:** 170-176.

Jung, H. S., Billington, N., Thirumurugan, K., Salzameda, B., Cremo, C., Chalovich, J., Chantler, P. and Knight, P. (2011) Role of the tail in the regulated state of myosin 2. *J. Mol. Biol*. **408:** 863-878.

Kaur-Atwal, G., Reynolds, J., Mussell, C., Champarnaud, E., Knapman, T., Ashcroft, A., O'Connor, G., Christie, S. and Creaser, C. (2011) Determination of testosterone and epitestosterone glucuronides in urine by ultra performance liquid chromatography-ion mobility-mass spectrometry. *Analyst* **136:** 3911-3916.

Khandelwal, N., Simpson, J., Taylor, G., Rafique, S., Whitehouse, A., Hiscox, J. and Stark, L. (2011) Nucleolar nf-kappa b/rela mediates apoptosis by causing cytoplasmic relocalization of nucleophosmin. *Cell Death Differ*. **18:** 1889-1903.

Knowling, S., Bartlett, A. and Radford, S. (2011) Dissecting key residues in folding and stability of the bacterial immunity protein 7. *Protein Eng. Des. Sel*. **24:** 517-523.

Krzeminski, L., Cronin, S., Ndamba, L., Canters, G., Aartsma, T., Evans, S. and Jeuken, L. (2011) Orientational control over nitrite reductase on modified gold electrode and its effects on the interfacial electron transfer. *J. Phys. Chem. B* **115:** 12607-12614.

Krzeminski, L., Ndamba, L., Canters, G., Aartsma, T., Evans, S. and Jeuken, L. (2011) Spectroelectrochemical investigation of intramolecular and interfacial electron-transfer rates reveals differences between nitrite reductase at rest and during turnover. *J. Am. Chem. Soc.* **133:** 15085-15093.

Kurtis, C., Knowles, P., Parsons, M., Gaule, T., Phillips, S. and McPherson, M. (2011) Tyrosine 381 in *E. coli* copper amine oxidase influences substrate specificity. *J. Neural Transm.* **118:** 1043-1053.

La Corte, A., Carter, A., Rice, G., Duan, Q. L., Rouleau, G., Adam, A., Grant, P. and Hooper, N. (2011) A functional xpnpep2 promoter haplotype leads to reduced plasma aminopeptidase p and increased risk of ace inhibitor-induced angioedema. *Hum. Mutat.* **32:** 1326-1331.

Lamont, F., Tomlinson, D., Cooper, P., Shnyder, S., Chester, J. and Knowles, M. (2011) Small molecule fgf receptor inhibitors block fgfr-dependent urothelial carcinoma growth in vitro and in vivo. *Br. J. Cancer* **104:** 75-82.

Lane, S., Dennis, C., Lane, C., Trinh, C., Rizkallah, P., Stockley, P. and Phillips, S. (2011) Construction and crystal structure of recombinant STNV capsids. *J. Mol. Biol*. **413:** 41-50.

Leddin, M., Perrod, C., Hoogenkamp, M., Ghani, S., Assi, S., Heinz, S., Wilson, N., Follows, G., Schoenheit, J., Vockentanz, L., Mosammam, A., Chen, W., Tenen, D., Westhead, D., Goettgens, B., Bonifer, C. and Rosenbauer, F. (2011) Two distinct auto-regulatory loops operate at the pu.1 locus in b cells and myeloid cells. *Blood* **117:** 2827-2838.

Leney, A., Phan, G., Allen, W., Verger, D., Waksman, G., Radford, S. and Ashcroft, A. (2011) Second order rate constants of donor-strand exchange reveal individual amino acid residues important in determining the subunit specificity of pilus biogenesis. *J. Am. Soc. Mass Spectrom.* **22:** 1214-1223.

Li, J., Cubbon, R., Wilson, L., Amer, M., McKeown, L., Hou, B., Majeed, Y., Tumova, S., Seymour, V., Taylor, H., Stacey, M., O'Regan, D., Foster, R., Porter, K., Kearney, M. and Beech, D. (2011) Orai1 and crac channel dependence of vegf-activated ca(2+) entry and endothelial tube formation. *Circul. Res.* **108:** 1190-U131.

Lynch, A., Chen, R. and Slater, N. (2011) Ph-responsive polymers for trehalose loading and desiccation protection of human red blood cells. *Biomaterials* **32:** 4443-4449.

Ma, P., Nishiguchi, K., Yuille, H. M., Davis, L. M., Nakayama, J. and Phillips-Jones, M. K. (2011) Anti-hiv siamycin i directly inhibits autophosphorylation activity of the bacterial fsrc quorum sensor and other ATP-dependent enzyme activities. *FEBS Lett.* **585:** 2660-2664.

Macnab, S., Turrell, S., Carr, I., Markham, A., Coletta, P. and Whitehouse, A. (2011) Herpesvirus saimiri-mediated delivery of the adenomatous polyposis coli tumour suppressor gene reduces proliferation of colorectal cancer cells. *Int. J. Oncol*. **39:** 1173-1181.

Majeed, Y., Amer, M., Agarwal, A., McKeown, L., Porter, K., O'Regan, D., Naylor, J., Fishwick, C., Muraki, K. and Beech, D. (2011) Stereo-selective inhibition of transient receptor potential trpc5 cation channels by neuroactive steroids. *Br. J. Pharmacol.* **162:** 1509-1520.

Mandal, P. and Turnbull, W. (2011) Studies on the synthesis of Lewis-Y oligosaccharides. *Carbohyd. Res.* **346:** 2113-2120.

Mariner, K., McPhillie, M., Trowbridge, R., Smith, C., O'Neill, A., Fishwick, C. and Chopra, I. (2011) Activity of and development of resistance to corallopyronin a, an inhibitor of RNA polymerase. *Antimicrob. Agents Chemother*. **55:** 2413-2416.

Mariner, K., Ooi, N., Roebuck, D., O'Neill, A. and Chopra, I. (2011) Further characterization of *Bacillus subtilis* antibiotic biosensors and their use for antibacterial mode-of-action studies. *Antimicrob. Agents Chemother.* **55:** 1784-1786.

McAllister, T., Nix, M. and Webb, M. (2011) Fmoc-chemistry of a stable phosphohistidine analogue. *Chem. Commun*. **47:** 1297-1299.

McFadden, N., Bailey, D., Carrara, G., Benson, A., Chaudhry, Y., Shortland, A., Heeney, J., Yarovinsky, F., Simmonds, P., Macdonald, A. and Goodfellow, I. (2011) Norovirus regulation of the innate immune response and apoptosis occurs via the product of the alternative open reading frame 4. *PLoS Pathog*. **7:** e1002413.

McGhee, A., Plante, J., Kilner, C. and Wilson, A. (2011) Solid-state structures of ureidoimidazoles. *Supramol. Chem*. **23:** 470-479.

McLaws, F., Larsen, A., Skov, R., Chopra, I. and O'Neill, A. (2011) Distribution of fusidic acid resistance determinants in methicillin-resistant *Staphylococcus aureus*. *Antimicrob. Agents Chemother*. **55:** 1173-1176.

McPhillie, M., Trowbridge, R., Mariner, K., O'Neill, A., Johnson, A., Chopra, I. and Fishwick, C. (2011) Structure-based ligand design of novel bacterial RNA polymerase inhibitors. *ACS Med. Chem. Lett.* **2:** 729-734.

Metanawin, T., Tang, T., Chen, R., Vernon, D. and Wang, X. (2011) Cytotoxicity and photocytotoxicity of structure-defined water-soluble C(60)/micelle supramolecular nanoparticles. *Nanotechnology* **22**:235604.

Mitchell, J., Laughton, C. and Harris, S. (2011) Atomistic simulations reveal bubbles, kinks and wrinkles in supercoiled DNA. *Nucleic Acids Res*. **39:** 3928-3938.

Moore, M., Bunka, D., Forzan, M., Spear, P., Stockley, P., McGowan, I. and James, W. (2011) Generation of neutralizing aptamers against herpes simplex virus type 2: Potential components of multivalent microbicides. *J. Gen. Virol*. **92:** 1493-1499.

Murrison, S., Maurya, S., Einzinger, C., McKeever-Abbas, B., Warriner, S. and Nelson, A. (2011) Synthesis of skeletally diverse alkaloid-like small molecules. *Eur. J. Org. Chem.* **12:**2354-2359.

Nam, J., Beales, P. and Vanderlick, T. (2011) Giant phospholipid/block copolymer hybrid vesicles: Mixing behavior and domain formation. *Langmuir* **27:** 1-6.

Nandasoma, U., McCormick, C., Griffin, S. and Harris, M. (2011) Nucleotide requirements at positions +1 to +4 for the initiation of hepatitis c virus positive-strand RNA synthesis. *J. Gen. Virol*. **92:** 1082-1086.

Newstead, S., Drew, D., Cameron, A., Postis, V., Xia, X., Fowler, P., Ingram, J., Carpenter, E., Sansom, M., McPherson, M., Baldwin, S. and Iwata, S. (2011) Crystal structure of a prokaryotic homologue of the mammalian oligopeptide-proton symporters, pept1 and pept2. *EMBO J*. **30:** 417-426.

Nicol, C., Bunka, D., Blair, G. and Stonehouse, N. (2011) Effects of single nucleotide changes on the binding and activity of rna aptamers to human papillomavirus 16 e7 oncoprotein. *Biochem. Biophys. Res. Commun*. **405:** 417-421.

Owen, R., Yorke, B., Gowdy, J. and Pearson, A. (2011) Revealing low-dose radiation damage using single-crystal spectroscopy. *J. Synch. Rad*. **18:** 367-373.

Pellizzaro, M., McGhee, A., Renton, L., Nix, M., Fisher, J., Turnbull, W. and Wilson, A. (2011) Conformer-independent ureidoimidazole motifs-tools to probe conformational and tautomeric

effects on the molecular recognition of triply hydrogen-bonded heterodimers. *Chemistry* ***17:****14508-14517.*

Ponnambalam, S. and Alberghina, M. (2011) Evolution of the VEGF-regulated vascular network from a neural guidance system. *Mol. Neurobiol*. **43:** 192-206.

Porter, M., Routledge, K., Radford, S. and Hewitt, E. (2011) Characterization of the response of primary cells relevant to dialysis-related amyloidosis to beta(2)-microglobulin monomer and fibrils. *PloS ONE* **DOI:** 10.1371/journal.pone.0027353.

Pritchard, C., Quaglia, M., Ashcroft, A. and O'Connor, G. (2011) Considering the advantages and pitfalls of the use of isotopically labeled protein standards for accurate protein quantification. *Bioanalysis* **3:** 2797-2802.

Ricchiuto, P., Brukhno, A. V., Paci, E. and Auer, S. (2011) Communication: Conformation state diagram of polypeptides: A chain length induced alpha-beta transition. *J. Chem. Phys*. **DOI:** 10.1063/1.3624928.

Richards, K. and Macdonald, A. (2011) Putting the brakes on the anti-viral response: Negative regulators of type i interferon (IFN) production. *Microb. Infect*. **13:** 291-302.

Robichaud, T., Appleyard, A., Herbert, R., Henderson, P. and Carruthers, A. (2011) Determinants of ligand binding affinity and cooperativity at the GLUT1 endofacial site. *Biochemistry* **50:** 3137-3148.

Santos, S., Barcons, V., Christenson, H., Font, J. and Thomson, N. (2011) The intrinsic resolution limit in the atomic force microscope: Implications for heights of nano-scale features. *PLoS ONE* **6**: e23821.

Santos, S., Barcons, V., Verdaguer, A., Font, J., Thomson, N. and Chiesa, M. (2011) How localized are energy dissipation processes in nanoscale interactions? *Nanotechnology* **DOI:**10.1088/0957-4484/22/34/345401.

Santos, S. and Thomson, N. (2011) Energy dissipation in a dynamic nanoscale contact. *App. Phys. Lett.* **DOI:**10.1063/1.3532097.

Santos, S., Verdaguer, A., Souier, T., Thomson, N. and Chiesa, M. (2011) Measuring the true height of water films on surfaces. *Nanotechnology* **DOI:** 10.1088/0957-4484/22/46/465705.

Shepherd, D., Veesler, D., Lichiere, J., Ashcroft, A. and Cambillau, C. (2011) Unraveling lactococcal phage baseplate assembly by mass spectrometry. *Mol. Cell. Prot.* **DOI:** 10.1074/mcp.M111.009787.

Skorski, S. and Olmsted, P. (2011) Loss of solutions in shear banding fluids driven by second normal stress differences. *J. Rheol*. **55:** 1219-1246.

Smith, D., Woods, L., Radford, S. and Ashcroft, A. (2011) Structure and dynamics of oligomeric intermediates in beta(2)-microglobulin self-assembly. *Biophys. J*. **101:** 1238-1247.

Stadler, L., Hoffmann, T., Tomlinson, D., Song, Q., Lee, T., Busby, M., Nyathi, Y., Gendra, E., Tiede, C., Flanagan, K., Cockell, S., Wipat, A., Harwood, C., Wagner, S., Knowles, M., Davis, J., Keegan, N. and Ferrigno, P. K. (2011) Structure-function studies of an engineered scaffold

protein derived from stefin a. Ii: Development and applications of the SQT variant. *Prot. Eng. Des. Sel.* **24:** 751-763.

Standeven, K., Hess, K., Carter, A., Rice, G., Cordell, P., Balmforth, A., Lu, B., Scott, D., Turner, A., Hooper, N. and Grant, P. (2011) Neprilysin, obesity and the metabolic syndrome. *Int. J. Obes.* **35:** 1031-1040.

Stead, L., Wood, I. and Westhead, D. (2011) Kvsnp: Accurately predicting the effect of genetic variants in voltage-gated potassium channels. *Bioinformatics* **27:** 2181-2186.

Stephens, C., Kim, Y.-Y., Evans, S., Meldrum, F. and Christenson, H. (2011) Early stages of crystallization of calcium carbonate revealed in picoliter droplets. *J. Am. Chem. Soc*. **133:** 5210-5213.

Taylor, A., Jackson, B., Noerenberg, M., Hughes, D., Boyne, J., Verow, M., Harris, M. and Whitehouse, A. (2011) Mutation of a C-terminal motif affects Kaposi's sarcoma-associated herpesvirus ORF57 RNA binding, nuclear trafficking, and multimerization. *J. Virol*. **85:** 7881-7891.

Tedbury, P., Welbourn, S., Pause, A., King, B., Griffin, S. and Harris, M. (2011) The subcellular localization of the hepatitis C virus non-structural protein NS2 is regulated by an ion channel-independent function of the p7 protein. *J. Gen. Virol*. **92:** 819-830.

Teoh, C., Pham, C., Todorova, N., Hung, A., Lincoln, C., Lees, E., Lam, Y. H., Binger, K., Thomson, N., Radford, S., Smith, T., Mueller, S., Engel, A., Griffin, M., Yarovsky, I., Gooley, P. and Howlett, G. (2011) A structural model for apolipoprotein c-ii amyloid fibrils: Experimental characterization and molecular dynamics simulations. *J. Mol. Biol.* **405:** 1246-1266.

Toropova, K., Stockley, P. and Ranson, N. (2011) Visualising a viral RNA genome poised for release from its receptor complex. *J. Mol. Biol.* **408:** 408-419.

Tosatti, P., Campbell, A., House, D., Nelson, A. and Marsden, S. (2011) Catalyst control in sequential asymmetric allylic substitution: Stereodivergent access to n,n-diprotected unnatural amino acids. *J. Org. Chem*. **76:** 5495-5501.

Towey, J., Soper, A. and Dougan, L. (2011) Preference for isolated water molecules in a concentrated glycerol-water mixture. *J. Phys. Chem. B* **115:** 7799-7807.

Towey, J., Soper, A. and Dougan, L. (2011) The structure of glycerol in the liquid state: A neutron diffraction study. *Phys. Chem. Chem. Phys.* **13:** 9397-9406.

Tunnicliffe, R., Hautbergue, G., Kalra, P., Jackson, B., Whitehouse, A., Wilson, S. and Golovanov, A. (2011) Structural basis for the recognition of cellular mRNA export factor ref by herpes viral proteins HSV-1 ICP27 and HVS ORF57. *PLoS Pathog.* **7:** e1001244.

Turrell, S. and Whitehouse, A. (2011) Mutation of herpesvirus saimiri ORF51 glycoprotein specifically targets infectivity to hepatocellular carcinoma cell lines. *J. Biomed. Biotechnol.* **DOI:**10.1155/2011/785158.

Tych, K., Burnett, A., Wood, C., Cunningham, J., Pearson, A., Davies, A. and Linfield, E. (2011) Applying broadband terahertz time-domain spectroscopy to the analysis of crystalline proteins: A dehydration study. *J. Appl. Cryst.* **44:** 129-133.

Ulyatt, C., Walker, J. and Ponnambalam, S. (2011) Hypoxia differentially regulates VEGFR1 and vegfr2 levels and alters intracellular signaling and cell migration in endothelial cells. *Biochem. Biophys. Res. Commun.* **404:** 774-779.

van Wezel, G. and McDowall, K. (2011) The regulation of the secondary metabolism of streptomyces: New links and experimental advances. *Natural Product Reports* **28:** 1311-1333.

Vehar, B., Hrast, M., Kovac, A., Konc, J., Mariner, K., Chopra, I., O'Neill, A., Janezic, D. and Gobec, S. (2011) Ellipticines and 9-acridinylamines as inhibitors of d-alanine:D-alanine ligase. *Bioorg. Med. Chem.* **19:** 5137-5146.

Wagner, B., Gilbert, T., Hanai, J.-i., Imamura, S., Bodycombe, N., Bon, R., Waldmann, H., Clemons, P., Sukhatme, V. and Mootha, V. (2011) A small-molecule screening strategy to identify suppressors of statin myopathy. *ACS Chem. Biol.* **6:** 900-904.

Walden, M., Jenkins, H. and Edwards, T. (2011) Structure of the drosophila melanogaster rab6 gtpase at 1.4 angstrom resolution. *Acta Crystallogr. Sect. F* **67:** 744-748.

Walter, C., Bento, D., Alonso, A. G. and Barr, J. (2011) Amino acid changes within the bunyamwera virus nucleocapsid protein differentially affect the mRNA transcription and RNA replication activities of assembled ribonucleoprotein templates. *J. Gen. Virol.* **92:** 80-84.

Woods, L., Platt, G., Hellewell, A., Hewitt, E., Homans, S., Ashcroft, A. and Radford, S. (2011) Ligand binding to distinct states diverts aggregation of an amyloid-forming protein. *Nat. Chem. Biol.* **7:** 730-739.

Woon, E., Zervosen, A., Sauvage, E., Simmons, K., Zivec, M., Inglis, S., Fishwick, C., Gobec, S., Charlier, P., Luxen, A. and Schofield, C. (2011) Structure guided development of potent reversibly binding penicillin binding protein inhibitors. *ACS Med. Chem. Lett.* **2:** 219-223.

Wu, W., Munday, D., Howell, G., Platt, G., Barr, J. and Hiscox, J. (2011) Characterization of the interaction between human respiratory syncytial virus and the cell cycle in continuous cell culture and primary human airway epithelial cells. *J. Virol.* **85:** 10300-10309.

Yao, S., Ng, A., Cass, C., Baldwin, S. and Young, J. (2011) Nucleobase transport by human equilibrative nucleoside transporter 1 (hent1). *J. Biol. Chem.* **286:** 32552-32562.

Yoon, J., Whipple, R., Balzer, E., Cho, E., Matrone, M., Peckham, M. and Martin, S. (2011) Local anesthetics inhibit kinesin motility and microtentacle protrusions in human epithelial and breast tumor cells. *Breast Cancer Res. Treat.* **129:** 691-701.

Zhang, S., Nelson, A., Coldrick, Z. and Chen, R. (2011) The effects of substituent grafting on the interaction of ph-responsive polymers with phospholipid monolayers. *Langmuir* **27:** 8530-8539.

Zhang, X., Lousa, C. D. M., Schutte-Lensink, N., Ofman, R., Wanders, R., Baldwin, S., Baker, A., Kemp, S. and Theodoulou, F. (2011) Conservation of targeting but divergence in function and quality control of peroxisomal ABC transporters: An analysis using cross-kingdom expression. *Biochem. J.* **436:** 547-557.

Zhang, Y., Zhang, H., Hollins, J., Webb, M. and Zhou, D. (2011) Small-molecule ligands strongly affect the forster resonance energy transfer between a quantum dot and a fluorescent protein. *Phys Chem Chem Phys* **13:** 19427-19436.

Zhou, D., Li, Y., Hall, E., Abell, C. and Klenerman, D. (2011) A chelating dendritic ligand capped quantum dot: Preparation, surface passivation, bioconjugation and specific DNA detection. *Nanoscale* **3:** 201-211.

UNIVERSITY OF LEEDS

Leeds, United Kingdom
LS2 9JT
Tel. 0113 243 1751
www.leeds.ac.uk